DYNAMICS OF A THREE-AXIS GYRO STABILIZED PLATFORM

A Thesis

Presented to

the Faculty of the College of Engineering

University of Houston

In Partial Fulfillment

of the Requirements for the Degree

Master of Science

---

by

Frank N. Barnes

August 1970

545121

ACKNOWLEDGMENTS

I am grateful to have had the opportunity to do my thesis research and preparation at the Lockheed Electronics Company.

My appreciation to Professor William Schneider, my thesis advisor, for his advice and suggestions which contributed greatly to the preparation of this paper.

A note of thanks to my fellow colleagues at LEC and NASA-MSC for their suggestions and interest in this work. Special recognition is due Al Turley (MSC) for suggesting this topic, Richard Theobald (LEC) for his review of the mathematical model development, and Leonard White (LEC) for programming support.

I am very grateful to those who aided in the preparation of this manuscript: to Suzan Lockett for editing; to Erma L. Pharr for typing; and to the Technical Illustrations group for preparing excellent figures.

This thesis was prepared under the auspices of the National Aeronautics and Space Administration under Contract NAS 9-5384. Publication of this report does not constitute approval by NASA or the Lockheed Electronics Company of the findings or conclusions contained herein. It is published only for the exchange and stimulation of ideas.

DYNAMICS OF A THREE-AXIS GYRO STABILIZED PLATFORM

An Abstract of a Thesis

Presented to

the Faculty of the College of Engineering

University of Houston

In Partial Fulfillment

of the Requirements for the Degree

Master of Science

---

by

Frank N. Barnes

August 1970

DYNAMICS OF A THREE-AXIS GYRO

STABILIZED PLATFORM

ABSTRACT

A detailed development of the equations of motion for the stable member of a three-gimbal platform is presented. These equations are combined with models of the three platform control loops to formulate a model for the system.

The system model is simplified and a digital simulation is developed for studying the motion of the stable member under conditions of dynamic vehicle angular environment.

Test cases are presented for a typical inertial measurement unit.

TABLE OF CONTENTS

LIST OF FIGURES

CHAPTER I

INTRODUCTION

An inertial navigation system consists of an inertial measurement unit (IMU), navigation computer, and computer interface. The IMU measures the acceleration and attitude of the vehicle in an inertial coordinate system; these inertial coordinates are transferred to the computer, which determines the vehicle position in the desired reference frame.

The requirement that the IMU measure vehicle acceleration in an inertial reference frame led to the concept of an inertial platform or stable member on which to mount the accelerometers. This stable platform provides a controlled angular environment, which reduces sensor dynamic error during vehicle oscillation.

The predominant configuration for an IMU is a group of inertial sensors mounted on a gimbal-supported platform. These sensors consist of three accelerometers and three single-degree-of-freedom rate integrating gyroscopes (gyros) which detect attitude errors (Figure 1).

Torquers mounted in the gimbal pivots are activated by the gyros to null the disturbing torques transmitted to the platform and return the platform to the correct reference

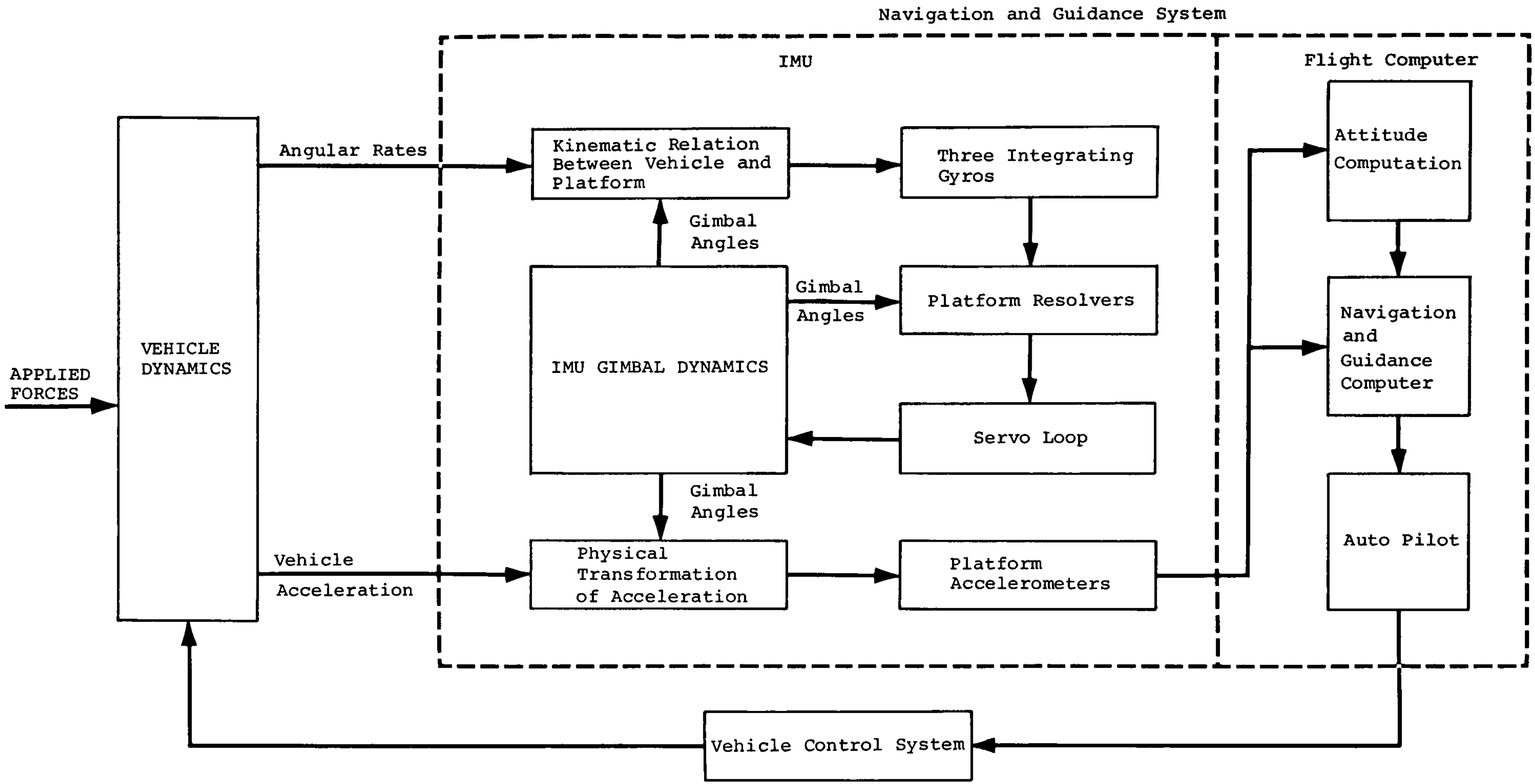

FIGURE 1

GIMBALED SYSTEM CONFIGURATION

attitude. The disturbing torques are due to friction in the pivots, mass unbalance of the gimbals, and anisoinertial effects. Driving the gimbals so that the gyro float angles are nulled returns the stable member to its original attitude, which causes negligible commutative error.

The platform-mounted accelerometers measure the components of translational acceleration to which the vehicle is subjected in a set of reference inertial coordinates; the acceleration may be integrated in the reference system to determine the vehicle state vector (velocity and position). The state vector may be used for guidance and navigation computations.

The gimbaled platform (IMU) is the classical form of an inertial navigation system. There are two standard gimbal configurations: the three-gimbal system, which is deprived of a degree of freedom when the pitch and roll gimbals become aligned (gimbal lock) as the middle gimbal angle approaches $\pi/2$ radians; the four-gimbal configuration, which eliminates the possibility of gimbal-lock, can experience instantaneous reorientation of a gimbal by π radians (gimbal flip). The four-gimbal system allows the vehicle a complete sphere of movement without loss of reference attitude if gimbal flip can be accommodated.

The three-gimbal system places logistic constraints on mission profiles; profiles must be designed such that the middle gimbal angle does not become excessive (approach $\pi/2$ radians). The attitude constraint is relative to a particular alignment (inertial reference) and therefore may be varied by a change in alignment.

The effects of the vehicle's rotational environment on the inertial instruments' environment is a primary concern. The filtering effect of the gimbal control loops is a function of the vehicle attitude relative to the reference coordinate system, and is not readily analyzed for an arbitrary vehicle motion. A mathematical model and digital simulation of a three-gimbal IMU was developed to study the effects of vehicle motion on the stable member (inertial instrument environment).

The system kinematic model is defined in Chapter II, and consists of a seven-body (case, outer gimbal, inner gimbal, platform, and three gyros) topological tree with one degree of freedom between adjacent bodies. All bodies are considered to be rigid, and their respective coordinate systems and appropriate linear transformations are defined. Kinematic relations between the members of a perfect platform are defined and extended to an imperfect or real system.

In Chapter III, the equations of motion are developed for each body of the system in the form $\vec{M} = {}^{i}\dot{\vec{H}}$ where $\vec{M}$ is the net torque on a given member of the system, and consists of the torque applied by the adjacent outer and inner members; ${}^{i}\dot{\vec{H}}$ is the inertial derivative of the body angular momentum. The equations of motion for the gimbals and gyros are a set of six second-order differential equations of state, where the state variables are the three system Euler angles, the three gyro float angles, and their respective derivatives.

$$\begin{bmatrix} \ddot{\phi} \\ \ddot{\psi} \\ \ddot{\theta} \\ \ddot{\alpha}_x \\ \ddot{\alpha}_y \\ \ddot{\alpha}_z \\ \dot{\phi} \\ \dot{\psi} \\ \dot{\theta} \\ \dot{\alpha}_x \\ \dot{\alpha}_y \\ \dot{\alpha}_z \end{bmatrix} = \begin{bmatrix} A \end{bmatrix} \begin{bmatrix} \dot{\phi} \\ \dot{\psi} \\ \dot{\theta} \\ \dot{\alpha}_x \\ \dot{\alpha}_y \\ \dot{\alpha}_z \\ \phi \\ \psi \\ \theta \\ \alpha_x \\ \alpha_y \\ \alpha_z \end{bmatrix} \tag{1-1}$$

The elements closing the loop between the gyro outputs $\vec{\alpha}$ and the control torques applied to the gimbals are modeled in Chapter IV. The resolvers, demodulator, compensation filters, amplifiers, and torque motors are included.

In Chapter V, the complete system model is analyzed and reduced in order; this was achieved by eliminating high-frequency terms, thus facilitating digital simulation. The low-frequency platform model is simulated in FORTRAN on a CDC 3800.

Criteria are developed in Appendix D to evaluate the stable-member motion under test conditions, and are included in the simulation. The figures of merit include the root-mean-square (rms) value of the total misalignment angles about the three axes, and the mean and variance of the individual misalignment angles. These criteria are plotted against time for the test cases run. The simulation was run for a range of environmental conditions on a typical space-vehicle platform and the results are presented.

CHAPTER II

KINEMATIC RELATIONSHIPS

The three-gimbaled Inertial Measurement Unit (IMU) supporting structure consists of the platform, inner gimbal, outer gimbal, and the case (Figure 2); each member is assumed to be rigid. The following definitions apply to the angles and rates relating the four members of the gimbaled system.

θ — The relative angle between the inner gimbal and the platform, measured about the platform Y-axis (Y_p).

$\dot{\theta}$ — The relative angular rate between the inner gimbal and the platform, measured about the platform Y-axis (Y_p).

ψ — The relative angle between the outer and inner gimbals, measured about the inner gimbal Z-axis (Z_I).

$\dot{\psi}$ — The relative angular rate between the outer and inner gimbals, measured about the inner gimbal Z-axis (Z_I).

ϕ — The relative angle between the case and the outer gimbals, measured about the outer gimbal X-axis (X_o).

$\dot{\phi}$ — The relative angular rate between the case and the outer gimbal, measured about the outer gimbal X-axis (X_o).

The above-defined angles and angular rates represent a 1,3,2 (ϕ,ψ,θ) Euler sequence from the case to the platform.

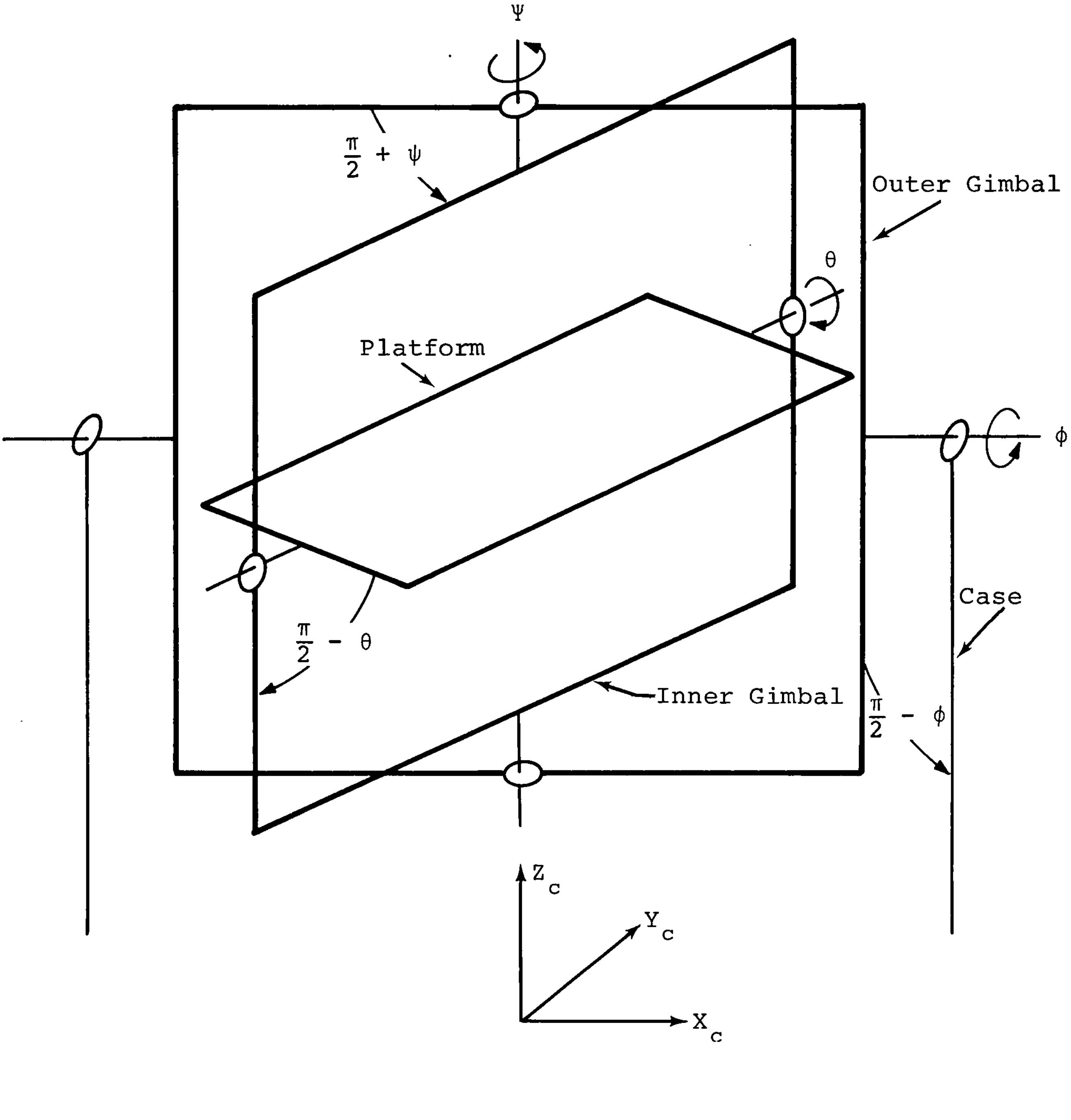

FIGURE 2

THREE-GIMBAL STRUCTURE

I. COORDINATE SYSTEMS

Gimbal Coordinate System. An orthogonal coordinate system is defined rotating with each member of the gimbaled system (Figure 3): platform (X_p, Y_p, Z_p), inner gimbal (X_I, Y_I, Z_I), outer gimbal (X_o, Y_o, Z_o), and case (X_c, Y_c, Z_c). A vector may be represented in the coordinates of any of the members and transformed from member to member by the appropriate linear transformation $[B_{pI}]$, $[B_{Io}]$, $[B_{oc}]$, etc.*

The inner gimbal and the platform are related by θ, the inner gimbal angle (IGA); the direction cosine transformation matrix from the platform to the inner gimbal is $[B_{pI}]$.

$$[B_{pI}] = \begin{bmatrix} \cos\theta & 0 & -\sin\theta \\ 0 & 1 & 0 \\ \sin\theta & 0 & \cos\theta \end{bmatrix} \tag{2-1}$$

*Note: Notation Convention, Appendix C.

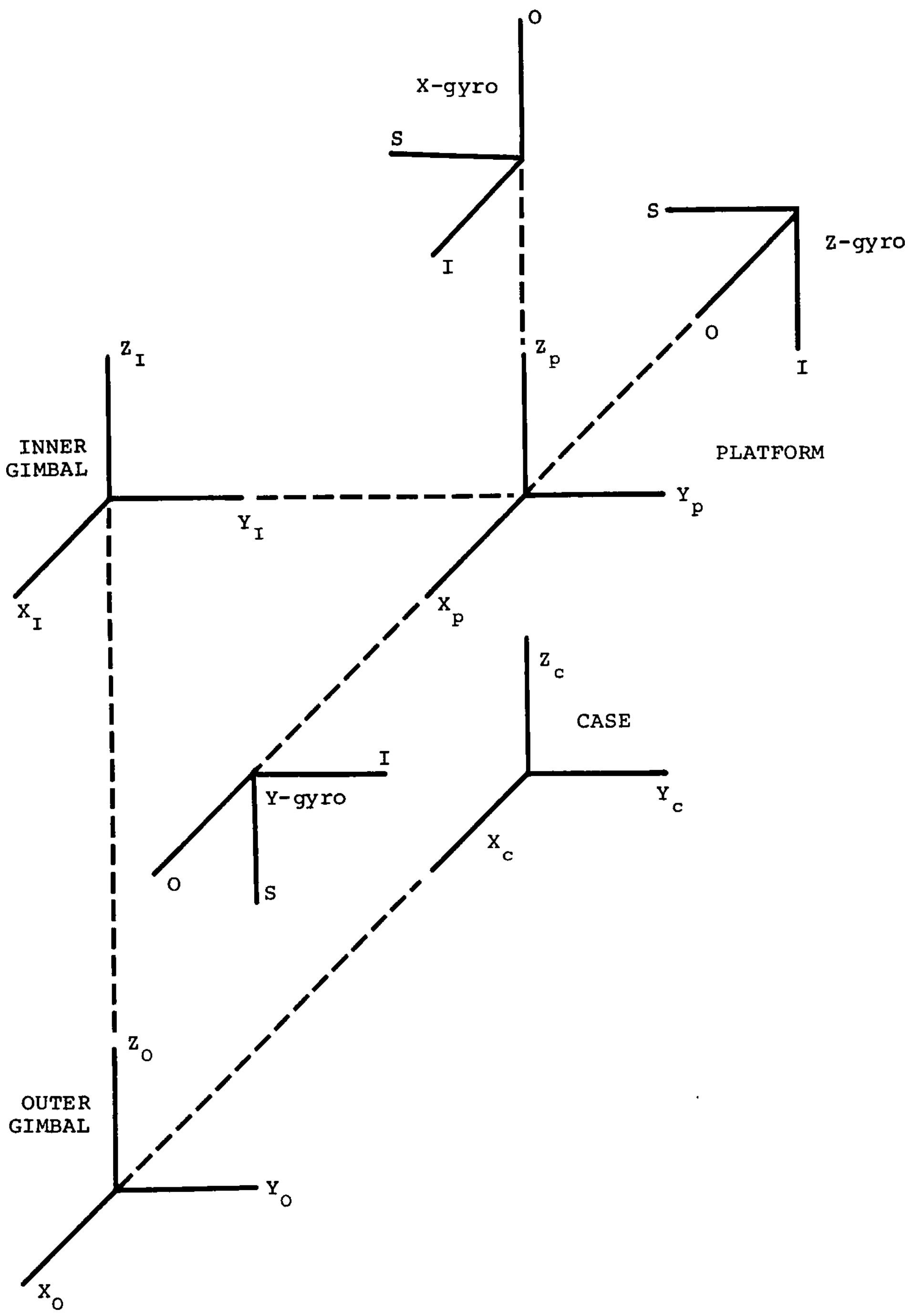

FIGURE 3

SYSTEM TOPOLOGY

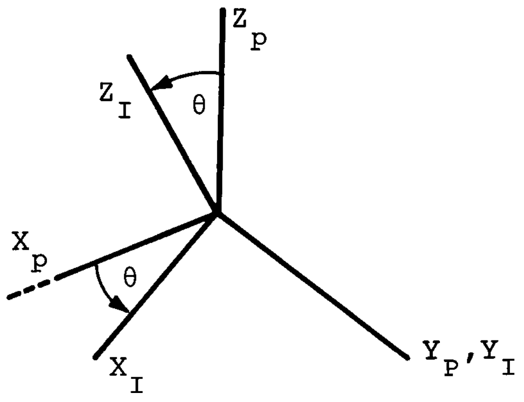

FIGURE 4

RELATIONSHIP BETWEEN PLATFORM AND INNER GIMBAL COORDINATE SYSTEMS

The outer gimbal is related to the inner gimbal by ψ , the middle gimbal angle (MGA).

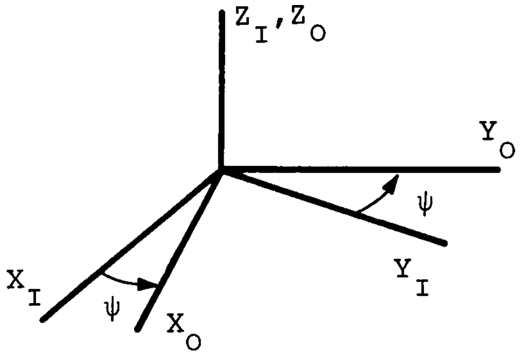

FIGURE 5

RELATIONSHIP BETWEEN INNER AND OUTER GIMBAL COORDINATE SYSTEMS

The direction cosine transformation matrix from the inner gimbal to the outer gimbal is $[B_{Io}]$.

$$[B_{Io}] = \begin{bmatrix} \cos\psi & \sin\psi & 0 \\ -\sin\psi & \cos\psi & 0 \\ 0 & 0 & 1 \end{bmatrix} \qquad (2\text{-}2)$$

The fourth member of the system is the case, which is related to the outer gimbal by ϕ, the outer gimbal angle (OGA).

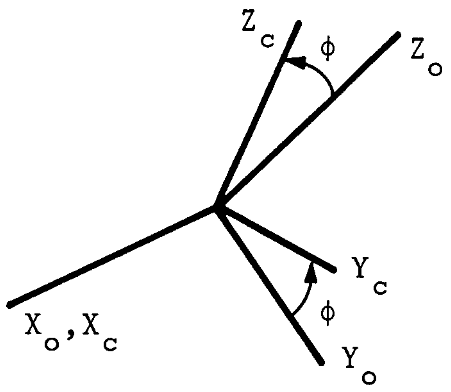

FIGURE 6

RELATIONSHIP BETWEEN OUTER GIMBAL

AND CASE COORDINATE SYSTEM

Transformation from the outer gimbal to the case is represented in matrix form by $[B_{oc}]$.

$$[B_{oc}] = \begin{bmatrix} 1 & 0 & 0 \\ 0 & \cos\phi & \sin\phi \\ 0 & -\sin\phi & \cos\phi \end{bmatrix} \tag{2-3}$$

The transformation from the platform to the case coordinate system is formed by

$$[B_{pc}] = [B_{oc}][B_{Io}][B_{pI}] \tag{2-4}$$

$$[B_{pc}] = \begin{bmatrix} \cos\theta\cos\psi & \sin\psi & -\sin\theta\cos\psi \\ \begin{matrix}\sin\theta\sin\psi \\ -\cos\theta\cos\phi\sin\psi\end{matrix} & \cos\psi\cos\phi & \begin{matrix}\sin\theta\sin\psi\cos\phi \\ +\sin\theta\sin\phi\end{matrix} \\ \begin{matrix}\cos\theta\sin\psi\sin\phi \\ +\sin\theta\cos\phi\end{matrix} & -\cos\psi\sin\phi & \begin{matrix}\cos\theta\cos\phi \\ -\sin\theta\sin\psi\sin\phi\end{matrix} \end{bmatrix} \tag{2-5}$$

Gyro Coordinate System. The system gyros are assumed to be mounted on the platform with no misalignment between the gyro cases and the platform. Each gyro has a coordinate system (Figure 7) mounted in the float with axes S, I, and O representing the spin axis of the rotor, float input axis and output axis, respectively. One degree of freedom (float angles α_X, α_Y, and α_Z) exists between the float of each gyro and the platform.

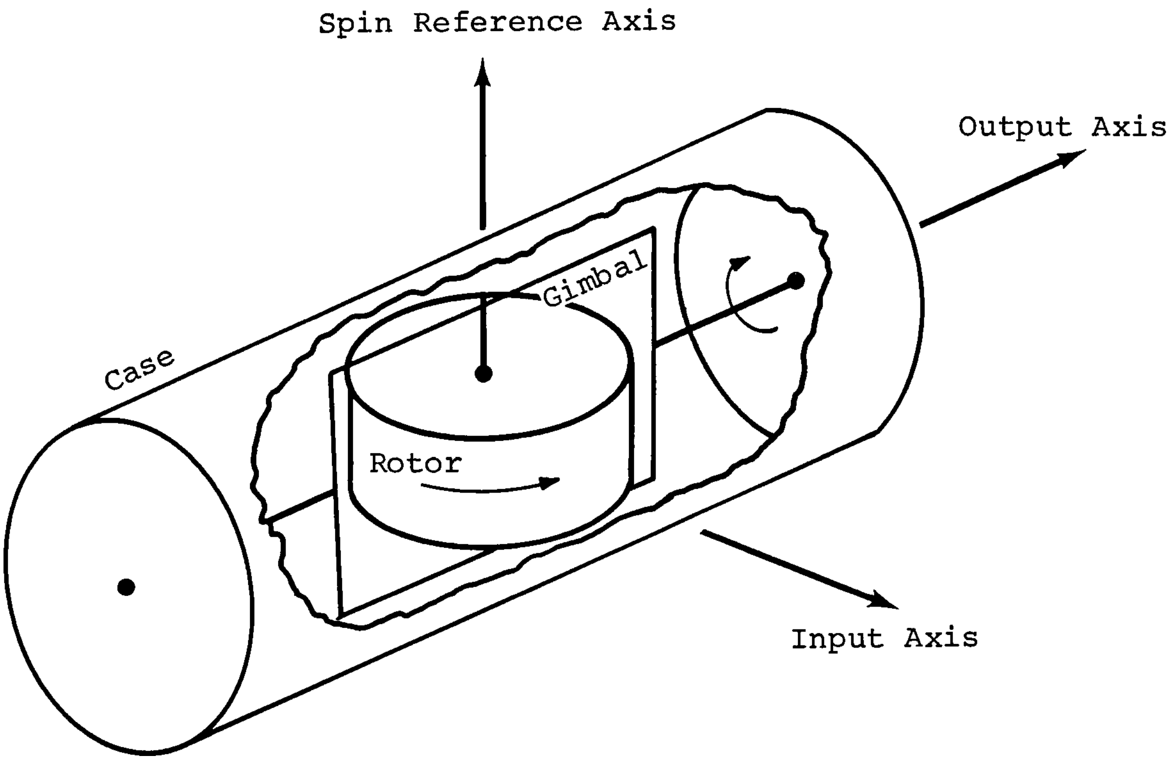

FIGURE 7

SINGLE-DEGREE-OF-FREEDOM GYRO

Figure 8 illustrates the orientation of the gyro triad to the platform.

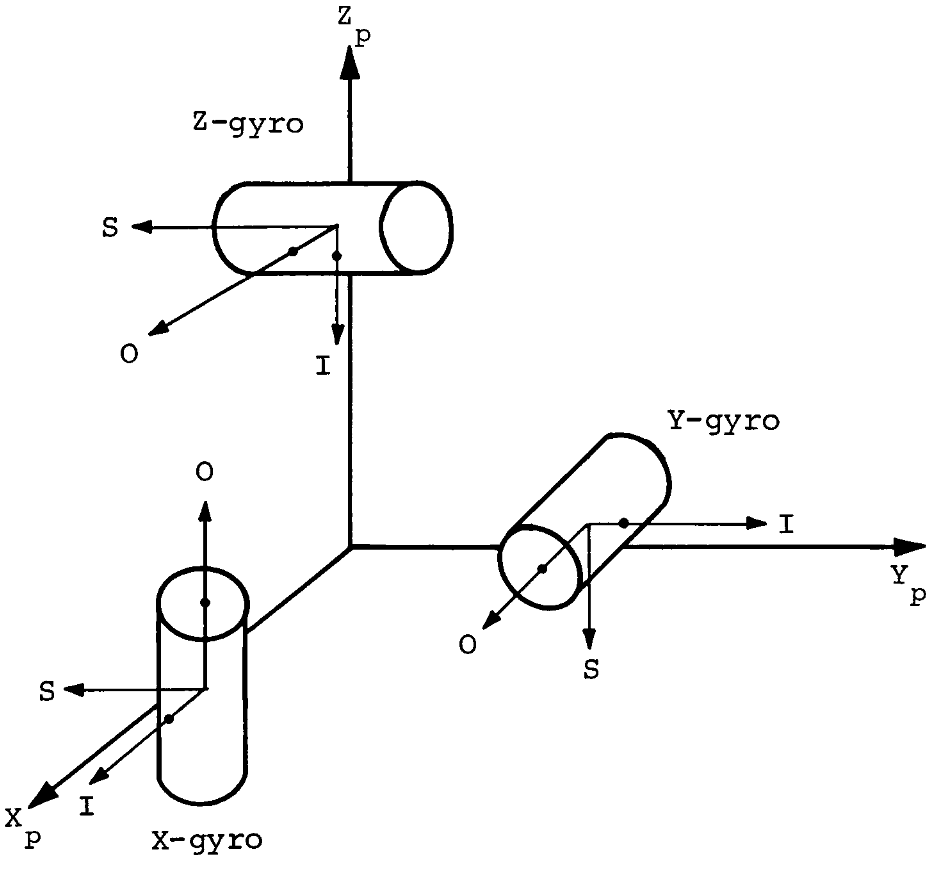

FIGURE 8

ORIENTATION OF GYRO AND PLATFORM AXES

The direction cosine transformations from the platform to the X, Y, and Z gyro floats are $[B_{pgx}]$, $[B_{pgy}]$, and $[B_{pgz}]$, where

$$[B_{pgx}] = \begin{bmatrix} \sin\alpha_X & -\cos\alpha_X & 0 \\ \cos\alpha_X & \sin\alpha_X & 0 \\ 0 & 0 & 1 \end{bmatrix} \qquad (2\text{-}6)$$

$$[B_{pgy}] = \begin{bmatrix} 0 & \sin\alpha_Y & -\cos\alpha_Y \\ 0 & \cos\alpha_Y & \sin\alpha_Y \\ 1 & 0 & 0 \end{bmatrix} \qquad (2\text{-}7)$$

$$[B_{pgz}] = \begin{bmatrix} 0 & -\cos\alpha_Z & -\sin\alpha_Z \\ 0 & \sin\alpha_Z & -\cos\alpha_Z \\ 1 & 0 & 0 \end{bmatrix} \qquad (2\text{-}8)$$

II. VECTOR TRANSFORMATION BETWEEN GIMBALS

Defining $\hat{u}$ as a unit vector with coordinates $[U_{px}, U_{py}, U_{pz}]^T$, $[U_{Ix}, U_{Iy}, U_{Iz}]^T$, $[U_{ox}, U_{oy}, U_{oz}]^T$, and $[U_{cx}, U_{cy}, U_{cz}]^T$ in the platform, inner and outer gimbals, and case coordinate systems, respectively.

Let

$$
* \qquad \hat{u}^{p} = \begin{bmatrix} U_{px} \\ U_{py} \\ U_{pz} \end{bmatrix} , \quad \hat{u}^{I} = \begin{bmatrix} U_{Ix} \\ U_{Iy} \\ U_{Iz} \end{bmatrix}
$$

$$
\hat{u}^{o} = \begin{bmatrix} U_{ox} \\ U_{oy} \\ U_{oz} \end{bmatrix} , \quad \hat{u}^{c} = \begin{bmatrix} U_{cx} \\ U_{cy} \\ U_{cz} \end{bmatrix} \tag{2-9}
$$

The following relationships may be used to transform vector coordinates between the various members of the system.

Platform and Inner Gimbals.

$$
\hat{u}^{I} = [B_{pI}]\hat{u}^{p} \tag{2-10}
$$

Since $[B_{pI}]$ is normal orthogonal

$$
[B_{pI}]^{-1} = [B_{pI}]^{T} = [B_{Ip}] \tag{2-11}
$$

Therefore

$$
\hat{u}^{p} = [B_{Ip}]\hat{u}^{I} \tag{2-12}
$$

*Note: Notation Convention, Appendix C.

Inner and Outer Gimbals.

$$\hat{u}^{o} = [B_{Io}]\hat{u}^{I} \tag{2-13}$$

$$[B_{Io}]^{-1} = [B_{Io}]^{T} = [B_{oI}] \tag{2-14}$$

Therefore

$$\hat{u}^{I} = [B_{oI}]\hat{u}^{o} \tag{2-15}$$

Outer Gimbal and Case.

$$\hat{u}^{c} = [B_{oc}]\hat{u}^{o} \tag{2-16}$$

$$[B_{oc}]^{-1} = [B_{oc}]^{T} = [B_{co}] \tag{2-17}$$

Therefore

$$\hat{u}^{o} = [B_{co}]\hat{u}^{c} \tag{2-18}$$

Platform and Case.

$$\hat{u}^{c} = [B_{pc}]\hat{u}^{p} \tag{2-19}$$

$$[B_{pc}]^{-1} = [B_{pc}]^{T} = [B_{cp}] \tag{2-20}$$

Therefore

$$\hat{u}^{p} = [B_{cp}]\hat{u}^{c} \tag{2-21}$$

III. VECTOR TRANSFORMATION BETWEEN GYROS AND PLATFORMS

Unit vectors in gyro float coordinates for the triad are defined as

$$\hat{u}^{gx} = \begin{bmatrix} U_{gxS} \\ U_{gxI} \\ U_{gxO} \end{bmatrix}, \quad \hat{u}^{gy} = \begin{bmatrix} U_{gyS} \\ U_{gyI} \\ U_{gyO} \end{bmatrix}, \quad \hat{u}^{gz} = \begin{bmatrix} U_{gzS} \\ U_{gzI} \\ U_{gzO} \end{bmatrix} \tag{2-22}$$

The transformation of vector coordinates between the gyro coordinate systems and the platform is described by the following equations.

<u>Platform and X-Gyro</u>.

$$\hat{u}^{gx} = [B_{pgx}]\hat{u}^{p} \tag{2-23}$$

$$[B_{pgx}]^{-1} = [B_{pgx}]^{T} = [B_{gxp}] \tag{2-24}$$

Therefore

$$\hat{u}^{p} = [B_{gxp}]\hat{u}^{gx} \tag{2-25}$$

<u>Platform and Y-Gyro</u>.

$$\hat{u}^{gy} = [B_{pgy}]\hat{u}^{p} \tag{2-26}$$

$$[B_{pgy}]^{-1} = [B_{pgy}]^T = [B_{gyp}] \tag{2-27}$$

Therefore

$$\hat{u}^p = [B_{gyp}]\hat{u}^{gy} \tag{2-28}$$

Platform and Z-Gyro.

$$\hat{u}^{gz} = [B_{pgz}]\hat{u}^p \tag{2-29}$$

$$[B_{pgz}]^{-1} = [B_{pgz}]^T = [B_{gzp}] \tag{2-30}$$

Therefore

$$\hat{u}^p = [B_{gzp}]\hat{u}^{gz} \tag{2-31}$$

IV. PERFECT PLATFORM KINEMATICS

If a perfectly balanced, frictionless set of pivots is assumed, an arbitrary rate $\vec{\Omega}$ may be applied to the case without disturbing the platform. In case coordinates, $\vec{\Omega}$ may be expressed

$$\vec{\Omega}^c = \begin{bmatrix} \omega_{cx} \\ \omega_{cy} \\ \omega_{cz} \end{bmatrix} \tag{2-32}$$

The following kinematic relation may be written for the perfect platform; assuming $\vec{\omega}_p = 0$, then

$$\vec{\Omega} = \vec{\omega}_{cp} \tag{2-33}$$

where

$$\vec{\omega}_{cp} = \vec{\omega}_{Ip} + \vec{\omega}_{oI} + \vec{\omega}_{co} \tag{2-34}$$

$$\begin{bmatrix} \omega_{cx} \\ \omega_{cy} \\ \omega_{cz} \end{bmatrix} = [B_{oc}]\left\{[B_{Io}]\begin{bmatrix} 0 \\ \dot{\theta} \\ 0 \end{bmatrix} + \begin{bmatrix} 0 \\ 0 \\ \dot{\psi} \end{bmatrix}\right\} + \begin{bmatrix} \dot{\phi} \\ 0 \\ 0 \end{bmatrix}$$

$$= \begin{bmatrix} 1 & 0 & 0 \\ 0 & \cos\phi & \sin\phi \\ 0 & -\sin\phi & \cos\phi \end{bmatrix}\left[\begin{bmatrix} \cos\psi & \sin\psi & 0 \\ -\sin\psi & \cos\psi & 0 \\ 0 & 0 & 1 \end{bmatrix}\begin{bmatrix} 0 \\ \dot{\theta} \\ 0 \end{bmatrix} + \begin{bmatrix} 0 \\ 0 \\ \dot{\psi} \end{bmatrix}\right] + \begin{bmatrix} \dot{\phi} \\ 0 \\ 0 \end{bmatrix} \tag{2-35}$$

Written in component form

$$\omega_{cx} = \dot{\theta}\sin\psi + \dot{\phi} \tag{2-36}$$

$$\omega_{cy} = \dot{\theta}\cos\psi\cos\phi + \dot{\psi}\sin\phi \tag{2-37}$$

$$\omega_{cz} = -\dot{\theta} \cos \psi \sin \phi + \dot{\psi} \cos \phi \tag{2-38}$$

Solving for the Euler angle rates

$$\dot{\phi} = \omega_{cx} - \dot{\theta} \sin \psi \tag{2-39}$$

$$\dot{\psi} = \omega_{cz} \cos \phi + \omega_{cy} \sin \phi \tag{2-40}$$

$$\dot{\theta} = \frac{\omega_{cy} \cos \phi - \omega_{cz} \sin \phi}{\cos \psi} \tag{2-41}$$

Equations 2-39, 2-40, and 2-41 can be integrated and the resulting Euler angles substituted into Equation 2-5 evaluating the direction cosine matrix representing the relative attitude between the platform and case, assuming frictionless pivots and a stable platform ($\omega_{xp} = \omega_{yp} = \omega_{zp} = 0$).

V. IMPERFECT PLATFORM KINEMATICS

The kinematic relations used to derive the equations for a perfect platform may be generalized and extended to determine the relationship between the members of an imperfect platform.

Angular Rate Relationships Between Gimbals. Assume that the angular rate of the case is that of the carrier or vehicle

$$\vec{\omega}_c = \vec{\omega}_v \tag{2-42}$$

$$\vec{\omega}_v^v = \begin{bmatrix} p \\ q \\ r \end{bmatrix} \tag{2-43}$$

Therefore

$$\vec{\omega}_c^v = \begin{bmatrix} p \\ q \\ r \end{bmatrix} \tag{2-44}$$

Let the case coordinate system be aligned with the vehicle system

$$\vec{\omega}_c^c = \begin{bmatrix} p \\ q \\ r \end{bmatrix} \tag{2-45}$$

The outer gimbal rate $\vec{\omega}_o$ is equal to the vector sum of the case rate $\vec{\omega}_c$ and the relative rate $\vec{\omega}_{oc}$ between the case and the outer gimbal

$$\vec{\omega}_o = \vec{\omega}_c + \vec{\omega}_{oc} \tag{2-46}$$

In case coordinates

$$\vec{\omega}_o^c = \begin{bmatrix} p \\ q \\ r \end{bmatrix} - \begin{bmatrix} \dot{\phi} \\ 0 \\ 0 \end{bmatrix} \tag{2-47}$$

$$\vec{\omega}_o^c = \begin{bmatrix} p - \dot{\phi} \\ q \\ r \end{bmatrix} \tag{2-48}$$

In outer gimbal coordinates $\vec{\omega}_o^o = [B_{co}]\vec{\omega}_o^c$

where

$$[B_{co}] = \begin{bmatrix} 1 & 0 & 0 \\ 0 & \cos\phi & -\sin\phi \\ 0 & \sin\phi & \cos\phi \end{bmatrix} \tag{2-49}$$

$$\vec{\omega}_o^o = \begin{bmatrix} \omega_{ox} \\ \omega_{oy} \\ \omega_{oz} \end{bmatrix} = \begin{bmatrix} p - \dot{\phi} \\ q\cos\phi - r\sin\phi \\ q\sin\phi + r\cos\phi \end{bmatrix} \tag{2-50}$$

Likewise, the inner gimbal rate $\vec{\omega}_I$ is equal to the vector sum of the outer gimbal rate $\vec{\omega}_o$ and the relative rate $\vec{\omega}_{Io}$ between the outer and inner gimbals

$$\vec{\omega}_I = \vec{\omega}_o + \vec{\omega}_{Io} \tag{2-51}$$

In outer gimbal coordinates

$$\vec{\omega}_I^o = \begin{bmatrix} p - \dot{\phi} \\ q \cos \phi - r \sin \phi \\ q \sin \phi + r \cos \phi \end{bmatrix} + \begin{bmatrix} 0 \\ 0 \\ \dot{\psi} \end{bmatrix} \tag{2-52}$$

Transforming to inner gimbal coordinates

$$\vec{\omega}_I^I = [B_{oI}]\vec{\omega}_I^o \tag{2-53}$$

where

$$[B_{oI}] = \begin{bmatrix} \cos \psi & -\sin \psi & 0 \\ \sin \psi & \cos \psi & 0 \\ 0 & 0 & 1 \end{bmatrix}$$

$$\vec{\omega}_I^I = \begin{bmatrix} \omega_{Ix} \\ \omega_{Iy} \\ \omega_{Iz} \end{bmatrix}$$

$$= \begin{bmatrix} (p + \dot{\phi}) \cos \psi - (q \cos \phi - r \sin \phi) \sin \psi \\ (p + \dot{\phi}) \sin \psi + (q \cos \phi - r \sin \phi) \cos \psi \\ q \sin \phi + r \cos \phi + \dot{\psi} \end{bmatrix} \tag{2-54}$$

The platform rate $\vec{\omega}_p$ is kinematically described by

$$\vec{\omega}_p = \vec{\omega}_I + \vec{\omega}_{pI} \tag{2-55}$$

In inner gimbal coordinates

$$\vec{\omega}_p^I = \begin{bmatrix} (p + \dot{\phi}) \cos \psi - (q \cos \phi - r \sin \phi) \sin \psi \\ (p + \dot{\phi}) \sin \psi + (q \cos \phi - r \sin \phi) \cos \psi \\ q \sin \phi + r \cos \phi + \dot{\psi} \end{bmatrix} + \begin{bmatrix} 0 \\ \dot{\theta} \\ 0 \end{bmatrix} \tag{2-56}$$

Transforming to platform coordinate

$$\vec{\omega}_p^p = [B_{Ip}]\vec{\omega}_p^I \tag{2-57}$$

$$[B_{Ip}] = \begin{bmatrix} \cos \theta & 0 & \sin \theta \\ o & 1 & o \\ -\sin \theta & 0 & \cos \theta \end{bmatrix} \tag{2-58}$$

$$\vec{\omega}_p^p = \begin{bmatrix} \omega_{px} \\ \omega_{py} \\ \omega_{pz} \end{bmatrix} \tag{2-59}$$

$$\vec{\omega}_p^p = \begin{bmatrix} [(p + \dot{\phi}) \cos \psi - (q \cos \phi - r \sin \phi) \sin \psi] \cos \theta \\ \quad + [q \sin \phi + r \cos \phi + \dot{\psi}] \sin \theta \\ (p + \dot{\phi}) \sin \psi + (q \cos \phi - r \sin \phi) \cos \psi + \dot{\theta} \\ -[(p + \dot{\phi}) \cos \psi - (q \cos \phi - r \sin \phi) \sin \psi] \sin \theta \\ \quad + [q \sin \phi + r \cos \phi + \dot{\psi}] \cos \theta \end{bmatrix} \tag{2-60}$$

<u>Angular Acceleration Relations Between Gimbals</u>. The generalized kinematic relations for the imperfect platform must also include the acceleration relationships because the platform can no longer be assumed to remain motionless.

To determine the angular acceleration of the members, assume that the inertial derivative of the case angular velocity equals that of vehicle

$$* \qquad {}^{i}\dot{\vec{\omega}}{}^{c}_{c} = {}^{i}\dot{\vec{\omega}}{}^{c}_{\text{vehicle}} = \begin{bmatrix} \dot{p} \\ \dot{q} \\ \dot{r} \end{bmatrix} \tag{2-61}$$

The derivative taken in the case reference system is

$${}^{c}\dot{\vec{\omega}}{}^{c}_{c} = {}^{i}\dot{\vec{\omega}}{}^{c}_{c} \tag{2-62}$$

The inertial angular acceleration of the outer gimbal is equal to the vector sum of the inertial angular acceleration of the case and the inertial relative angular acceleration between the case and outer gimbal. That is

$${}^{i}\dot{\vec{\omega}}_{o} = {}^{i}\dot{\vec{\omega}}_{c} + {}^{i}\dot{\vec{\omega}}_{oc} \tag{2-63}$$

Note that

$${}^{c}\dot{\vec{\omega}}_{o} = {}^{i}\dot{\vec{\omega}}_{o} \tag{2-64}$$

*Note: Notation Convention, Appendix C.

Expressed in case coordinates

$$ {}^{i}\dot{\vec{\omega}}_{o}^{c} = {}^{i}\dot{\vec{\omega}}_{c}^{c} + {}^{c}\dot{\vec{\omega}}_{co}^{c} + \vec{\omega}_{c}^{c} \times \vec{\omega}_{oc}^{c} \qquad (2\text{-}65) $$

In component form

$$ {}^{i}\dot{\vec{\omega}}_{o}^{c} = \begin{bmatrix} \dot{p} \\ \dot{q} \\ \dot{r} \end{bmatrix} + \begin{bmatrix} \ddot{\phi} \\ 0 \\ 0 \end{bmatrix} + \begin{bmatrix} \hat{e}_{cx} & \hat{e}_{cy} & \hat{e}_{cz} \\ p & q & r \\ \dot{\phi} & 0 & 0 \end{bmatrix} \qquad (2\text{-}66) $$

where $\hat{e}_{cx}$, $\hat{e}_{cy}$, and $\hat{e}_{cz}$ are unit vectors in the case coordinate system.

$$ {}^{i}\dot{\vec{\omega}}_{o}^{c} = \begin{bmatrix} \dot{p} + \ddot{\phi} \\ \dot{q} + r\dot{\phi} \\ \dot{r} - q\dot{\phi} \end{bmatrix} \qquad (2\text{-}67) $$

Transforming to outer gimbal coordinates

$$ {}^{i}\dot{\vec{\omega}}_{o}^{o} = [B_{co}]\, {}^{i}\dot{\vec{\omega}}_{o}^{c} \qquad (2\text{-}68) $$

$$ {}^{i}\dot{\vec{\omega}}_{o}^{o} = \begin{bmatrix} \dot{p} + \ddot{\phi} \\ (\dot{q} + r\dot{\phi}) \cos \phi - (\dot{r} - q\dot{\phi}) \sin \phi \\ (\dot{q} + r\dot{\phi}) \sin \phi + (\dot{r} - q\dot{\phi}) \cos \phi \end{bmatrix} $$

$$ (2\text{-}69) $$

Similarly

$$ {}^{i}\dot{\vec{\omega}}_{I} = {}^{i}\dot{\vec{\omega}}_{o} + {}^{i}\dot{\vec{\omega}}_{Io} \qquad (2\text{-}70) $$

$$ {}^{i}\dot{\vec{\omega}}_{I} = {}^{i}\dot{\vec{\omega}}_{o} + {}^{o}\dot{\vec{\omega}}_{Io} + \vec{\omega}_{o} \times \vec{\omega}_{Io} \qquad (2\text{-}71) $$

Expressing in outer gimbal coordinates

$$ {}^{i}\dot{\vec{\omega}}_{I}^{o} = \begin{bmatrix} \dot{p} + \ddot{\phi} \\ (\dot{q} + r\dot{\phi}) \cos \phi - (\dot{r} - q\dot{\phi}) \sin \phi \\ (\dot{q} + r\dot{\phi}) \sin \phi + (\dot{r} - q\dot{\phi}) \cos \phi \end{bmatrix} + \begin{bmatrix} 0 \\ 0 \\ \ddot{\psi} \end{bmatrix} + \begin{bmatrix} \hat{e}_{ox} & \hat{e}_{oy} & \hat{e}_{oz} \\ p + \dot{\phi} & q \cos \phi - r \sin \phi & r \cos \phi + q \sin \phi \\ 0 & 0 & \dot{\psi} \end{bmatrix} $$

(2-72)

where $\hat{e}_{ox}$, $\hat{e}_{oy}$, and $\hat{e}_{oz}$ are unit vectors in the outer gimbal coordinate system

$$ {}^{i}\dot{\vec{\omega}}_{I}^{o} = \begin{bmatrix} \dot{p} + \ddot{\phi} + (q \cos \phi - r \sin \phi)\dot{\psi} \\ (\dot{q} + r\dot{\phi}) \cos \phi - (\dot{r} - q\dot{\phi}) \sin \phi - (p + \dot{\phi})\dot{\psi} \\ (\dot{q} + r\dot{\phi}) \sin \phi + (\dot{r} - q\dot{\phi}) \cos \phi + \ddot{\psi} \end{bmatrix} $$

(2-73)

Transforming to inner gimbal coordinates

$$ {}^{i}\dot{\vec{\omega}}_{I}^{I} = [B_{oI}]\,{}^{i}\dot{\vec{\omega}}_{I}^{o} \tag{2-74} $$

$$ {}^{i}\dot{\vec{\omega}}_{I}^{I} = \begin{bmatrix} [\dot{p} + \ddot{\phi} + (q\cos\phi - r\sin\phi)\dot{\psi}]\cos\psi - [(\dot{q} + r\dot{\phi}) \\ \times \cos\phi - (\dot{r} - q\dot{\phi})\sin\phi - (p + \dot{\phi})\dot{\psi}]\sin\psi \\ \\ [\dot{p} + \ddot{\phi} + (q\cos\phi - r\sin\phi)\dot{\psi}]\sin\psi + [(\dot{q} + r\dot{\phi}) \\ \times \cos\phi - (\dot{r} - q\dot{\phi})\sin\phi - (p + \dot{\phi})\dot{\psi}]\cos\psi \\ \\ (\dot{q} + r\dot{\phi})\sin\phi + (\dot{r} - q\dot{\phi})\cos\phi + \ddot{\psi} \end{bmatrix} \tag{2-75} $$

For the platform

$$ {}^{i}\dot{\vec{\omega}}_{p} = {}^{i}\dot{\vec{\omega}}_{I} + {}^{i}\dot{\vec{\omega}}_{pI} \tag{2-76} $$

$$ {}^{i}\dot{\vec{\omega}}_{p} = {}^{i}\dot{\vec{\omega}}_{I} + {}^{I}\dot{\vec{\omega}}_{pI} + \vec{\omega}_{I} \times \vec{\omega}_{pI} \tag{2-77} $$

$$ {}^{i}\dot{\vec{\omega}}_{p}^{p} = [B_{Ip}]\,{}^{i}\dot{\vec{\omega}}_{p}^{I} \tag{2-78} $$

Evaluating ${}^{i}\dot{\vec{\omega}}_{p}$ in platform coordinates in the same manner as the previous members

$$
{}^{i}\dot{\vec{\omega}}_{p}^{p} = \begin{bmatrix}
\begin{aligned}
&\Big\{[\dot{p} + \ddot{\phi} + (q \cos \phi - r \sin \phi)\dot{\psi}] \cos \psi - [(\dot{q} + r\dot{\phi}) \\
&\quad \times \cos \phi - (\dot{r} - q\dot{\phi}) \sin \phi - (p + \dot{\phi})\dot{\psi}] \sin \psi \\
&\quad - (q \sin \phi + r \cos \phi + \dot{\psi})\dot{\theta}\Big\} \cos \theta \\
&\quad + \Big\{(\dot{q} + r\dot{\phi}) \sin \phi + (\dot{r} - q\dot{\phi}) \cos \phi + \ddot{\psi} \\
&\quad + [(p + \dot{\phi}) \cos \psi - (q \cos \phi - r \sin \phi) \\
&\quad \times \sin \psi]\dot{\theta}\Big\} \sin \theta
\end{aligned} \\[2ex]
\begin{aligned}
&\Big\{\dot{p} + \ddot{\phi} + (q \cos \phi - r \sin \phi)\dot{\psi}\Big\} \sin \psi + [(\dot{q} + r\dot{\phi}) \\
&\quad \times \cos \phi - (\dot{r} - q\dot{\phi}) \sin \phi - (p + \dot{\phi})\dot{\psi}] \cos \psi + \ddot{\theta}
\end{aligned} \\[2ex]
\begin{aligned}
&-\Big\{[\dot{p} + \ddot{\phi} + (q \cos \phi - r \sin \phi)\dot{\psi}] \cos \psi - [(\dot{q} + r\dot{\phi}) \\
&\quad \times \cos \phi - (\dot{r} - q\dot{\phi}) \sin \phi - (p + \dot{\phi})\dot{\psi}] \sin \psi \\
&\quad - (q \sin \phi + r \cos \phi + \dot{\psi})\dot{\theta}\Big\} \sin \theta \\
&\quad + \Big\{(\dot{q} + r\dot{\phi}) \sin \phi + (\dot{r} - q\dot{\phi}) \cos \phi + \ddot{\psi} \\
&\quad + [(p + \dot{\phi}) \cos \psi - (q \cos \phi - r \sin \phi) \\
&\quad \times \sin \psi]\dot{\theta}\Big\} \cos \theta
\end{aligned}
\end{bmatrix} \tag{2-79}
$$

Gyro Kinematic Relationships. The system gyros are orthogonally mounted on the innermost member (platform) of the system. If there is no misalignment of the case, the gyro float is related to the platform by the float angle α . The platform-to-gyro (float) transformation Equations 2-6, 2-7, and 2-8 are used to develop the kinematic relationships of the three individual gyros and the platform.

The angular velocity relationship of the gyros to the platform is

$$\vec{\omega}_{g}^{g} = [B_{pg}]\vec{\omega}_{p}^{p} + \vec{\omega}_{gp}^{g} \tag{2-80}$$

For the X-gyro

$$\vec{\omega}^{gx}_{gx} = [B_{pgx}]\vec{\omega}^{p}_{p} + \vec{\omega}^{gx}_{gxp} \tag{2-81}$$

Expanding in X-gyro coordinates

$$\vec{\omega}^{gx}_{gx} = \begin{bmatrix} \omega_{gxS} \\ \omega_{gxI} \\ \omega_{gxO} \end{bmatrix} = \begin{bmatrix} \sin\alpha_x & -\cos\alpha_x & 0 \\ \cos\alpha_x & \sin\alpha_x & 0 \\ 0 & 0 & 1 \end{bmatrix} \begin{bmatrix} \omega_{px} \\ \omega_{py} \\ \omega_{pz} \end{bmatrix} + \begin{bmatrix} 0 \\ 0 \\ \dot{\alpha}_x \end{bmatrix} \tag{2-82}$$

$$\vec{\omega}^{gx}_{gx} = \begin{bmatrix} \omega_{gxS} \\ \omega_{gxI} \\ \omega_{gxO} \end{bmatrix} = \begin{bmatrix} \omega_{px}\sin\alpha_x - \omega_{py}\cos\alpha_x \\ \omega_{px}\cos\alpha_x + \omega_{py}\sin\alpha_x \\ \omega_{pz} + \dot{\alpha}_x \end{bmatrix} \tag{2-83}$$

If α_x, the X-gyro float angle is a small angle, then

$$\vec{\omega}^{gx}_{gx} = \begin{bmatrix} \omega_{gxS} \\ \omega_{gxI} \\ \omega_{gxO} \end{bmatrix} = \begin{bmatrix} -\omega_{py} \\ \omega_{px} \\ \omega_{pz} + \dot{\alpha}_x \end{bmatrix} \tag{2-84}$$

Similarly, for the Y- and Z-gyros

$$\vec{\omega}^{gy}_{gy} = [B_{pgy}]\vec{\omega}^{p}_{p} + \vec{\omega}^{gy}_{gyp} \tag{2-85}$$

and

$$\vec{\omega}^{gz}_{gz} = [B_{pgz}]\vec{\omega}^{p}_{p} + \vec{\omega}^{gz}_{gzp} \tag{2-86}$$

Expanding in the respective gyro coordinates and assuming α_y and α_z are small angles, we compute

$$\vec{\omega}^{gy}_{gy} = \begin{bmatrix} \omega_{gyS} \\ \omega_{gyI} \\ \omega_{gyO} \end{bmatrix} = \begin{bmatrix} -\omega_{pz} \\ \omega_{py} \\ \omega_{px} + \dot{\alpha}_y \end{bmatrix} \tag{2-87}$$

and

$$\vec{\omega}^{gz}_{gz} = \begin{bmatrix} \omega_{gzS} \\ \omega_{gzI} \\ \omega_{gzO} \end{bmatrix} = \begin{bmatrix} -\omega_{py} \\ -\omega_{pz} \\ \omega_{px} + \dot{\alpha}_z \end{bmatrix} \tag{2-88}$$

The angular acceleration of the gyros with respect to the platform is described by

$$^{i}\dot{\vec{\omega}}^{p}_{g} = {}^{i}\dot{\vec{\omega}}^{p}_{p} + {}^{p}\dot{\vec{\omega}}^{p}_{gp} + \vec{\omega}^{p}_{p} \times \vec{\omega}^{p}_{gp} \tag{2-89}$$

Specifically, for the X-gyro

$$^{i}\dot{\vec{\omega}}^{p}_{gx} = {}^{i}\dot{\vec{\omega}}^{p}_{p} + {}^{p}\dot{\vec{\omega}}^{p}_{gxp} + \vec{\omega}^{p}_{p} \times \vec{\omega}^{p}_{gxp} \tag{2-90}$$

$$ {}^{i}\dot{\vec{\omega}}^{p}_{gx} = \begin{bmatrix} \dot{\omega}_{px} \\ \dot{\omega}_{py} \\ \dot{\omega}_{pz} \end{bmatrix} + \begin{bmatrix} 0 \\ 0 \\ \ddot{\alpha} \end{bmatrix} + \begin{bmatrix} \hat{e}_{px} & \hat{e}_{py} & \hat{e}_{pz} \\ \omega_{px} & \omega_{py} & \omega_{pz} \\ 0 & 0 & \dot{\alpha}_x \end{bmatrix} \tag{2-91} $$

where $\hat{e}_{px}$, $\hat{e}_{py}$, and $\hat{e}_{pz}$ are unit vectors aligned with the respective platform axes.

Therefore

$$ {}^{i}\dot{\vec{\omega}}^{p}_{gx} = \begin{bmatrix} \dot{\omega}_{px} + \dot{\alpha}_x \omega_{py} \\ \dot{\omega}_{py} - \dot{\alpha}_x \omega_{px} \\ \dot{\omega}_{pz} + \ddot{\alpha}_x \end{bmatrix} \tag{2-92} $$

Transforming to X-gyro coordinates, we compute

$$ {}^{i}\dot{\vec{\omega}}^{gx}_{px} = [B_{pgx}] \left[{}^{i}\dot{\vec{\omega}}^{p}_{gx} \right] \tag{2-93} $$

$$ {}^{i}\dot{\vec{\omega}}^{gx}_{gx} = \begin{bmatrix} \sin\alpha_x & -\cos\alpha_x & 0 \\ \cos\alpha_x & \sin\alpha_x & 0 \\ 0 & 0 & 1 \end{bmatrix} \begin{bmatrix} \dot{\omega}_{px} + \dot{\alpha}_x \omega_{py} \\ \dot{\omega}_{py} - \dot{\alpha}_x \omega_{px} \\ \dot{\omega}_{pz} + \ddot{\alpha}_x \end{bmatrix} \tag{2-94} $$

Assuming α_x is very small

$$\vec{\dot{\omega}}^{gx}_{gx} {}^{i} = \begin{bmatrix} -\dot{\omega}_{py} + \dot{\alpha}_x \omega_{px} \\ \dot{\omega}_{px} + \dot{\alpha}_x \omega_{py} \\ \dot{\omega}_{pz} + \ddot{\alpha}_x \end{bmatrix} \tag{2-95}$$

Expanding in state variables

$$\vec{\dot{\omega}}^{gx}_{gx} {}^{i} = \begin{bmatrix} \ddot{\phi} \sin\psi + \ddot{\theta} + \dot{\alpha}_x W_{px} - \dot{W}_{py} \\ -\ddot{\phi} \cos\theta \cos\psi - \ddot{\psi} \sin\theta + \dot{\alpha}_x W_{py} + \dot{W}_{px} \\ \ddot{\phi} \sin\theta \cos\psi - \ddot{\psi} \cos\theta + \ddot{\alpha}_x + \dot{W}_{pz} \end{bmatrix}$$

(2-96)

The vector equations for the Y and Z gyro are

$$ {}^{i}\vec{\dot{\omega}}^{p}_{gy} = {}^{i}\vec{\dot{\omega}}^{p}_{p} + {}^{p}\vec{\dot{\omega}}^{p}_{gyp} + \vec{\omega}^{p}_{p} \times \vec{\omega}_{gyp} \tag{2-97}$$

$$ {}^{i}\vec{\dot{\omega}}^{p}_{gz} = {}^{i}\vec{\dot{\omega}}^{p}_{p} + {}^{p}\vec{\dot{\omega}}^{p}_{gzp} + \vec{\omega}^{p}_{p} \times \vec{\omega}_{gzp} \tag{2-98}$$

Evaluating and transforming to Y- and Z-gyro coordinates, respectively, and assuming small α_y and α_z angles

$$ {}^{i}\vec{\dot{\omega}}^{gy}_{gy} = \begin{bmatrix} -\dot{\omega}_{pz} + \dot{\alpha}_y \omega_{py} \\ \dot{\omega}_{py} + \dot{\alpha}_y \omega_{pz} \\ \dot{\omega}_{px} + \ddot{\alpha}_y \end{bmatrix} \tag{2-99}$$

$$
{}^{i}\vec{\dot{\omega}}_{gz}^{gz} = \begin{bmatrix} -\dot{\omega}_{py} - \dot{\alpha}_z \omega_{pz} \\ -\dot{\omega}_{pz} + \dot{\alpha}_z \omega_{py} \\ \dot{\omega}_{px} + \ddot{\alpha}_z \end{bmatrix} \tag{2-100}
$$

Expanding in state variables

$$
{}^{i}\vec{\dot{\omega}}_{gy}^{gy} = \begin{bmatrix} -\ddot{\phi} \sin\theta \cos\psi + \ddot{\psi} \cos\theta - \dot{W}_{pz} + \dot{\alpha}_y W_{py} \\ -\ddot{\phi} \sin\psi - \ddot{\theta} + \dot{W}_{py} + \dot{\alpha}_y W_{pz} \\ -\ddot{\phi} \cos\theta \cos\psi - \ddot{\psi} \sin\theta + \ddot{\alpha}_y + \dot{W}_{px} \end{bmatrix} \tag{2-101}
$$

and

$$
{}^{i}\vec{\dot{\omega}}_{gz}^{gz} = \begin{bmatrix} \ddot{\phi} \sin\psi + \ddot{\theta} - \dot{W}_{py} - \dot{\alpha}_z W_{pz} \\ -\ddot{\phi} \sin\theta \cos\psi + \ddot{\psi} \cos\theta - \dot{W}_{pz} + \dot{\alpha}_z W_{py} \\ -\ddot{\phi} \cos\theta \cos\psi - \ddot{\psi} \sin\theta + \ddot{\alpha}_z + \dot{W}_{px} \end{bmatrix} \tag{2-102}
$$

<u>Coefficients</u>.

Outer gimbal kinematic coefficients

$$
\begin{aligned}
W_{ox} &= p - \dot{\phi} \\
W_{oy} &= q \cos\phi - r \sin\phi \\
W_{oz} &= q \sin\phi + r \cos\phi
\end{aligned} \tag{2-103}
$$

$$\dot{W}_{ox} = \dot{p}$$

$$\dot{W}_{oy} = \dot{q} \cos \phi - \dot{r} \sin \phi - \dot{\phi} W_{oz} \qquad (2\text{-}103)$$

$$\dot{W}_{oz} = \dot{q} \sin \phi + \dot{r} \cos \phi + \dot{\phi} W_{oy}$$

Inner gimbal kinematic coefficients

$$W_{Ix} = W_{ox} \cos \psi - W_{oy} \sin \psi$$

$$W_{Iy} = W_{ox} \sin \psi + W_{oy} \cos \psi$$

$$W_{Iz} = W_{oz} - \dot{\psi}$$

$$(2\text{-}104)$$

$$\dot{W}_{Ix} = \dot{p} \cos \psi - \dot{W}_{oy} \sin \psi - W_{Iy} \dot{\psi}$$

$$\dot{W}_{Iy} = \dot{p} \sin \psi + \dot{W}_{oy} \cos \psi + W_{Ix} \dot{\psi}$$

$$\dot{W}_{Iz} = \dot{W}_{oz}$$

Platform kinematic coefficients

$$W_{px} = W_{Ix} \cos \theta + W_{Iz} \sin \theta$$

$$W_{py} = W_{Iy} - \dot{\theta} \qquad (2\text{-}105)$$

$$W_{pz} = -W_{Ix} \sin \theta + W_{Iz} \cos \theta$$

$$\dot{W}_{px} = \dot{\theta}W_{pz} + \dot{W}_{Ix} \cos \theta + \dot{W}_{Iz} \sin \theta$$

$$\dot{W}_{py} = \dot{W}_{Iy} \tag{2-105}$$

$$\dot{W}_{pz} = -\dot{\theta}W_{px} - \dot{W}_{Ix} \sin \theta + \dot{W}_{Iz} \cos \theta$$

where p, q, r, $\dot{p}$, $\dot{q}$, and $\dot{r}$ are the known rates and respective case accelerations.

CHAPTER III

SYSTEM DYNAMICAL EQUATIONS

Each member of the system is treated as a rigid body, and the torque equation 3-1 is developed.

$$\vec{M} = {}^{i}\dot{\vec{H}} \tag{3-1}$$

The net torque $\vec{M}$ consists of driving torque applied by the adjacent outer member and reaction torque applied by the adjacent inner member.

The equations are presented in the coordinate system of the member under consideration. The adjacent members may be noted from Figure 3, the topological diagram.

The system consists of seven rigid bodies (X-gyro, Y-gyro, Z-gyro, platform, inner and outer gimbals, and case), each with one degree of freedom respective to its adjacent bodies.

The dynamical equations of the system are developed starting with the gyros and working progressively out to the case.

I. ROTATIONAL DYNAMIC EQUATIONS

The rigid-body rotational equation of motion is

$$\vec{M} = {}^{i}\dot{\vec{H}} \tag{3-2}$$

where

$$^{i}\dot{\vec{H}} = \frac{d\vec{H}}{dt} \tag{3-3}$$

$$^{i}\dot{\vec{H}} = {}^{m}\dot{\vec{H}} + \vec{\omega}_{m} \times \vec{H} \tag{3-4}$$

$^{i}\dot{\vec{H}}$ — inertial derivative of the vector $\vec{H}$.

$^{m}\dot{\vec{H}}$ — derivative of H calculated in a rotating frame of reference.

$\vec{\omega}_{m}$ — absolute rotational rate of the moving reference frame.

$\vec{H}$ — inertial angular momentum.

$\vec{M}$ — external torque applied to the body.

The equations of motion for three of the system members and the three integrating gyros are developed based on the preceding definitions. The results are a set of second-order differential equations for the gimbals and the three gyros.

Each member is treated as a rigid body, and three equations are written for the coordinates of the external torque $\vec{M}$.

The moment coordinate denoted by M^* is on the free or dynamic axis (represented by the dashed line in Figure 3) of the member under consideration, and the other two coordinates are constraints. The constraints represent the reaction torques in the locked axis of the hinge; the free axis torque represents the single degree of freedom between two adjacent members of the system. The terms in the equations represented by W and $\dot{W}$ are lumped parameters, e.g., W_{px} and $\dot{W}_{px}$.

II. GYRO EQUATIONS OF MOTION

The generalized angular momentum of a gyro may be expressed in vector form

$$\vec{H}_g = [I_g]\vec{\omega}_g + \vec{H}_\omega \tag{3-5}$$

assuming a massless case.

$\vec{H}_g$ — total angular momentum of the gyro float.
$[I_g]$ — inertia tensor of the gyro float.
$\vec{\omega}_g$ — absolute angular velocity of the gyro float.
$\vec{H}_\omega$ — wheel angular momentum.

The first derivative of $\vec{H}_g$ viewed from an inertial reference is

$${}^{i}\dot{\vec{H}}_g = {}^{g}\dot{\vec{H}}_g + \vec{\omega}_g \times \vec{H}_g \tag{3-6}$$

For an inertial derivative of $\vec{H}_g$

$$\vec{M}_g = {}^{i}\dot{\vec{H}}_g \tag{3-7}$$

<u>X-gyro Equations of Motion</u>. Expanding equation 3-7 for the X-gyro in S (spin axis), I (input axis), and O (output axis) coordinates

$$\vec{M}_{gx} = {}^{i}\dot{\vec{H}}_{gx} \tag{3-8}$$

$$M_{gxS} = I_{gxS}\,{}^{gx}\dot{\omega}_{gxS} + (I_{gxO} - I_{gxI})\,\omega_{gxO}\omega_{gxI} \tag{3-9}$$

$$M_{gxI} = I_{gxI}\,{}^{gy}\dot{\omega}_{gxI} + H_{\omega x}\omega_{gxO} + (I_{gxS} - I_{gxO})\,\omega_{gxO}\omega_{gxS} \tag{3-10}$$

$$M^{*}_{gxO} = I_{gxO}\,{}^{gx}\dot{\omega}_{gxO} - H_{\omega x}\omega_{gxI} + (I_{gxI} - I_{gxS})\,\omega_{gxI}\omega_{gxS} \tag{3-11}$$

The equation of motion for the dynamic axis gxO may be written in terms of state variables by substituting $-D_{gxO}\dot{\alpha}_x = M^{*}_{gxO}$, viscous float damping, and substituting the output axis component of Equation 2-96 for ${}^{gx}\dot{\omega}_{gxO}$.

$$-D_{gxO}\dot{\alpha}_x = I_{gxO}(\ddot{\phi}\sin\theta\cos\psi - \ddot{\psi}\cos\theta + \ddot{\alpha}_x + \dot{W}_{pz}) - H_{\omega x}W_{gxI} + (I_{gxI} - I_{gxS})W_{gxI}W_{gxS} \tag{3-12}$$

Arranging the highest derivative of the state variables on the left side

$$\ddot{\phi} \sin\theta \cos\psi - \ddot{\psi} \cos\theta + \ddot{\alpha}_x = \frac{H_{\omega x}}{I_{gxO}} W_{gxI} - \frac{(I_{gxI} - I_{gxS})}{I_{gxO}} W_{gxI} W_{gxS} - \frac{D_{gxO}\dot{\alpha}_x}{I_{gxO}} - \dot{W}_{pz} \tag{3-13}$$

The moments $-M_{gxS}$, $-M_{gxI}$, and $-M^*_{gxO}$ are transformed to platform coordinates and included in the platform equations of motion as reaction torques.

<u>Y- and Z-Gyro Equations of Motion</u>. The Y- and Z-gyro rotational equations are similarly developed in Y- and Z-gyro coordinates, respectively.

Y-gyro:

$$M_{gyS} = I_{gyS}\,{}^{gy}\dot{\omega}_{gyS} + (I_{gyO} - I_{gyI})\,\omega_{gyO}\omega_{gyI} \tag{3-14}$$

$$M_{gyI} = I_{gyI}\,{}^{gy}\dot{\omega}_{gyI} + H_{\omega y}\omega_{gyO} + (I_{gyS} - I_{gyO})\,\omega_{gyO}\omega_{gyS} \tag{3-15}$$

$$M^*_{gyO} = I_{gyO}\,{}^{gy}\dot{\omega}_{gyO} - H_{\omega y}\omega_{gyI} + (I_{gyI} - I_{gyS})\,\omega_{gyI}\omega_{gyS} \tag{3-16}$$

Z-gyro:

$$M_{gzS} = I_{gzS}\,{}^{gz}\dot{\omega}_{gzS} + (I_{gzO} - I_{gzI})\omega_{gzO}\omega_{gzI} \tag{3-17}$$

$$M_{gzI} = I_{gzI}\,{}^{gz}\dot{\omega}_{gzI} + H_{\omega z}\omega_{gzO} + (I_{gzS} - I_{gzO})\omega_{gzS}\omega_{gzO} \tag{3-18}$$

$$M^*_{gzO} = I_{gzO}\,{}^{gz}\dot{\omega}_{gzO} - H_{\omega z}\omega_{gzI} + (I_{gzI} - I_{gzS})\omega_{gzI}\omega_{gzS} \tag{3-19}$$

The equations for the dynamic axes may be expanded in terms of the state variable by substituting

$$\begin{aligned} M^*_{gyO} &= -D_{gyO}\dot{\alpha}_y \\ M^*_{gzO} &= -D_{gzO}\dot{\alpha}_z \end{aligned} \tag{3-20}$$

and substituting the output axis components of Equations 2-101 and 2-102 for ${}^{gy}\dot{\omega}_{gyO}$ and ${}^{gz}\dot{\omega}_{gzO}$, respectively.

$$\begin{aligned} -\ddot{\phi}\cos\theta\cos\psi - \ddot{\psi}\sin\theta + \ddot{\alpha}_y &= \frac{H_{\omega y}}{I_{gyO}} W_{gyI} \\ &\quad - \frac{(I_{gyI} - I_{gyS})}{I_{gyO}} W_{gyI}W_{gyS} - \frac{D_{gyO}\dot{\alpha}_y}{I_{gyO}} - \dot{W}_{px} \end{aligned} \tag{3-21}$$

$$-\ddot{\phi} \cos\theta \cos\psi - \ddot{\psi} \sin\theta + \ddot{\alpha}_z = \frac{H_{\omega z}}{I_{gzO}} W_{gzI}$$

$$- \frac{(I_{gzI} - I_{gzS})}{I_{gzO}} W_{gzS} W_{gzI} - \frac{D_{gzO} \dot{\alpha}_z}{I_{gzO}} - \dot{W}_{px} \tag{3-22}$$

III. GYRO OUTPUT AXIS EQUATIONS

The three dynamic gyro equations (3-13, 3-21, and 3-22) may be expressed as second-order differential equations in terms of the state variables

$$G_{x\phi} \ddot{\Phi} + G_{x\psi} \ddot{\Psi} + \ddot{\alpha}_x = LGX \tag{3-23}$$

$$G_{y\phi} \ddot{\Phi} + G_{y\psi} \ddot{\Psi} + \ddot{\alpha}_y = LGY \tag{3-24}$$

$$G_{z\phi} \ddot{\Phi} + G_{z\psi} \ddot{\Psi} + \ddot{\alpha}_z = LGZ \tag{3-25}$$

where

$$\begin{aligned}
G_{x\phi} &= \sin\theta \cos\psi \\
G_{x\psi} &= -\cos\theta \\
G_{y\phi} &= -\cos\theta \cos\psi \\
G_{y\psi} &= -\sin\theta \\
G_{z\phi} &= -\cos\theta \cos\psi \\
G_{z\psi} &= -\sin\theta
\end{aligned} \tag{3-26}$$

$$LGX = \frac{H_{\omega x}}{I_{gxO}} W_{gxI} - \frac{(I_{gxI} - I_{gxS})}{I_{gxO}} W_{gxI} W_{gxS} - \frac{D_{gxO}\dot{\alpha}_x}{I_{gxO}} - \dot{W}_{pz} \tag{3-27}$$

$$LGY = \frac{H_{\omega y}}{I_{gyO}} W_{gyI} - \frac{(I_{gyI} - I_{gyS})}{I_{gyO}} W_{gyI} W_{gyS} - \frac{D_{gyO}\dot{\alpha}_y}{I_{gyO}} - \dot{W}_{px} \tag{3-28}$$

$$LGZ = \frac{H_{\omega z}}{I_{gzO}} W_{gzI} - \frac{(I_{gzI} - I_{gzS})}{I_{gzO}} W_{gzS} W_{gzI} - \frac{D_{gzO}\dot{\alpha}_z}{I_{gzO}} - \dot{W}_{px} \tag{3-29}$$

Gyro Rate Coefficients.

$$\begin{aligned} W_{gxS} &= -W_{py} \\ W_{gxI} &= W_{px} \\ W_{gxO} &= W_{pz} + \dot{\alpha}_x \end{aligned} \tag{3-30}$$

$$\begin{aligned} W_{gyS} &= -W_{pz} \\ W_{gyI} &= W_{py} \\ W_{gyO} &= W_{px} + \dot{\alpha}_y \end{aligned} \tag{3-31}$$

$$W_{gzS} = -W_{py}$$

$$W_{gzI} = -W_{pz} \tag{3-32}$$

$$W_{gzO} = W_{px} + \dot{\alpha}_z$$

$\vec{W}_o$, $\dot{\vec{W}}_o$, $\vec{W}_I$, $\dot{\vec{W}}_I$, $\vec{W}_p$, and $\dot{\vec{W}}_p$ are defined in equation groups 2-104, 2-105, and 2-106.

<u>Gyro Reaction Torques</u>. The reaction moment of the gyros on the platform is expressed by transforming the negative of the gyro moments to platform coordinates.

Gyro-to-Platform Reaction Moment:

$$\vec{M}_{gp} = \begin{bmatrix} M_{gpx} \\ M_{gpy} \\ M_{gpz} \end{bmatrix} \tag{3-33}$$

Evaluating for X-, Y-, and Z-gyros

$$\begin{bmatrix} M_{gpx} \\ M_{gpy} \\ M_{gpz} \end{bmatrix} = -[B_{gxp}] \begin{bmatrix} M_{gxS} \\ M_{gxI} \\ M^*_{gxO} \end{bmatrix} - [B_{gyp}] \begin{bmatrix} M_{gyS} \\ M_{gyI} \\ M^*_{gyO} \end{bmatrix} - [B_{gzp}] \begin{bmatrix} M_{gzS} \\ M_{gzI} \\ M^*_{gzO} \end{bmatrix}$$

(3-34)

where

$$[B_{gxp}] = \begin{bmatrix} \sin\alpha_x & \cos\alpha_x & 0 \\ -\cos\alpha_x & \sin\alpha_x & 0 \\ 0 & 0 & 1 \end{bmatrix} \qquad (3\text{-}35)$$

$$[B_{gyp}] = \begin{bmatrix} 0 & 0 & 1 \\ \sin\alpha_y & \cos\alpha_y & 0 \\ -\cos\alpha_y & \sin\alpha_y & 0 \end{bmatrix} \qquad (3\text{-}36)$$

$$[B_{gzp}] = \begin{bmatrix} 0 & 0 & 1 \\ -\cos\alpha_z & \sin\alpha_z & 0 \\ -\sin\alpha_z & -\cos\alpha_z & 0 \end{bmatrix} \qquad (3\text{-}37)$$

Assuming that α_x, α_y, and α_z are small

$$[B_{gxp}] = \begin{bmatrix} 0 & 1 & 0 \\ -1 & 0 & 0 \\ 0 & 0 & 1 \end{bmatrix} \qquad (3\text{-}38)$$

$$[B_{gyp}] = \begin{bmatrix} 0 & 0 & 1 \\ 0 & 1 & 0 \\ -1 & 0 & 0 \end{bmatrix} \qquad (3\text{-}39)$$

$$[B_{gzp}] = \begin{bmatrix} 0 & 0 & 1 \\ -1 & 0 & 0 \\ 0 & -1 & 0 \end{bmatrix} \tag{3-40}$$

The gyro reaction moment in platform coordinates

$$\vec{M}^{p}_{gp} = \begin{bmatrix} -M_{gxI} \\ M_{gxS} \\ -M^{*}_{gxO} \end{bmatrix} + \begin{bmatrix} -M^{*}_{gyO} \\ -M_{gyI} \\ M_{gyS} \end{bmatrix} + \begin{bmatrix} -M^{*}_{gzO} \\ M_{gzS} \\ M_{gzI} \end{bmatrix} \tag{3-41}$$

$$\vec{M}^{p}_{gp} = \begin{bmatrix} -(M_{gxI} + M^{*}_{gyO} + M^{*}_{gzO}) \\ (M_{gxS} - M_{gyI} + M_{gzS}) \\ -(M^{*}_{gxO} - M_{gyS} - M_{gzI}) \end{bmatrix} \tag{3-42}$$

Expanding in state variables

$$\begin{aligned} M^{p}_{gpx} = {} & I_{gxI}\ddot{\phi} \cos\theta \cos\psi + I_{gxI}\ddot{\psi} \sin\theta - I_{gxI}\dot{\alpha}_x W_{py} \\ & - I_{gxI}\dot{W}_{px} - H_{\omega x} W_{gxO} - (I_{gxS} - I_{gxO}) W_{gxO} W_{gxS} \\ & + D_{gyO}\dot{\alpha}_y + D_{gzO}\dot{\alpha}_z \end{aligned} \tag{3-43}$$

Substituting

$$\begin{aligned} MGX = {} & -I_{gxI}(\dot{\alpha}_x W_{py} + \dot{W}_{px}) - H_{\omega x} W_{gxO} \\ & - (I_{gxS} - I_{gxO}) W_{gxO} W_{gxS} + D_{gyO}\dot{\alpha}_y + D_{gzO}\dot{\alpha}_z \end{aligned} \tag{3-44}$$

Results in

$$M^p_{gpx} = I_{gxI}\ddot{\phi} \cos \theta \cos \psi + I_{gxI}\ddot{\psi} \sin \theta + MGX \tag{3-45}$$

Similarly

$$M^p_{gpy} = \ddot{\phi} \sin \psi (I_{gxS} + I_{gyI} + I_{gzS}) + \ddot{\theta}(I_{gxS} + I_{gyI} + I_{gzS}) + MGY \tag{3-46}$$

where

$$\begin{aligned} MGY = {} & I_{gxS}\dot{\alpha}_x W_{px} - I_{gyI}\dot{\alpha}_y W_{pz} - I_{gzS}\dot{\alpha}_z W_{pz} - \dot{W}_{py}(I_{gxS} + I_{gyI} \\ & + I_{gzS}) + (I_{gxO} - I_{gxI})W_{gxO}W_{gxI} \\ & - (I_{gyS} - I_{gyO})W_{gyO}W_{gyS} + (I_{gzO} - I_{gzI})W_{gzO}W_{gzI} \\ & - H_{\omega y}W_{gyO} - H_{\omega x}W_{gxO}\alpha_x - H_{\omega z}W_{gzO}\alpha_z \end{aligned} \tag{3-47}$$

and

$$M^p_{gpz} = -\ddot{\phi} \sin \theta \cos \psi (I_{gyS} + I_{gzI}) + \ddot{\psi} \cos \theta (I_{gyS} + I_{gzI}) + MGZ \tag{3-48}$$

where

$$MGZ = -\dot{W}_{pz}(I_{gyS} + I_{gzI}) + I_{gyS}\dot{\alpha}_y W_{py} + I_{gzI}\dot{\alpha}_z W_{py} + (I_{gyO} - I_{gyI})W_{gyO}W_{gyI} + (I_{gzS} - I_{gzO})W_{gzO}W_{gzS} + D_{gxO}\dot{\alpha}_x + H_{\omega z}W_{gzO} - H_{\omega y}W_{gyO}\alpha_y \qquad (3\text{-}49)$$

IV. DYNAMIC EQUATION OF GIMBALED MEMBERS

Platform Equations of Motion.

$$\vec{M}_p = {}^i\dot{\vec{H}}_p \qquad (3\text{-}50)$$

$${}^i\dot{\vec{H}}_p = {}^p\dot{\vec{H}}_p + \vec{\omega}_p \times \vec{H}_p \qquad (3\text{-}51)$$

Expanding in platform coordinates

$$M_{Ipx} = I_{px}{}^p\dot{\omega}_{px} + (I_{pz} - I_{py})\omega_{pz}\omega_{py} - M_{gpx} \qquad (3\text{-}52)$$

$$M^*_{Ipy} = I_{py}{}^p\dot{\omega}_{py} + (I_{px} - I_{pz})\omega_{pz}\omega_{px} - M_{gpy} \qquad (3\text{-}53)$$

$$M_{Ipz} = I_{pz}{}^p\dot{\omega}_{pz} + (I_{py} - I_{px})\omega_{px}\omega_{py} - M_{gpz} \qquad (3\text{-}54)$$

M_{Ipx}, M^*_{Ipy}, and M_{Ipz} are the coordinates of the driving torque applied by the inner gimbal on the platform axes (X_p, Y_p, Z_p) in platform coordinates. The respective gyro reaction torque coordinates are M_{gpx}, M_{gpy}, and M_{gpz}, previously defined in Equations 3-45, 3-46, and 3-48.

Expanding in terms of the state variables, the locked-axes (X_p and Z_p) equations are

$$M_{Ipx} = -\ddot{\phi} \cos\theta \cos\psi (I_{px} + I_{gxI}) - \ddot{\psi} \sin\theta (I_{px} + I_{gxI}) + MPX \tag{3-55}$$

where

$$MPX = I_{px}\dot{W}_{px} + (I_{pz} - I_{py})W_{pz}W_{py} + MGX \tag{3-56}$$

MGX is defined in Equation 3-44, and

$$M_{Ipz} = \ddot{\phi} \sin\theta \cos\psi (I_{pz} + I_{gyS} + I_{gzI}) - \ddot{\psi} \cos\theta (I_{pz} + I_{gyS} + I_{gzI}) + MPZ \tag{3-57}$$

where $$MPZ = I_{pz}\dot{W}_{pz} + (I_{py} - I_{px})W_{px}W_{py} - MGZ \tag{3-58}$$

MGZ is defined in Equation 3-49. The dynamic Y-axis (Y_p) of the platform is expanded to form the fourth state variable differential equation

$$-\ddot{\phi} \sin \psi \left(\frac{(I_{gxS} + I_{gyI} + I_{gzS})}{I_{py}} + 1 \right)$$

$$- \ddot{\theta} \left(\frac{(I_{gxS} + I_{gyI} + I_{gzS})}{I_{py}} + 1 \right) = MPY \qquad (3\text{-}59)$$

where

$$MPY = \frac{M^*_{Ipy}}{I_{py}} + \frac{MGY}{I_{py}} - \dot{W}_{py} \qquad (3\text{-}60)$$

MGY is defined in Equation 3-47, and

$$M^*_{Ipy} = D_{Ip}\dot{\theta} + F_{Ip}(SGN\dot{\theta}) - T_{II} \qquad (3\text{-}61)$$

D_{Ip} — viscous friction between the inner gimbal and the platform.

$F_{Ip}(SGN\dot{\theta})$ — function representing Coulomb friction and striction.

T_{II} — motor torque, inner axis.

Inner Gimbal Equations of Motion. The inner gimbal rotational equations of motion are

$$\vec{M}_I = {}^i\dot{\vec{H}}_I \qquad (3\text{-}62)$$

$$ {}^{i}\dot{\vec{H}}_{I} = {}^{I}\dot{\vec{H}}_{I} + \vec{\omega}_{I} \times \vec{H}_{I} \tag{3-63}$$

Expanding in inner gimbal coordinates

$$M_{oIx} = I_{Ix}\,{}^{I}\dot{\omega}_{Ix} + (I_{Iz} - I_{Iy})\omega_{Iz}\omega_{Iy} - M_{pIx} \tag{3-64}$$

$$M_{oIy} = I_{Iy}\,{}^{I}\dot{\omega}_{Iy} + (I_{Ix} - I_{Iz})\omega_{Ix}\omega_{Iz} - M_{pIy} \tag{3-65}$$

$$M^{*}_{oIz} = I_{Iz}\,{}^{I}\dot{\omega}_{Iz} + (I_{Iy} - I_{Ix})\omega_{Ix}\omega_{Iy} - M_{pIz} \tag{3-66}$$

The driving torque applied to the inner gimbal by the outer gimbal is $\vec{M}_{oI}$.

$$\vec{M}^{I}_{oI} = \begin{bmatrix} M_{oIx} \\ M_{oIy} \\ M^{*}_{oIz} \end{bmatrix} \tag{3-67}$$

$\vec{M}_{pI}$ is the reaction torque of the platform on the inner gimbal; $\vec{M}_{pI} = -\vec{M}_{Ip}$ where $\vec{M}_{Ip}$ was determined in Equations 3-55, 3-61, and 3-57.

$$\vec{M}^{I}_{pI} = \begin{bmatrix} M_{pIx} \\ M_{pIy} \\ M_{pIz} \end{bmatrix} = -[B_{pI}] \begin{bmatrix} M_{Ipx} \\ M^{*}_{Ipy} \\ M_{Ipz} \end{bmatrix} \tag{3-68}$$

In terms of the state variables, the inner gimbal equations of motion for the locked axes (X_I and Y_I) are

$$M_{oIx} = -\ddot{\phi} \cos \psi [I_{Ix} + \cos^2 \theta (I_{px} + I_{gxI}) + \sin^2 \theta (I_{pz} + I_{gyS} + I_{gzI})] - \ddot{\psi} \cos \theta (I_{px} + I_{gxI} - I_{pz} - I_{gyS} - I_{gzI}) + MIX \tag{3-69}$$

where

$$MIX = (I_{Iz} - I_{Iy}) W_{Iz} W_{Iy} + I_{Ix} \dot{W}_{Ix} + MPX \cos \theta - MPZ \sin \theta \tag{3-70}$$

MPX and MPZ are defined in Equations 3-56 and 3-58, respectively.

$$M_{oIy} = -\ddot{\phi} \sin \psi \, I_{Iy} + MIY \tag{3-71}$$

where

$$MIY = \dot{W}_{Iy} I_{Iy} + (I_{Ix} - I_{Iz}) W_{Iz} W_{Ix} + M^*_{Ipy} \tag{3-72}$$

M^*_{Ipy} is defined in Equation 3-61.

The Z-axis of the inner gimbal is the driven or dynamic axis; expanding in state variables, the fifth system differential equation is formed.

$$-\ddot{\phi}\sin\theta\cos\theta\cos\psi\,\frac{(I_{px}+I_{gxI}-I_{pz}-I_{gyS}-I_{gzI})}{I_{Iz}}$$

$$-\ddot{\psi}\left[1+\sin^2\theta\,\frac{(I_{px}+I_{gxI})}{I_{Iz}}\right.$$

$$\left.+\cos^2\theta\,\frac{(I_{pz}+I_{gyS}+I_{gzI})}{I_{Iz}}\right] = MIZ \qquad (3\text{-}73)$$

where the dynamic torque

$$MIZ = \frac{M^*_{oIz}}{I_{Iz}} - \frac{(I_{Iy}-I_{Ix})}{I_{Iz}}W_{Ix}W_{Iy}$$

$$-\frac{MPX\sin\theta}{I_{Iz}} - \frac{MPZ\cos\theta}{I_{Iz}} - \dot{W}_{Iz} \qquad (3\text{-}74)$$

$$M^*_{oIz} = D_{oI}\dot{\psi} + F_{oI}(SGN\dot{\psi}) - T_{mm} \qquad (3\text{-}75)$$

D_{oI} — viscous friction between inner and outer gimbals.

$F_{oI}(SGN\dot{\psi})$ — function representing stiction and Coulomb friction.

T_{mm} — middle-axis motor torque

<u>Outer Gimbal Equations of Motion</u>. The sixth state equation describing the system is obtained from the equation of motion for the outer gimbal X-axis.

$$M^*_{cox} = I_{ox} \overset{o}{\dot{\omega}}_{ox} + (I_{oz} - I_{oy})\omega_{oz}\omega_{oy} - M_{Iox} \tag{3-76}$$

where

$$\vec{M}^o_{Io} = -\left[B_{Io}\right]\vec{M}^I_{oI} \tag{3-77}$$

Substituting state variables

$$-\ddot{\phi}\left[1 + \cos^2\psi\left\{\frac{I_{Ix} + \cos^2\theta(I_{px} + I_{gxI})}{I_{ox}}\right.\right.$$

$$\left.\left. + \frac{\sin^2\theta(I_{pz} + I_{gyS} + I_{gzI})}{I_{ox}}\right\} + \sin^2\psi\,\frac{I_{Iy}}{I_{ox}}\right]$$

$$- \ddot{\psi}\cos\theta\sin\theta\cos\psi\left(\frac{I_{px} + I_{gxI} - I_{pz}}{I_{ox}}\right.$$

$$\left. - \frac{I_{gyS} - I_{gzI}}{I_{ox}}\right) = MOX \tag{3-78}$$

where

$$MOX = \frac{M^*_{cox}}{I_{ox}} - \frac{(I_{oz} - I_{oy})}{I_{ox}} W_{oz}W_{oy}$$

$$- \frac{MIX\cos\psi}{I_{ox}} - \frac{MIY\sin\psi}{I_{ox}} - \dot{P} \tag{3-79}$$

and

$$M^*_{cox} = D_{co}\dot{\phi} + F_{co}(SGN\dot{\phi}) - T_{oo} \qquad (3\text{-}80)$$

D_{co} — viscous friction between the case and outer gimbal.

$F_{co}(SGN\dot{\phi})$ — function representing stiction and Coulomb friction.

T_{oo} — outer axis motor torque.

V. GIMBAL SYSTEM STATE EQUATIONS

The three equations of motion (3-59, 3-73, and 3-78) representing the gimbaled system may be expressed as a set of second-order differential equations in the state variables.

$$A_{p\phi}\ddot{\Phi} + A_{p\theta}\ddot{\Theta} = MPY \qquad (3\text{-}81)$$

$$A_{I\phi}\ddot{\Phi} + A_{I\psi}\ddot{\Psi} = MIZ \qquad (3\text{-}82)$$

$$A_{o\phi}\ddot{\Phi} + A_{o\psi}\ddot{\Psi} = MOX \qquad (3\text{-}83)$$

Coefficients are defined as

$$A_{p\phi} = -\sin\psi\left[\frac{(I_{gxS} + I_{gyI} + I_{gzS})}{I_{py}} + 1\right] \qquad (3\text{-}84)$$

$$A_{p\theta} = -\left[\frac{(I_{gxS} + I_{gyI} + I_{gzS})}{I_{py}} + 1\right] \tag{3-85}$$

$$A_{I\psi} = -\left[1 + \sin^2\theta \frac{(I_{px} + I_{gxI})}{I_{Iz}} + \cos^2\theta \frac{(I_{pz} + I_{gyS} + I_{gzI})}{I_{Iz}}\right] \tag{3-86}$$

$$A_{I\phi} = -\sin\theta \cos\theta \cos\psi \frac{(I_{px} - I_{pz} + I_{gxI} - I_{gyS} - I_{gzI})}{I_{Iz}} \tag{3-87}$$

$$A_{o\phi} = -\left[1 + \cos^2\psi \frac{(I_{Ix} + \cos^2\theta(I_{px} + I_{gxI})}{I_{ox}} + \frac{\sin^2\theta(I_{pz} + I_{gyS} + I_{gzI})}{I_{ox}} + \sin^2\psi \frac{I_{Iy}}{I_{ox}}\right] \tag{3-88}$$

$$A_{o\psi} = -\cos\theta \sin\theta \cos\psi \frac{(I_{px} + I_{gxI} - I_{pz} - I_{gyS} - I_{gzI})}{I_{ox}} \tag{3-89}$$

VI. SOLVED DYNAMICAL EQUATIONS (GIMBALS AND GYROS)

The differential equations of motion for the three gyros mounted on the platform were previously derived and presented in Equations 3-23, 3-24, and 3-25. Equations 3-81, 3-82, and 3-83 describe the motion of the gimbaled members. Solving the aforementioned system of six differential equations for the highest derivative of the state variables

$$\ddot{\Phi} = \frac{MIZ\ A_{o\psi} - MOX\ A_{I\psi}}{A_{I\phi}A_{o\psi} - A_{I\psi}A_{o\phi}} \tag{3-90}$$

$$\ddot{\Psi} = \frac{MOX\ A_{I\phi} - MIZ\ A_{o\phi}}{A_{I\phi}A_{o\psi} - A_{I\psi}A_{o\phi}} \tag{3-91}$$

$$\ddot{\Theta} = \frac{A_{p\phi}\left[MOX\ A_{I\psi} - MIX\ A_{o\psi}\right]}{A_{p\theta}(A_{I\phi}A_{o\psi} - A_{I\phi}A_{o\psi})} + \frac{MPY}{A_{p\theta}} \tag{3-92}$$

$$\ddot{\alpha}_x = LGX - G_{x\phi}\ddot{\Phi} - G_{x\psi}\ddot{\Psi} \tag{3-93}$$

$$\ddot{\alpha}_y = LGY - G_{y\phi}\ddot{\Phi} - G_{y\psi}\ddot{\Psi} \tag{3-94}$$

$$\ddot{\alpha}_z = LGZ - G_{z\phi}\ddot{\Phi} - G_{z\psi}\ddot{\Psi} \tag{3-95}$$

CHAPTER IV

THE CLOSED-LOOP SYSTEM

The IMU studied is composed of four mechanical members (case, outer and inner gimbals, and platform) with three gyros orthogonally mounted on the innermost member or platform.

I. ATTITUDE ERROR MEASUREMENT

The gyros are of the integrating type and serve as instruments to measure the angular displacement of the platform about their respective input axes. The triad formed by the three gyro measurements may be treated as a vector representing the change in attitude of the platform, providing that commutation is negligible. No order of rotation is assumed when the attitude variation of the platform is treated as a vector. This assumption breaks down during periods of extreme platform disturbance, and a commutation error may be observed. A commutation error results in an unrecoverable platform-attitude error. The platform-attitude error vector is represented by a triad of the gyro float angles.

$$\vec{\alpha} = \begin{bmatrix} \alpha_X \\ \alpha_Y \\ \alpha_Z \end{bmatrix} \tag{4-1}$$

The $\vec{\alpha}$ vector is the error signal in the IMU control loop. There are three degrees of freedom between the case and the platform, the X-, Z-, and Y-Euler sequence, as discussed previously. The dynamic or driven axis between each member of the system has a torque motor mounted such that it may attempt to drive the platform to a position nulling $\vec{\alpha}$; which returns the platform to its initial position (inertial reference) if there has been no commutation.

Resolving Errors. The Euler rotation axes generally form a nonorthogonal set, and $\vec{\alpha}$ must be transformed as follows to form the error signal $\vec{\varepsilon}$ for the three control loops

$$\vec{\varepsilon} = \begin{bmatrix} \varepsilon_{II} \\ \varepsilon_{mm} \\ \varepsilon_{oo} \end{bmatrix} \tag{4-2}$$

Note: The bases II, mm, and oo are not generally orthogonal.

<u>Determination of ε_{II}, ε_{mm}, and ε_{oo}</u> . For small $\vec{\alpha}$, $\vec{\alpha} = \vec{\alpha}^p$

$$\vec{\alpha}^I = \left[B_{pI}\right]\vec{\alpha}^p \tag{4-3}$$

$$\begin{bmatrix} \alpha_x^I \\ \alpha_y^I \\ \alpha_z^I \end{bmatrix} = \begin{bmatrix} \cos\theta & 0 & -\sin\theta \\ 0 & 1 & 0 \\ \sin\theta & 0 & \cos\theta \end{bmatrix} \begin{bmatrix} \alpha_x^p \\ \alpha_y^p \\ \alpha_z^p \end{bmatrix} \tag{4-4}$$

The error signal for the inner gimbal loop ε_{II} is equal to α_y^I or the output of the Y-axis gyro α_y

$$\varepsilon_{II} = \alpha_y \tag{4-5}$$

$$\vec{\alpha}^o = \left[B_{Io}\right]\vec{\alpha}^I \tag{4-6}$$

$$\begin{bmatrix} \alpha_x^o \\ \alpha_y^o \\ \alpha_z^o \end{bmatrix} \quad \begin{bmatrix} \cos\psi & \sin\psi & 0 \\ -\sin\psi & \cos\psi & 0 \\ 0 & 0 & 1 \end{bmatrix} \begin{bmatrix} \alpha_x^I \\ \alpha_y^I \\ \alpha_z^I \end{bmatrix} \tag{4-7}$$

The middle gimbal loop error is α_z^o

$$\varepsilon_{mm} = \alpha_z^o \tag{4-8}$$

$$\varepsilon_{mm} = \alpha_x \sin\theta + \alpha_z \cos\theta \tag{4-9}$$

In the system studies, the Z-axis gyro had its input oriented along the negative Z-axis; therefore

$$\varepsilon_{mm} = \alpha_x \sin\theta - \alpha_z \cos\theta \tag{4-10}$$

$$\vec{\alpha}^{c} = \left[B_{oc}\right]\vec{\alpha}^{o} \tag{4-11}$$

$$\begin{bmatrix} \alpha_x^c \\ \alpha_y^c \\ \alpha_z^c \end{bmatrix} = \begin{bmatrix} 1 & 0 & 0 \\ 0 & \cos\phi & \sin\phi \\ 0 & -\sin\phi & \cos\phi \end{bmatrix} \begin{bmatrix} \alpha_x^o \\ \alpha_y^o \\ \alpha_z^o \end{bmatrix} \tag{4-12}$$

The outer gimbal loop error is α_x^c

$$\varepsilon_{oo} = \alpha_x^c \tag{4-13}$$

$$\varepsilon_{oo} = \alpha_x \cos\theta \cos\psi - \alpha_z \sin\theta \cos\psi + \alpha_y \sin\psi \tag{4-14}$$

With the Z-axis gyro oriented along the negative Z-axis, the outer gimbal error becomes

$$\varepsilon_{oo} = \alpha_x \cos\theta \cos\psi + \alpha_z \sin\theta \cos\psi + \alpha_y \sin\psi \tag{4-15}$$

Summarizing the resolver equations for the system under consideration

$$\vec{\varepsilon} = \begin{bmatrix} \varepsilon_{II} \\ \varepsilon_{mm} \\ \varepsilon_{oo} \end{bmatrix} = \begin{bmatrix} 0 & 1 & 0 \\ \sin\theta & 0 & -\cos\theta \\ \cos\theta\cos\psi & \sin\psi & \sin\theta\cos\psi \end{bmatrix} \begin{bmatrix} \alpha_x \\ \alpha_y \\ \alpha_z \end{bmatrix} \tag{4-16}$$

II. PREAMPLIFIER DEMODULATOR

The signal generators or pickoffs on the gyro float and the resolvers are variable inductance transformer devices. The output of the resolvers is therefore an amplitude-modulated signal; the demodulator preamplifier for the control loops is modeled by the transfer function

$$\frac{K_a\left(\dfrac{s^2}{4613^2} + 1\right)}{\left(\dfrac{s}{3378} + 1\right)\left[\dfrac{s^2}{3604^2} + \dfrac{2(0.1786)s}{3604} + 1\right]}$$

$$\times \frac{1}{\left[\dfrac{s^2}{3787^2} + \dfrac{2(0.6192)s}{3787} + 1\right]} \tag{4-17}$$

A limiter follows the preamplifier to simulate saturation effects.

III. COMPENSATION AND SERVOAMPLIFIER

Each of the three loops has a servoamplifier to drive the torque motors and a compensation network to achieve the required loop response and noise attenuation. The three filter/servoamplifiers are modeled by the following functions, which represent the inner, middle, and outer gimbal loops, respectively. Saturation effects are included in the loop, Figure 9

$$K_{II} \frac{(s + 5)(s + 160)}{(s + .125)(s + 2000)} \tag{4-18}$$

$$K_{mm} \frac{(s + 5)(s + 160)}{(s + .125)(s + 2000)} \tag{4-19}$$

$$K_{oo} \frac{(s + 5)(s + 160)}{(s + .125)(s + 2000)} \tag{4-20}$$

IV. DYNAMIC AXES TORQUES

<u>Motor Torques</u>. The torque motors are modeled as first-order lags

$$\frac{\vec{K}_t}{\tau_t s + 1} \tag{4-21}$$

and produce the driving torque $\vec{T}$ applied to the three dynamic axes

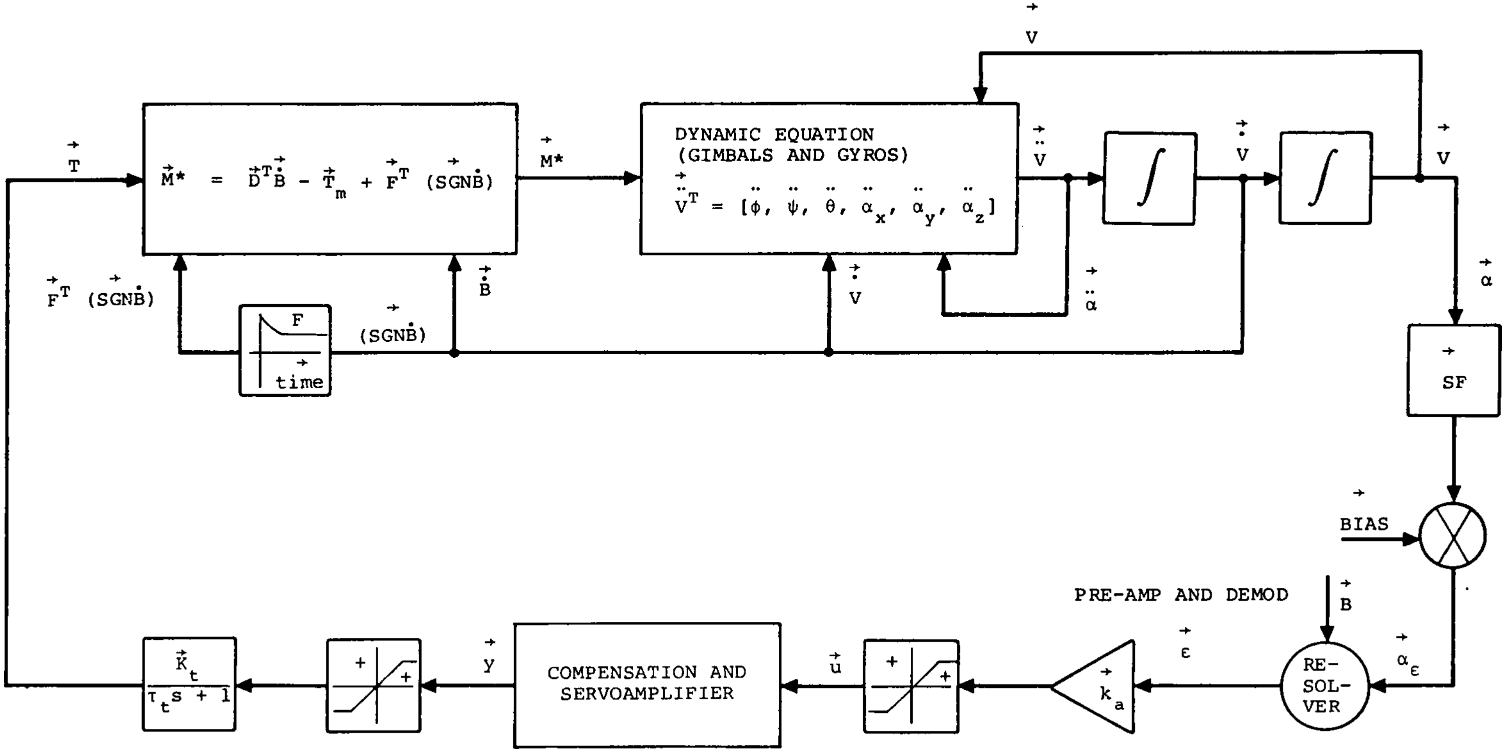

$\ddot{\vec{V}}^T = [\ddot{\theta}, \ddot{\psi}, \ddot{\phi}, \ddot{\alpha}_x, \ddot{\alpha}_y, \ddot{\alpha}_z]$

$\dot{\vec{V}}^T = [\dot{\theta}, \dot{\psi}, \dot{\phi}, \dot{\alpha}_x, \dot{\alpha}_y, \dot{\alpha}_z]$

$\vec{V}^T = [\theta, \psi, \phi, \alpha_x, \alpha_y, \alpha_z]$

$\ddot{\vec{\alpha}}^T = [\ddot{\alpha}_x, \ddot{\alpha}_y, \ddot{\alpha}_z]$

$\vec{\alpha}^T = [\alpha_x, \alpha_y, \alpha_z]$

$\dot{\vec{B}}^T = [\dot{\theta}, \dot{\psi}, \dot{\phi}]$

$\vec{B}^T = [\theta \;\; \psi \;\; \phi]$

$\vec{\alpha}_\varepsilon^T = [\alpha_{\varepsilon x}, \alpha_{\varepsilon y}, \alpha_{\varepsilon z}]$

$\vec{\varepsilon}^T = [\varepsilon_{II}, \varepsilon_{mm}, \varepsilon_{oo}]$

$\vec{u}^T = [U_{II}, U_{mm}, U_{oo}]$

$\vec{y}^T = [y_{II}, y_{mm}, y_{oo}]$

$\vec{K}_t^T = [K_{tII}, K_{tmm}, K_{too}]$

$\vec{T}^T = [T_{II}, T_{mm}, T_{oo}]$

$\vec{M}^{*T} = [M^*_{Ipy}, M^*_{oIz}, M^*_{COX}]$

$\vec{D}^T = [D_{Ip}, D_{oI}, D_{co}]$

$\vec{F}^T = [F_{Ip}, F_{oI}, F_{co}]$

$\overrightarrow{SGN\dot{B}}^T = [SGN\dot{\theta}, SGN\dot{\psi}, SGN\dot{\phi}]$

$\vec{BIAS} = [BIAS_x, BIAS_y, BIAS_z]$

$\vec{SF} = [SF_x, SF_y, SF_z]$

$\vec{k}_a = [k_{aII}, k_{amm}, k_{aoo}]$

FIGURE 9

BLOCK DIAGRAM FOR THREE-AXIS PLATFORM

$$\vec{K}_t = \begin{bmatrix} K_{tII} \\ K_{tmm} \\ K_{too} \end{bmatrix} \qquad (4\text{-}22)$$

$$\vec{T} = \begin{bmatrix} T_{II} \\ T_{mm} \\ T_{oo} \end{bmatrix} \qquad (4\text{-}23)$$

where

$$\tau_t = 50 \ \mu\text{sec}$$

Net Torque. The net torque on the driven dynamic axes is $\vec{M}^*$

$$\vec{M}^* = \begin{bmatrix} M^*_{Ipy} \\ M^*_{oIz} \\ M^*_{cox} \end{bmatrix} \qquad (4\text{-}24)$$

where M^*_{Ipy}, M^*_{oIz}, and M^*_{cox} are defined in equations 3-61, 3-75, and 3-80, respectively.

In vector form

$$\vec{M}^* = \vec{D}^T \dot{\vec{B}} + F^T (S\vec{G}N\dot{B}) - \vec{T} \qquad (4\text{-}25)$$

where viscous friction is

$$D^T\dot{\vec{B}} = \begin{bmatrix} D_{Ip} & D_{oI} & D_{co} \end{bmatrix} \begin{bmatrix} \dot{\theta} \\ \dot{\psi} \\ \dot{\phi} \end{bmatrix} \tag{4-26}$$

and Coulomb and static frictions are $\vec{F}^T(\overrightarrow{SGN\dot{B}})$.

Figures 9 and 10 are vector block and schematic diagrams of the three-axes platform, respectively.

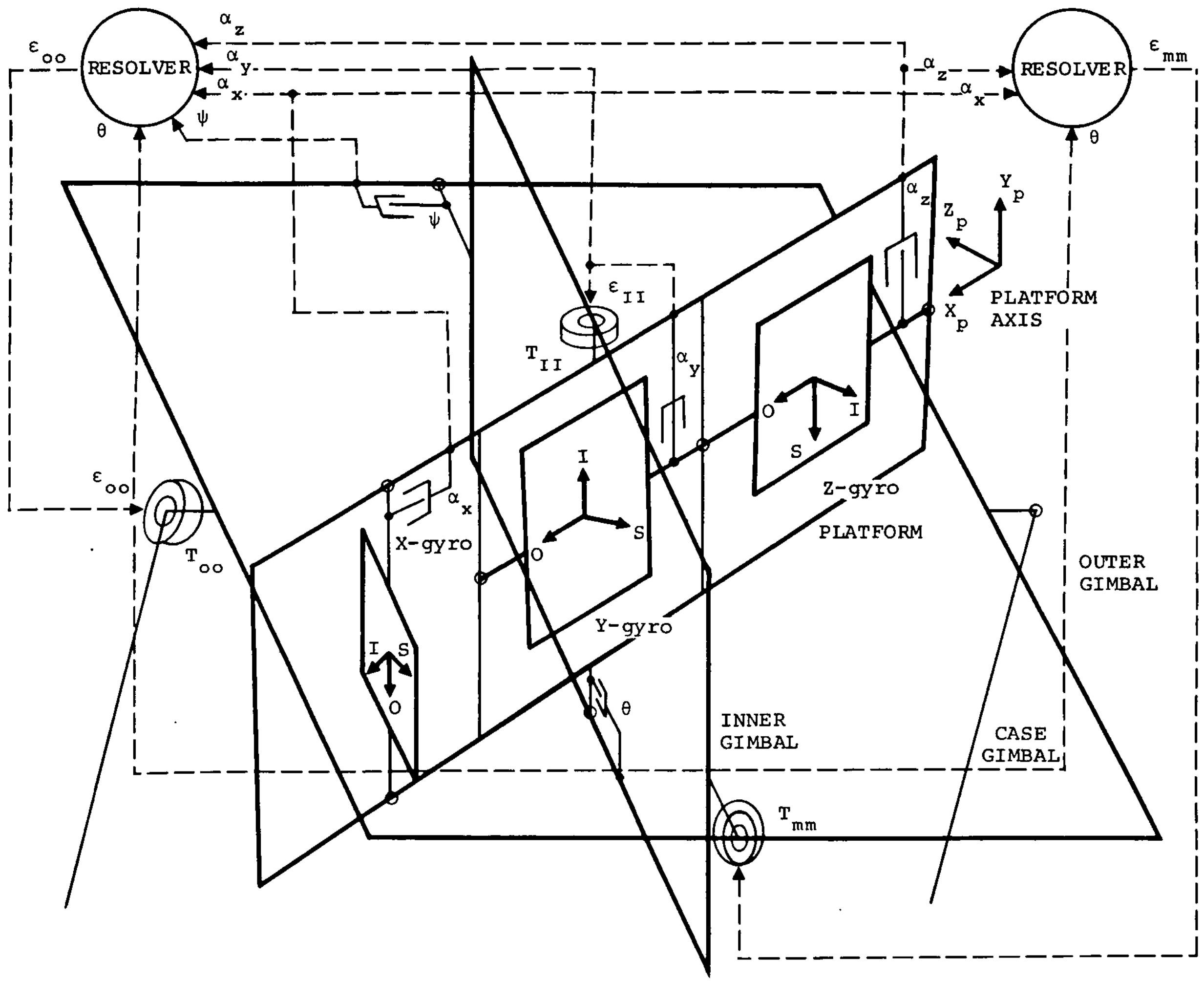

FIGURE 10

THREE-GIMBAL IMU SCHEMATIC DIAGRAM

CHAPTER V

SYSTEM SIMPLIFICATION AND SIMULATION

The system modeled in Chapters II, III, and IV is examined for reduction of high-frequency (small time constant) terms and programmed in FORTRAN for the CDC 3800 digital computer. High-frequency terms are removed from the models if system performance (simulated) is not extensively affected. This results in reduced computation times. The integration-stepsize is chosen as a function of the smallest time constant is retained.

I. INERTIAL MEASUREMENT UNIT MODEL SIMPLIFICATION

The IMU model summarized in Figure 10 consists of three second-order differential equations (3-90), (3-91), and (3-92) representing the motion of the mechanical members of the system, equations (3-93), (3-94), and (3-95) representing the three gyros, and the transfer functions (4-17) to (4-20) for the control-loop elements. The servoamplifier gain in each loop is adjusted to offset the variation in gimbal inertia so that the response and stability of the three loops are maintained. A single loop may be examined for elimination of high-frequency terms. The control loop to be analyzed is presented in Figure 11.

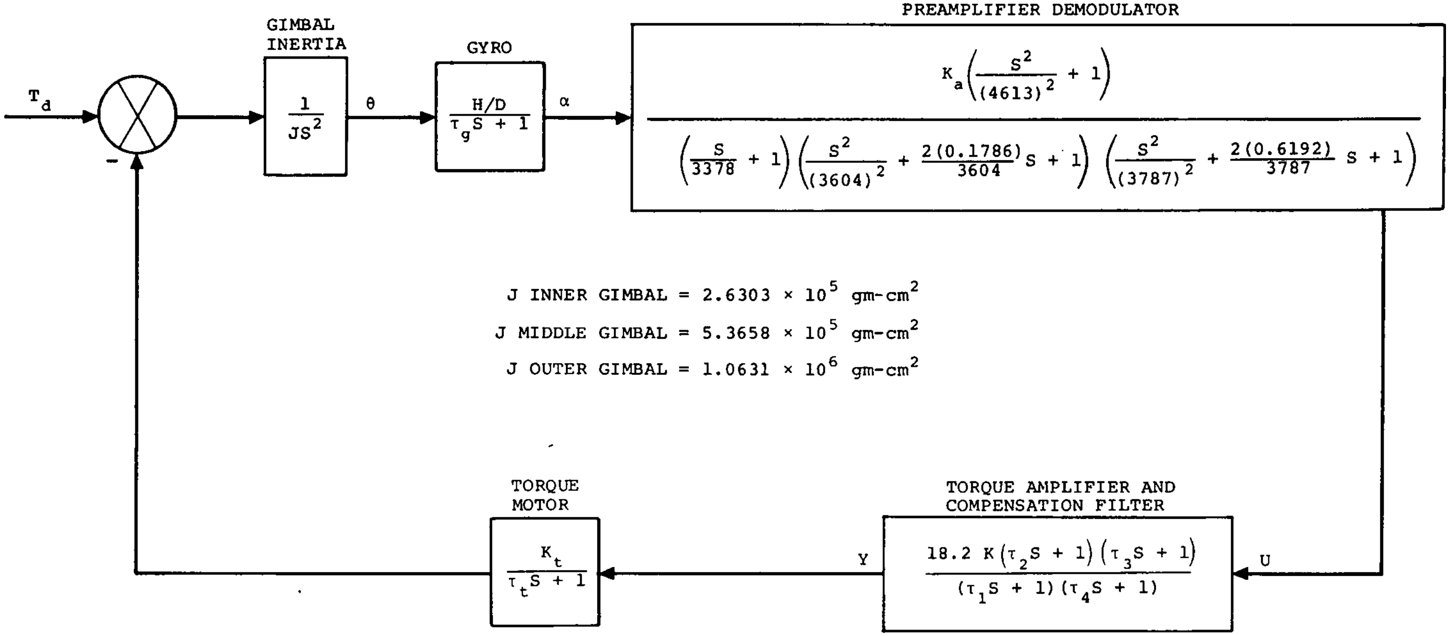

J INNER GIMBAL = 2.6303×10^5 gm-cm^2

J MIDDLE GIMBAL = 5.3658×10^5 gm-cm^2

J OUTER GIMBAL = 1.0631×10^6 gm-cm^2

K_t INNER GIMBAL = 1.52×10^7 $\frac{\text{dyn-cm}}{\text{A}}$

K_t MIDDLE GIMBAL = 1.52×10^7 $\frac{\text{dyn-cm}}{\text{A}}$

K_t OUTER GIMBAL = 1.23×10^7 $\frac{\text{dyn-cm}}{\text{A}}$

$\frac{1}{\tau_1}$ = .125 1/sec

$\frac{1}{\tau_g}$ = 1290 1/sec

$\frac{1}{\tau_t}$ = 2×10^4 1/sec

K INNER GIMBAL = 1 $\frac{\text{A}}{\text{Vrms}}$

K MIDDLE GIMBAL = 2 $\frac{\text{A}}{\text{Vrms}}$

K OUTER GIMBAL = 3 $\frac{\text{A}}{\text{Vrms}}$

$\frac{1}{\tau_2}$ = 5 1/sec

$\frac{1}{\tau_4}$ = 10^4 1/sec

H = 0.434×10^6 $\frac{\text{dyn-cm}}{\text{rad/sec}}$

D = 0.475×10^6 $\frac{\text{dyn-cm}}{\text{rad/sec}}$

$\frac{H}{D}$ = 0.915

$\frac{1}{\tau_3}$ = 160 1/sec

K_a (PURE GAIN) = 1650

FIGURE 11

SINGLE-AXIS IMU FUNCTIONAL DIAGRAM
(HIGH-FREQUENCY MODEL)

A frequency domain analysis is performed using a plot of the log of the gain versus the log of frequency (Figure 12).

It is clear that all terms with breakpoints above 160 radians per second may be dropped without appreciably affecting the system phase margin.

Phase Margin with High-Frequency Terms

P.M. = 39° for the inner and middle loop

P.M. = 32° for the outer loop

Phase Margin Without High-Frequency Terms

P.M. = 56° for the inner and middle loop

P.M. = 43° for the outer loop

This reduces the preamplifier demodulator to a gain, the gyro equations to first order, and the compensator to a lead. Figure 13 is a block diagram of the new low-frequency loop.

Preamplifier Demodulator. The preamplifier demodulator represented by the transfer function in equation (4-17) may be reduced to a pure gain K_a . The open loop, frequency-gain plot (Figure 12) indicates that the dynamic terms have no effect on system response, and the simulation does not contain any disturbance requiring attenuation of these frequencies.

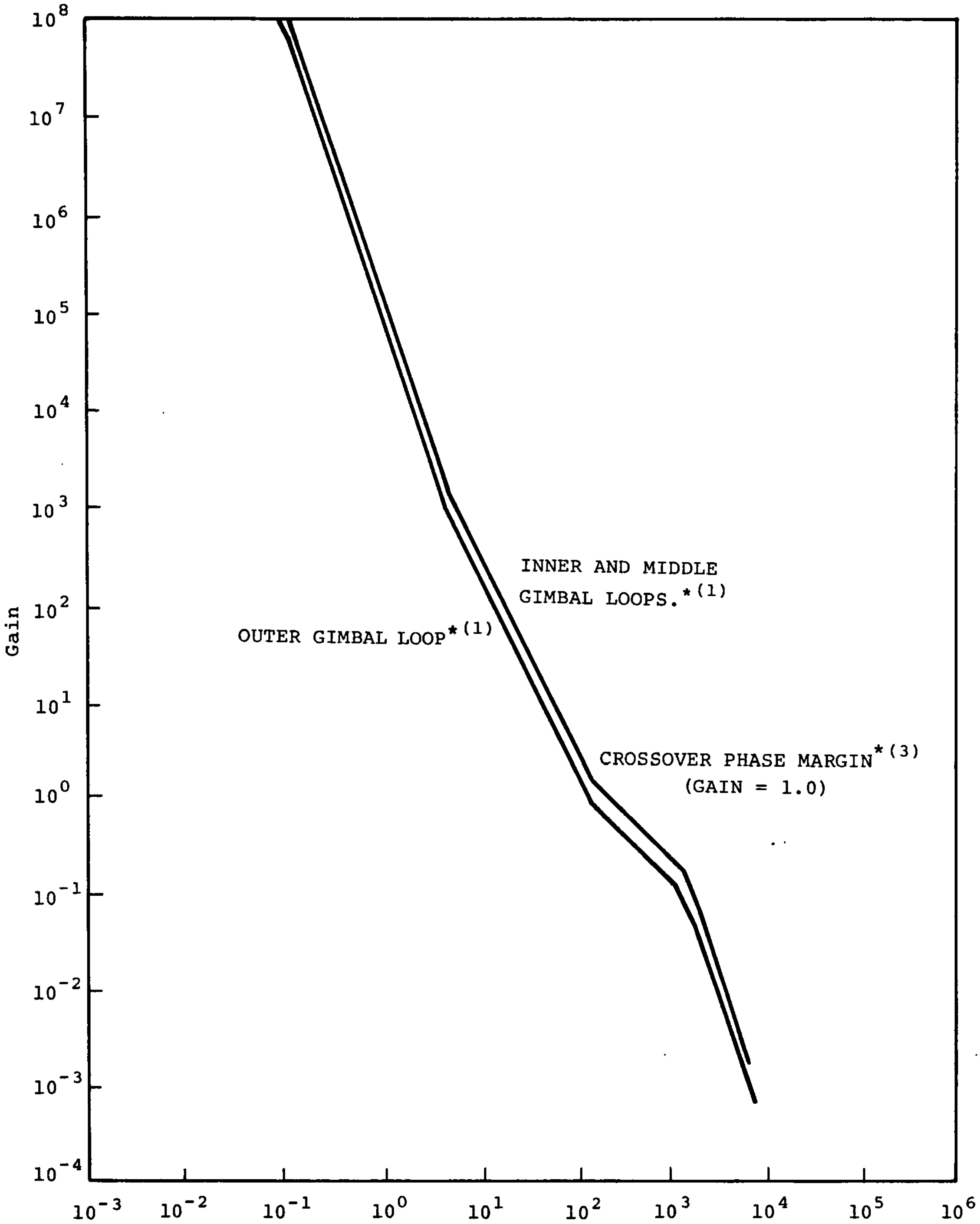

*REFER TO NOTES ON THE FOLLOWING TWO PAGES.

FIGURE 12

LOG GAIN VERSUS LOG FREQUENCY

NOTES

(1) OPEN-LOOP TRANSFER FUNCTION

$$-A(S) = \frac{50}{K_a S}\left(\frac{1200}{S\left(\frac{s}{1290}+1\right)}\right)\left(\frac{1.352\left(\frac{s^2}{4613^2}+1\right)}{\left(\frac{s}{3378}+1\right)\left(\frac{s^2}{3604^2}+\frac{2(0.1786)S}{3604}+1\right)}\right)$$

$$\left(\frac{1}{\left(\frac{s^2}{3787^2}+\frac{2(0.6192)s}{3787}+1\right)}\right)\left(\frac{18.2\ K_s\left(\frac{s}{5}+1\right)\left(\frac{s}{160}+1\right)}{\left(\frac{s}{0.125}+1\right)\left(\frac{s}{2000}+1\right)}\right)\left(K_{TH}\right)$$

where

GIMBAL LOOP	K_a	K_s	K_{TH}
INNER	1	1	1.12
MIDDLE	2	2	1.12
OUTER	4	3	0.105

(2) EVALUATING $-A(S)$ AS $S \to 0$

GIMBAL LOOP	$-A(S)$, $S \to 0$
INNER	1.65355×10^6
MIDDLE	1.65355×10^6
OUTER	1.12358×10^6

NOTES (Concluded)

ESTIMATING PHASE MARGIN

(3) HIGH-FREQUENCY MODEL

*INNER AND MIDDLE GIMBAL LOOP

Phase Angle at Crossover

$$\text{Phase Angle} = -\pi + \tan^{-1}\frac{240}{100} - \tan^{-1}\frac{240}{2000}$$

$$= -140.9$$

Phase Margin = 39.01

*OUTER GIMBAL LOOP

$$\text{Phase Angle} = -\pi + \tan^{-1}\frac{150}{160} - \tan^{-1}\frac{150}{1290} - \tan^{-1}\frac{150}{2000}$$

$$= -147.72$$

Phase Margin = 32.28

LOW-FREQUENCY MODEL

*INNER AND MIDDLE GIMBAL LOOP

$$\text{Phase Angle} = -\pi + \tan^{-1}\frac{240}{160}$$

$$= 123.64$$

Phase Margin = 56.36

*OUTER GIMBAL LOOP

$$\text{Phase Angle} = -\pi + \tan^{-1}\frac{150}{160}$$

$$= -136.85$$

Phase Margin = 43.15

<u>Compensation Network and Servoamplifier</u>. The transfer functions (equations 4-18, 4-19, and 4-20) representing the compensation network and servoamplifier for the control loops contain the following terms

$$\frac{K(s + 5)(s + 160)}{(s + .125)(s + 2,000)} \tag{5-1}$$

The lag at 2,000 radians may be eliminated with only minor effects on the simulation performance; however, this leaves an undesirable form for the remaining transfer function. The form $\frac{Q(S)}{P(S)}$ is physically unrealizable when Q(S) is of higher order than P(S). An examination of the remaining terms on the gain-frequency plot (Figure 12) reveals that the leads at 5 and 160 radians are required for loop response and stability. The total, open loop, transfer functions, after dropping the high frequency terms (Figure 13), is of the proper form; therefore a set of differential equations may be written incorporating the required compensation amplifier terms.

The compensation network and servoamplifier for the low-frequency model are represented by

$$\frac{K(s + 5)(s + 160)}{(s + .125)} \tag{5-2}$$

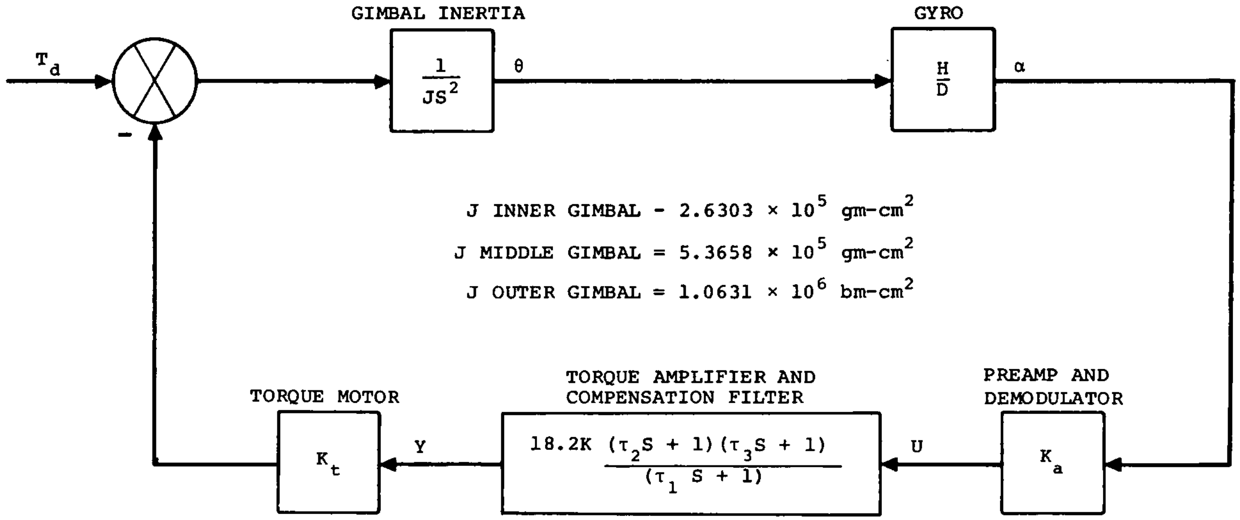

J INNER GIMBAL - 2.6303×10^5 gm-cm^2

J MIDDLE GIMBAL = 5.3658×10^5 gm-cm^2

J OUTER GIMBAL = 1.0631×10^6 bm-cm^2

$K_a = 1650$

K_t INNER GIMBAL = $1.52 \times 10^7 \frac{\text{dyn-cm}}{\text{A}}$

K_t MIDDLE GIMBAL = $1.52 \times 10^7 \frac{\text{dyn-cm}}{\text{A}}$

K_t OUTER GIMBAL = $1.23 \times 10^7 \frac{\text{dyn-cm}}{\text{A}}$

K INNER GIMBAL = $1 \frac{\text{A}}{\text{Vrms}}$

K MIDDLE GIMBAL = $2 \frac{\text{A}}{\text{Vrms}}$

K OUTER GIMBAL = $3 \frac{\text{A}}{\text{Vrms}}$

$D = 0.475 \times 10^6 \frac{\text{dyn-cm}}{\text{rad/sec}}$

$H = 0.434 \times 10^6 \frac{\text{dyn-cm}}{\text{rad/sec}}$

$\frac{H}{D} = 0.915$

$\frac{1}{\tau_1} = .125$ 1/sec

$\frac{1}{\tau_1} = 5$ 1/sec

$\frac{1}{\tau_3} = 160$ 1/sec

FIGURE 13

SINGLE-AXIS FUNCTIONAL DIAGRAM
(LOW-FREQUENCY MODEL)

The dynamic equations for the compensation filter illustrated in Figure 13 may be developed by the block algebra manipulation illustrated by Figure 14.

The differential equations representing the block diagram Figure 14 are

$$Y = K\dot{U} + 164.875\dot{X} + 800X \tag{5-3}$$

$$\dot{X} = KU - .125X \tag{5-4}$$

Relating the above equations to the three loops under consideration

$$\vec{y}^T = [Y_{II}, Y_{mm}, Y_{oo}] \tag{5-5}$$

$$\vec{u}^T = [U_{II}, U_{mm}, U_{oo}] \tag{5-6}$$

$$\vec{u}^T = K_a \vec{\varepsilon}^T \tag{5-7}$$

$$\dot{\vec{u}}^T = K_a \dot{\vec{\varepsilon}}^T \tag{5-8}$$

where

$$\varepsilon_{II} = \alpha_y$$

$$\varepsilon_{mm} = \alpha_x \sin\theta - \alpha_z \cos\theta \tag{5-9}$$

$$\varepsilon_{oo} = \alpha_x \cos\theta \cos\psi + \alpha_z \sin\theta \cos\psi + \alpha_y \sin\psi$$

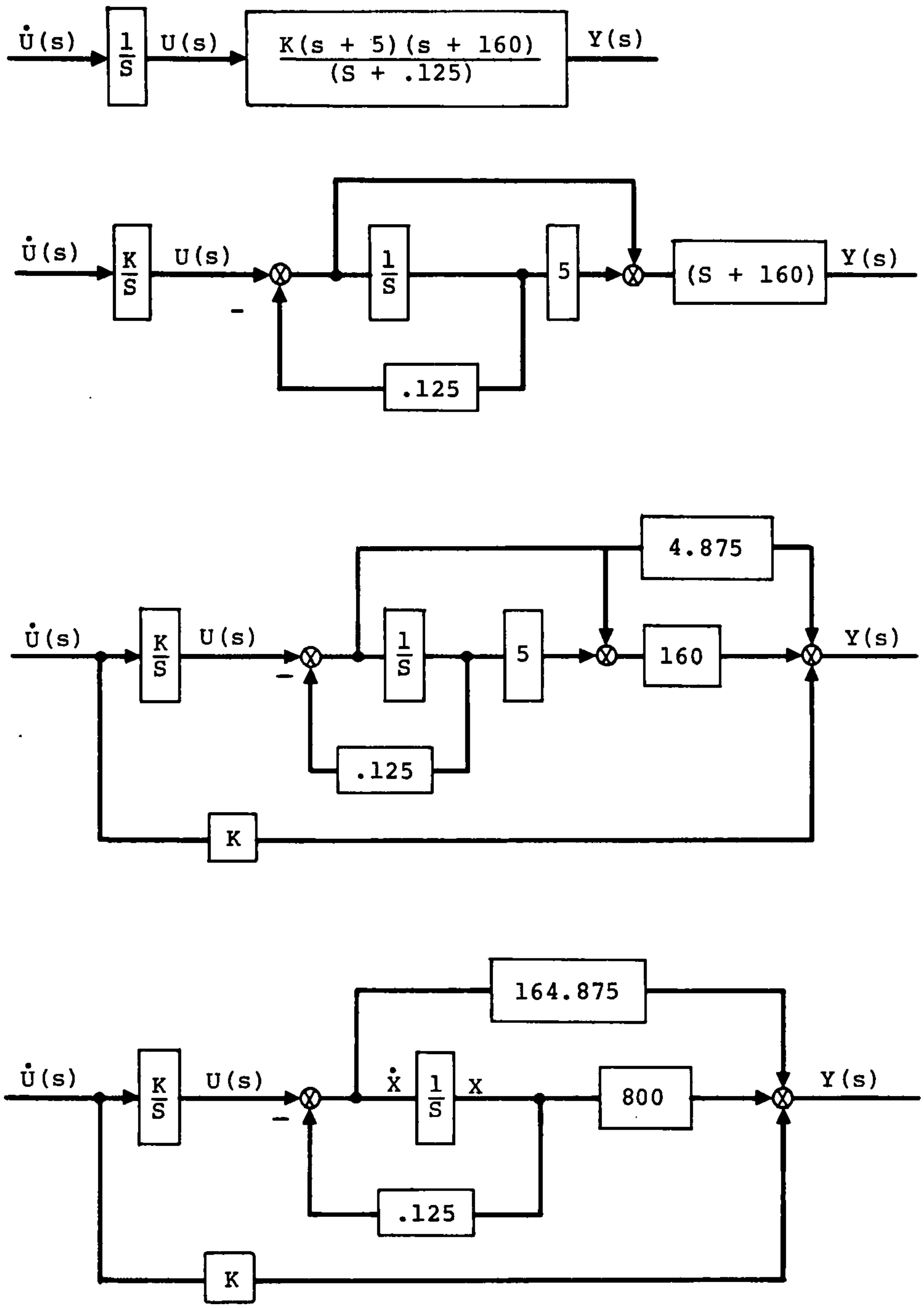

FIGURE 14

COMPENSATION NETWORK BLOCK ALGEBRA

$$\dot{\varepsilon}_{II} = \dot{\alpha}_y$$

$$\dot{\varepsilon}_{mm} = \dot{\alpha}_x \sin\theta - \dot{\alpha}_z \cos\theta \tag{5-10}$$

$$\dot{\varepsilon}_{oo} = \dot{\alpha}_x \cos\theta\cos\psi + \dot{\alpha}_z \sin\theta\cos\psi + \dot{\alpha}_y \sin\psi$$

Torque Motor. The torque motor represented by a first-order lag

$$\frac{K_t}{\tau_t s + 1}$$

has a very small time constant. This analysis assumes τ_t to be 50 μsec; based on this figure, the torquer is reduced to a pure gain K_t for use in the low-frequency model. Analysis of the gain-frequency plot (Figure 12) indicates that this reduction has a negligible effect on the system response.

Gyro Reduction. The gyro equations may be represented for a single channel by the second-order transfer function

$$\alpha(S) = \left[\frac{1}{S}\,\frac{H/D}{\tau_g S + 1}\right] \omega_p(S) \tag{5-11}$$

where $\tau_g = \frac{1}{1300}$.

This function may be reduced to the first-order transfer function

$$\alpha(S) = \left(\frac{H/D}{S}\right) \omega_p(S) \qquad (5\text{-}12)$$

by eliminating the $\ddot{\alpha}$ terms from Equations 3-23 to 3-25 and 3-81 to 3-83. Reducing the order of the gyro equations results in the following six simultaneous equations representing the motion of the gyros and gimbals of the system.

$$A_{p\phi}\ddot{\phi} + A_{p\theta}\ddot{\theta} + A_{px}\dot{\alpha}_x + A_{py}\dot{\alpha}_y + A_{pz}\dot{\alpha}_z = \text{MPYW} \qquad (5\text{-}13)$$

$$A_{I\phi}\ddot{\phi} + A_{I\psi}\ddot{\psi} + A_{Ix}\dot{\alpha}_x + A_{Iy}\dot{\alpha}_y + A_{Iz}\dot{\alpha}_z = \text{MIZW} \qquad (5\text{-}14)$$

$$A_{o\phi}\ddot{\phi} + A_{o\psi}\ddot{\psi} + A_{ox}\dot{\alpha}_x + A_{oy}\dot{\alpha}_y + A_{oz}\dot{\alpha}_z = \text{MOXW} \qquad (5\text{-}15)$$

$$A_{x\phi}\ddot{\phi} + A_{x\psi}\ddot{\psi} + \dot{\alpha}_x = \text{LGXW} \qquad (5\text{-}16)$$

$$A_{y\phi}\ddot{\phi} + A_{y\psi}\ddot{\psi} + \dot{\alpha}_y = \text{LGYW} \qquad (5\text{-}17)$$

$$A_{z\phi}\ddot{\phi} + A_{z\psi}\ddot{\psi} + \dot{\alpha}_z = \text{LGZW} \qquad (5\text{-}18)$$

Coefficients are defined as

$$A_{x\phi} = \frac{I_{gxO}}{D_{gxO}} \sin\theta \cos\psi \tag{5-19}$$

$$A_{x\psi} = -\frac{I_{gxO}}{D_{gxO}} \cos\theta \tag{5-20}$$

$$A_{y\phi} = -\frac{I_{gyO}}{D_{gyO}} \cos\theta \cos\psi \tag{5-21}$$

$$A_{y\psi} = -\frac{I_{gyO}}{D_{gyO}} \sin\theta \tag{5-22}$$

$$A_{z\phi} = -\frac{I_{gzO}}{D_{gzO}} \cos\theta \cos\psi \tag{5-23}$$

$$A_{z\psi} = -\frac{I_{gzO}}{D_{gzO}} \sin\theta \tag{5-24}$$

$$A_{ox} = \frac{1}{I_{ox}} (H_x \cos\theta \cos\psi + D_{gxO} \sin\theta \cos\psi) \tag{5-25}$$

$$A_{oy} = \frac{1}{I_{ox}} (H_y \sin\theta \cos\psi - D_{gyO} \cos\theta \cos\psi) \tag{5-26}$$

$$A_{oz} = \frac{1}{I_{ox}} (H_z \sin\theta \cos\psi - D_{gzO} \cos\theta \cos\psi) \tag{5-27}$$

$$A_{Ix} = \frac{1}{I_{Iz}} (H_x \sin\theta - D_{gxO} \cos\theta) \tag{5-28}$$

$$A_{Iy} = \frac{1}{I_{Iz}} (-H_y \cos\theta - D_{gyO} \sin\theta) \tag{5-29}$$

$$A_{Iz} = \frac{1}{I_{Iz}} (-H_z \cos\theta - D_{gzO} \sin\theta) \tag{5-30}$$

$$A_{px} = \frac{1}{I_{py}} (H_{px}) \tag{5-31}$$

$$A_{py} = \frac{1}{I_{py}} (H_{py}) \tag{5-32}$$

$$A_{pz} = \frac{1}{I_{py}} (H_{pz}) \tag{5-33}$$

$$H_x = I_{gx} W_{py} + H_{\omega x} \tag{5-34}$$

$$H_y = I_{gy} W_{py} - H_{\omega y} \alpha_y \tag{5-35}$$

$$H_z = I_{gz} W_{py} + H_{\omega z} \tag{5-36}$$

$$H_{px} = (I_{gxI} - I_{gxS} - I_{gxO}) W_{px} + H_{\omega x} \alpha_x \tag{5-37}$$

$$H_{py} = (I_{gyI} + I_{gyO} - I_{gyS}) W_{pz} + H_{\omega y} \tag{5-38}$$

$$H_{pz} = (I_{gzS} + I_{gzO} - I_{gzI})W_{pz} + H_{\omega z}\alpha_z \tag{5-39}$$

$$I_{gx} = I_{gxI} + I_{gxO} - I_{gxS} \tag{5-40}$$

$$I_{gy} = I_{gyS} + I_{gyO} - I_{gyI} \tag{5-41}$$

$$I_{gz} = I_{gzI} + I_{gzO} - I_{gzS} \tag{5-42}$$

$$LGXW = \frac{H_{\omega x}}{D_{gxO}} W_{gxI} - \frac{(I_{gxI} - I_{gxS})}{D_{gxO}} W_{gxI}W_{gxS} - \frac{I_{gxO}}{D_{gxO}} \dot{W}_{pz} \tag{5-43}$$

$$LGYW = \frac{H_{\omega y}}{D_{gyO}} W_{gyI} - \frac{(I_{gyI} - I_{gyS})}{D_{gyO}} W_{gyI}W_{gyS} - \frac{I_{gyO}}{D_{gyO}} \dot{W}_{px} \tag{5-44}$$

$$LGZW = \frac{H_{\omega z}}{D_{gzO}} W_{gzI} - \frac{(I_{gzI} - I_{gzS})}{D_{gzO}} W_{gzS}W_{gzI} - \frac{I_{gzO}}{D_{gzO}} \dot{W}_{px} \tag{5-45}$$

$$\begin{aligned} MOXW = \frac{1}{I_{ox}} \Big\{ & M^*_{cox} - MOZY - MIZY \cos\psi - MIXZ \sin\psi \\ & - M^*_{Ipy} \sin\psi - MGXW \cos\theta \cos\psi \\ & - MGZW \sin\theta \cos\psi - MPZY \cos\theta \cos\psi \\ & + MPYX \sin\theta \cos\psi \Big\} - \dot{W}_{ox} \end{aligned} \tag{5-46}$$

$$\begin{aligned} MIZW = \frac{1}{I_{Iz}} \Big\{ & M^*_{oIz} - MIYX - (MPZY + MGXW) \sin\theta \\ & - (MPYX - MGZW) \cos\theta \Big\} - \dot{W}_{Iz} \end{aligned} \tag{5-47}$$

$$MPYW = \frac{1}{I_{py}} \left\{ M^*_{Ipy} - MPXZ + MGYW \right\} - \dot{W}_{py} \tag{5-48}$$

$$MOZY = (I_{oz} - I_{oy}) W_{oz} W_{oy} \tag{5-49}$$

$$MIZY = (I_{Iz} - I_{Iy}) W_{Iz} W_{Iy} + I_{Ix} \dot{W}_{Ix} \tag{5-50}$$

$$MIXZ = (I_{Ix} - I_{Iz}) W_{Iz} W_{Ix} + I_{Iy} \dot{W}_{Iy} \tag{5-51}$$

$$MPZY = (I_{pz} - I_{py}) W_{pz} W_{py} + I_{px} \dot{W}_{px} \tag{5-52}$$

$$MPYX = (I_{py} - I_{px}) W_{px} W_{py} + I_{pz} \dot{W}_{pz} \tag{5-53}$$

$$MIYX = (I_{Iy} - I_{Ix}) W_{Ix} W_{Iy} \tag{5-54}$$

$$MPXZ = (I_{px} - I_{pz}) W_{px} W_{pz} \tag{5-55}$$

$$MGXW = I_{gxI} \dot{W}_{px} + H_{\omega x} W_{pz} + (I_{gxo} - I_{gxz}) W_{pz} W_{py} \tag{5-56}$$

$$\begin{aligned} MGYW = {} & (I_{gxO} + I_{gyS} + I_{gzI} - I_{gxI} - I_{gyO} \\ & - I_{gzO}) W_{pz} W_{px} - H_{\omega y} W_{px} - H_{\omega x} W_{pz} \alpha_x \\ & - H_{\omega z} W_{px} \alpha_z - (I_{gxS} + I_{gyI} + I_{gzS}) \dot{W}_{py} \end{aligned} \tag{5-57}$$

$$\begin{aligned} MGZW = {} & (I_{gyO} + I_{gzO} - I_{gyI} - I_{gzS}) W_{py} W_{px} \\ & + (H_{\omega y} - H_{\omega y} \alpha_y) W_{px} - (I_{gyS} + I_{gxI}) \dot{W}_{pz} \end{aligned} \tag{5-58}$$

Solving equations 5-13 through 5-18 simultaneously, we obtain

$$(1) \quad \ddot{\phi} = \frac{M_B C_\psi - M_C B_\psi}{B_\phi C_\psi - B_\psi C_\phi} \tag{5-59}$$

$$(2) \quad \ddot{\psi} = \frac{B_\phi M_C - M_B C_\phi}{B_\phi C_\psi - B_\psi C_\phi} \tag{5-60}$$

$$(3) \quad \ddot{\theta} = \frac{A_\phi \left(B_\psi M_C - C_\psi M_B\right) + A_\psi \left(B_\phi M_C - C_\phi M_B\right)}{A_\theta \left(B_\phi C_\psi - B_\psi C_\phi\right)} + \frac{M_A}{A_\theta} \tag{5-61}$$

$$(4) \quad \dot{\alpha}_x = LGXW - A_{x\phi}\ddot{\phi} - A_{x\psi}\ddot{\psi} \tag{5-62}$$

$$(5) \quad \dot{\alpha}_y = LGYW - A_{y\phi}\ddot{\phi} - A_{y\psi}\ddot{\psi} \tag{5-63}$$

$$(6) \quad \dot{\alpha}_z = LGZW - A_{z\phi}\ddot{\phi} - A_{z\psi}\ddot{\psi} \tag{5-64}$$

Coefficients are defined as

$$A_\phi = A_{p\phi} - A_{px}A_{x\phi} - A_{py}A_{y\phi} - A_{pz}A_{z\phi} \tag{5-65}$$

$$A_\psi = A_{px}A_{x\psi} + A_{py}A_{y\psi} + A_{pz}A_{z\psi} \tag{5-66}$$

$$A_\theta = A_{p\theta} \tag{5-67}$$

$$B_\phi = A_{I\phi} - A_{Ix}A_{x\phi} - A_{Iy}A_{y\phi} - A_{Iz}A_{z\phi} \tag{5-68}$$

$$B_\psi = A_{I\psi} - A_{Ix}A_{x\psi} - A_{Iy}A_{y\psi} - A_{Iz}A_{z\psi} \tag{5-69}$$

$$C_\phi = A_{o\phi} - A_{ox}A_{x\phi} - A_{oy}A_{y\phi} - A_{oz}A_{z\phi} \tag{5-70}$$

$$C_\psi = A_{o\psi} - A_{ox}A_{x\psi} - A_{oy}A_{y\psi} - A_{oz}A_{z\psi} \tag{5-71}$$

$$M_A = MPYW - A_{px}LGXW - A_{py}LGYW - A_{pz}LGZW \tag{5-72}$$

$$M_B = MIZW - A_{Ix}LGXW - A_{Iy}LGYW - A_{Iz}LGZW \tag{5-73}$$

$$M_C = MOXW - A_{ox}LGXW - A_{oy}LGYW - A_{oz}LGZW \tag{5-74}$$

Equations 5-59 through 5-64, combined with the following differential equations representing the compensation network and servoamplifier indicated in Figures 15 and 16, form the low-frequency model for the IMU under consideration. The smallest time constant represented is 6.25 milliseconds.

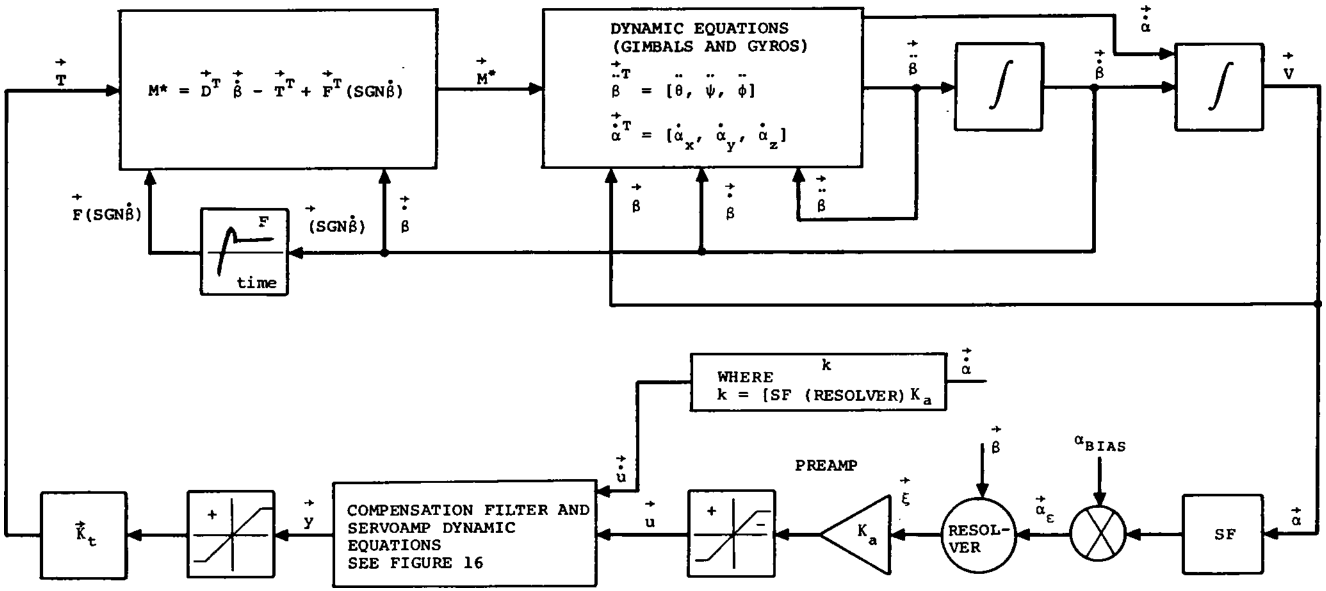

$\dot{\vec V}^T = [\dot\theta, \dot\psi, \dot\phi, \dot\alpha_x, \dot\alpha_y, \dot\alpha_z]$

$\vec V^T = [\theta, \psi, \phi, \alpha_x, \alpha_y, \alpha_z]$

$\dot{\vec\alpha}^T = [\dot\alpha_x, \dot\alpha_y, \dot\alpha_z]$

$\vec\alpha^T = [\alpha_x, \alpha_y, \alpha_z]$

$\ddot{\vec B}^T = [\ddot\theta, \ddot\psi, \ddot\phi]$

$\dot{\vec B}^T = [\dot\theta, \dot\psi, \dot\phi]$

$\vec B^T = [\theta, \psi, \phi]$

$\vec\alpha_\varepsilon^T = [\alpha_{\varepsilon x}, \alpha_{\varepsilon y}, \alpha_{\varepsilon z}]$

$\vec\varepsilon^T = [\varepsilon_{II}, \varepsilon_{mm}, \varepsilon_{oo}]$

$\vec u^T = [U_{II}, U_{mm}, U_{oo}]$

$\vec y^T = [Y_{II}, Y_{mm}, Y_{oo}]$

$\vec K_t^T = [K_{tII}, K_{Tmm}, K_{too}]$

$\vec T^T = [T_{II}, T_{mm}, T_{oo}]$

$\vec M^{*T} = [M^*_{Ipy}, M^*_{oIz}, M^*_{cox}]$

$\vec D^T = [D_{Ip}, D_{oI}, D_{co}]$

$\vec F^T = [F_{Ip}, F_{oI}, F_{co}]$

$\dot{\vec u}^T = [\dot U_{II}, \dot U_{mm}, \dot U_{oo}]$

$\vec{SGN\dot B}^T = [SGN\dot\theta, SGN\dot\psi, SGN\dot\phi]$

$\vec{BIAS} = [BIAS_x, BIAS_y, BIAS_z]$

$\vec{SF} = [SF_x, SF_y, SF_z]$

$\vec K_a = [A_{II}, A_{mm}, A_{oo}]$

FIGURE 15

BLOCK DIAGRAM FOR THREE-AXIS PLATFORM SIMULATION

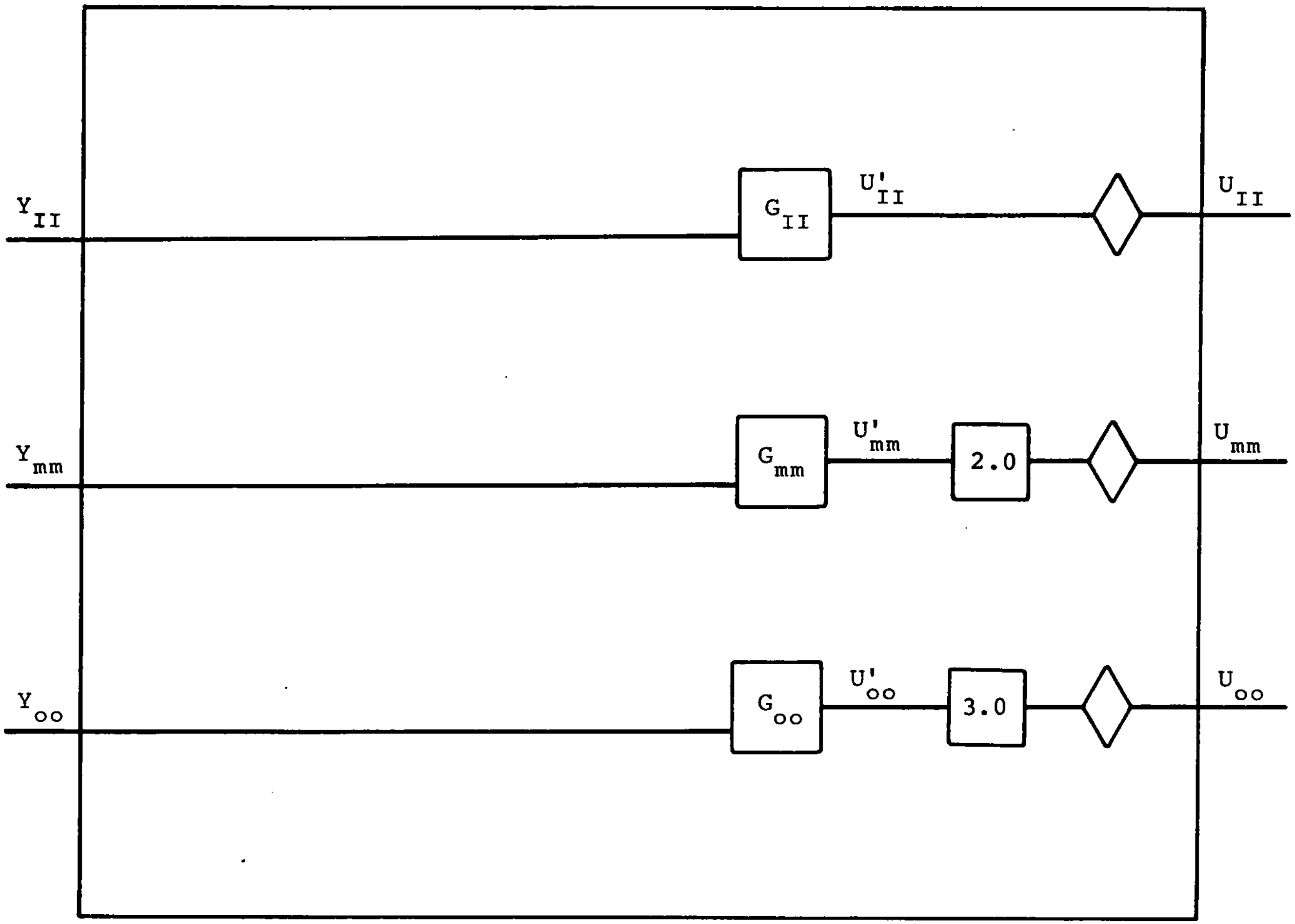

FIGURE 16

COMPENSATION AND SERVO AMP

The differential equations for the compensation networks and servoamplifiers are

$$G_{II} = G_{mm} = G_{oo} \tag{5-75}$$

$$G_{II} = \frac{Y_{II}}{U'_{II}} \tag{5-76}$$

$$G_{mm} = \frac{Y_{mm}}{U'_{mm}} \tag{5-77}$$

$$G_{oo} = \frac{Y_{oo}}{U'_{oo}} \tag{5-78}$$

$$G_{II} = \frac{Y_{II}}{Y'_{II}} = \frac{18.2}{6400}\left[\frac{(s + 5)(s + 160)}{(s + .125)}\right] \tag{5-79}$$

The differential equations to be solved representing the G_{II} transfer function are

$$\dot{x} = \frac{18.2}{6400} U_{II} - .125x \tag{5-80}$$

$$Y_{II} = 164.875\dot{x} + \frac{18.2}{6400} \dot{U}_{II} + 800x \tag{5-81}$$

Similarly, Y_{mm} and Y_{oo} may be determined as functions of U_{mm}, $\dot{U}_{mm}$, $\dot{U}_{oo}$, and U_{oo} , respectively. Resolving

α_x, α_y, α_z, $\dot{\alpha}_x$, $\dot{\alpha}_y$, and $\dot{\alpha}_z$ into error singals ε_{II}, ε_{mm}, ε_{oo}, $\dot{\varepsilon}_{II}$, $\dot{\varepsilon}_{mm}$, and $\dot{\varepsilon}_{oo}$, respectively, and adding resolver errors ε_θ and ε_ψ

$$\varepsilon_{II} = \alpha_y \tag{5-82}$$

$$\varepsilon_{mm} = \alpha_x \sin(\theta + \varepsilon_\theta) - \alpha_z \cos(\theta + \varepsilon_\theta) \tag{5-83}$$

$$\begin{aligned}\varepsilon_{oo} = {} & \alpha_x \cos(\theta + \varepsilon_\theta) \cos(\psi + \varepsilon_\psi) \\ & + \alpha_z \sin(\theta + \varepsilon_\theta) \cos(\psi + \varepsilon_\psi) \\ & + \alpha_y \sin(\psi + \varepsilon_\psi)\end{aligned} \tag{5-84}$$

$$\dot{\varepsilon}_{II} = \dot{\alpha}_y \tag{5-85}$$

$$\dot{\varepsilon}_{mm} = \dot{\alpha}_x \sin(\theta + \varepsilon_\theta) - \dot{\alpha}_z \cos(\theta + \varepsilon_\theta) \tag{5-86}$$

$$\begin{aligned}\dot{\varepsilon}_{oo} = {} & \dot{\alpha}_x \cos(\theta + \varepsilon_\theta) \cos(\psi + \varepsilon_\psi) \\ & + \dot{\alpha}_z \sin(\theta + \varepsilon_\theta) \cos(\psi + \varepsilon_\psi) \\ & + \dot{\alpha}_y \sin(\psi + \varepsilon_\psi)\end{aligned} \tag{5-87}$$

where ε_θ and ε_ψ are resolver errors.

The low-frequency model of the IMU system (Figures 15 and 16) and related equations were programmed and designated subroutine PLTFRM. This subroutine simulates the low-frequency dynamic behavior of a three-gimbaled IMU with an orthogonally mounted gyro triad on the platform (stable member).

The program is briefly outlined in the flow diagram (Figure 17). Block 1 of the flow diagram receives updates of the vehicle (IMU case) body angular accelerations $\dot{\vec{\omega}}_c$ from the external driver subroutine NEWACC four times per integration step. Block 2 transforms the gyro-float pickoff angles $\vec{\alpha}$ into error signals $\vec{\varepsilon}$ for each gimbal axis. The scale factor, bias, and resolver errors may be incorporated in $\vec{\alpha}$ at this point if desired.

The compensation filter differential equations are solved in block 3, assuring the desired loop response. The filter output $\vec{y}$ is multiplied by the motor gain $\vec{K}_t$ and the sign selected in block 4 such that the torque applied by the motor drives $\vec{\alpha}$ toward the null. Computations performed in block 5 calculate the Coulomb friction torque in each loop as a function of the SGN of the gimbal angle rates. The net torque $\vec{M}^*$, including motor torque, Coulomb friction, and viscous damping is computed in block 6. The derivatives of the state variables

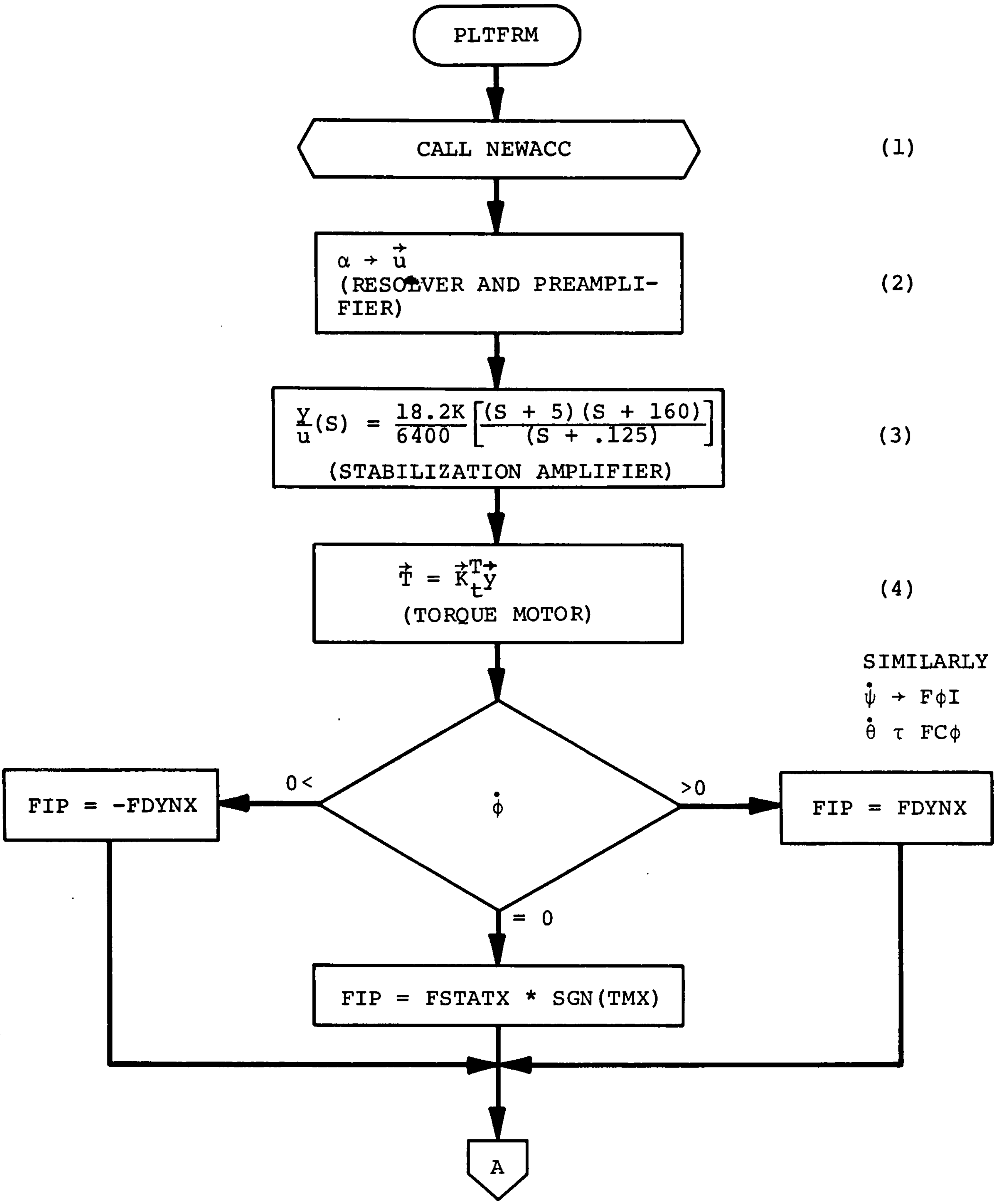

FIGURE 17

GENERAL FLOW DIAGRAM

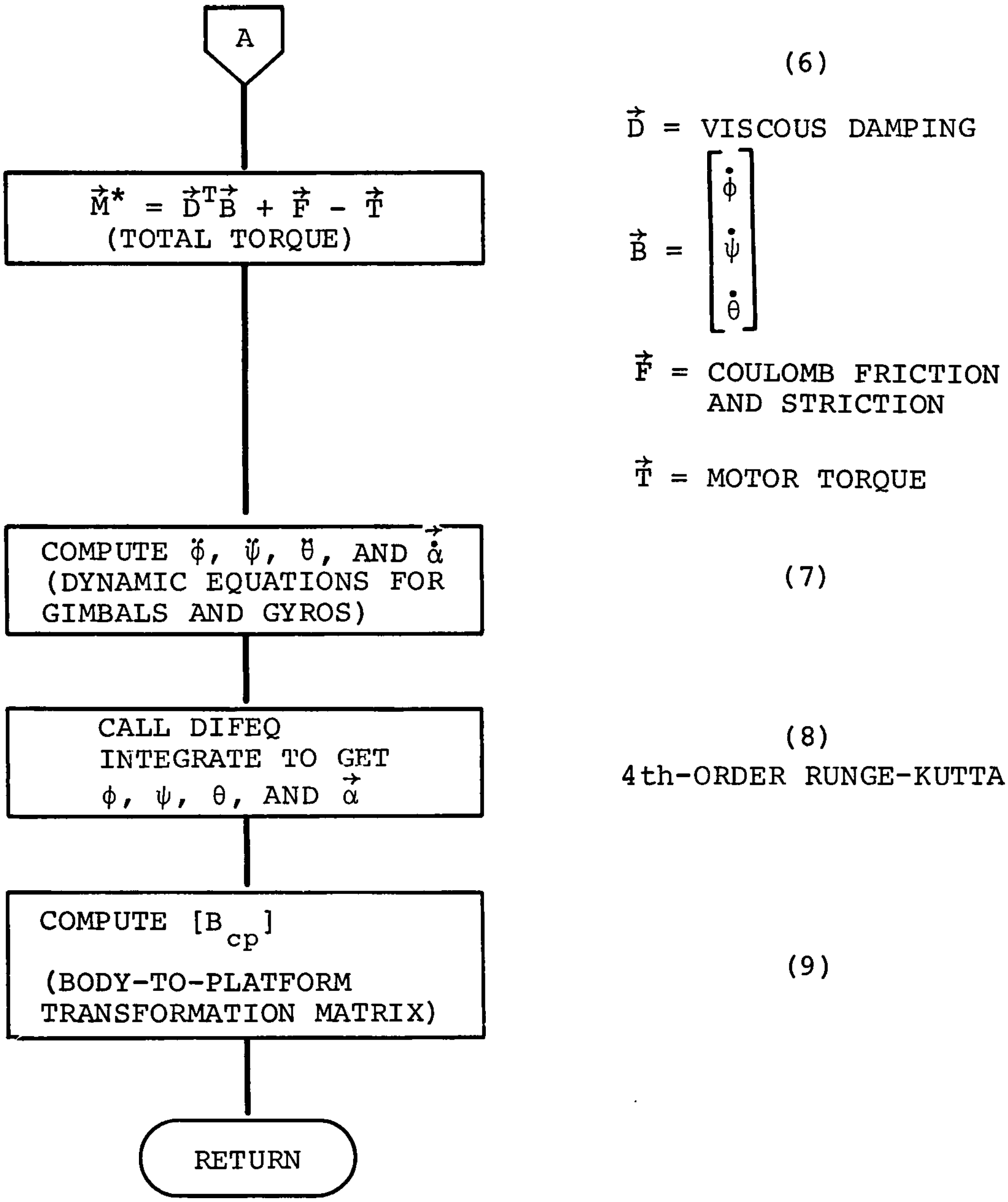

FIGURE 17 (Concluded)

GENERAL FLOW CHART

$\ddot{\phi}$, $\ddot{\psi}$, $\ddot{\theta}$, $\dot{\alpha}_x$, $\dot{\alpha}_y$, and $\dot{\alpha}_z$ are calculated in block 7, and are used by the integration subroutine. Subroutine DIFEQ is called in block 8 and the state equations are integrated using a 4th-order Runge-Kutta scheme. When an integration cycle has been completed, the program proceeds to block 9 where the body-to-platform transformation $[B_{cp}]$ is computed from the Euler angles. A comprehensive flow diagram with common locations defined and a FORTRAN listing of PLTFRMS, NEWACC, and DIFEQ are presented in Appendix A.

CHAPTER VI

CONCLUSIONS AND RECOMMENDATIONS

This thesis developed a mathematical model for the three-gimbal IMU stable member and a FORTRAN subroutine to simulate its motion.

The kinematic relationships between the system members were developed in Chapter II. Equations 2-60 and 2-79 represent the relationship between the case and the platform. The gyro-to-platform relationships are presented in Equations 2-84, 2-87, 2-88, 2-96, 2-101, and 2-102.

Chapter III developed the dynamic equations of motion (3-90 through 3-95) for the mechanical members (gimbals and gyros) of a three-gimbal IMU, including damping, friction, and inertial effects. The control loop components were modeled including demodulators, resolvers, compensation networks, and torque motors. A frequency-domain analysis indicated that the high-frequency (time constants less than 5 msec) terms may be eliminated without severely affecting the system response or stability. The equations of motion are reduced to Equations 5-59 through 5-64 for the low-frequency representation of the gimbals and gyros.

Figure 15 and the associated filter and resolver equations (5-80 through 5-85) represent the low-frequency mechanization of the three-gimbal IMU stable member. Subroutine PLTFRM is programmed from the low-frequency system representation.

This thesis developed subroutine PLTFRM to simulate the angular motion of a three-gimbal IMU stable member. This subroutine is a tool for studying the environment to which inertial instruments are subjected when mounted on the stable member.

PLTFRM was tested (described in Appendix D) under a variety of stationary axis and coning motion conditions. The results closely paralleled available Apollo test data.

The development of this simulation is prerequisite to performing extensive studies to relate specific mission profiles with the environment to which the inertial instruments are subjected. Realistic studies of platform-mounted instrument errors may be performed using PLTFRM to simulate the stable-member motion.

The high-frequency model presented can be used as the basis for developing a hybrid simulation which maintains all the dynamic terms of the system. A simulation of this nature would be of use in studying servoloop components.

REFERENCES

REFERENCES

Arnold, Ronald N., and Leonard Maunder. Gyrodynamics and its Engineering Applications. New York: Academic Press, 1961.

Beckett, Royce, and James Hart. Numerical Calculations and Algorithms. New York: McGraw-Hill Book Company, Inc., 1967.

Bode, H. W. Network Analysis and Feedback Amplifier Design. Princeton, N.J.: Van Nostrand Company, Inc., 1945.

Chestnut, Harold, and R. W. Mayer. Servomechanisms and Regulating System Design. Vol I. New York: John Wiley and Sons, Inc., 1951.

Gibson, John E. Nonlinear Automatic Control. New York: McGraw-Hill Book Company, Inc., 1963.

Goodman, L. E., and A. R. Robinson. "Effects of Finite Rotations on Gyroscope Sensing Devices," J. Appl. Mech., Vol. XXV, June 1958.

Greenwood, Donald T. Principles of Dynamics. New York: Prentice-Hall, Inc., 1965.

Halfman, Robert L. Dynamics. Vol I. New York: Addition Wesley Publishing Company, Inc., 1962.

Hildebrand, Francis B. Methods of Applied Mathematics. New York: Prentice-Hall, Inc., 1952.

Richardson, L. I. T. The Gyroscope Applied. London: Hutchinson's Scientific and Technical Publications, 1954.

Savet, Paul H. (ed.) Gyroscopes: Theory and Design. New York: McGraw-Hill Book Company, Inc., 1961.

Sutherland, A. A., Jr., and William S. Beebee. "Design of Strapdown Gyroscopes for a Dynamic Environment," Houston: NASA Contractor Report CR-1396.

Thomson, William T. Introduction to Space Dynamics. New York: John Wiley and Sons, Inc., 1961.

APPENDIXES

APPENDIX A

COMPUTER PROGRAM DOCUMENTATION

The program documentation consists of a detailed flow diagram (Figure 18), a description of the input common for subroutine PLTFRM (page 110), and a FORTRAN listing of subroutine PLTFRM (page 113), with its associated subroutines NEWACC, DEFEQ, MXV, and REAL FUNCTION SGN. Chapter V described the program organization and included a general flow diagram.

Mr. L. A. White of the Lockheed Electronics Company performed the programming and checkout of PLTFRM and its associated routines.

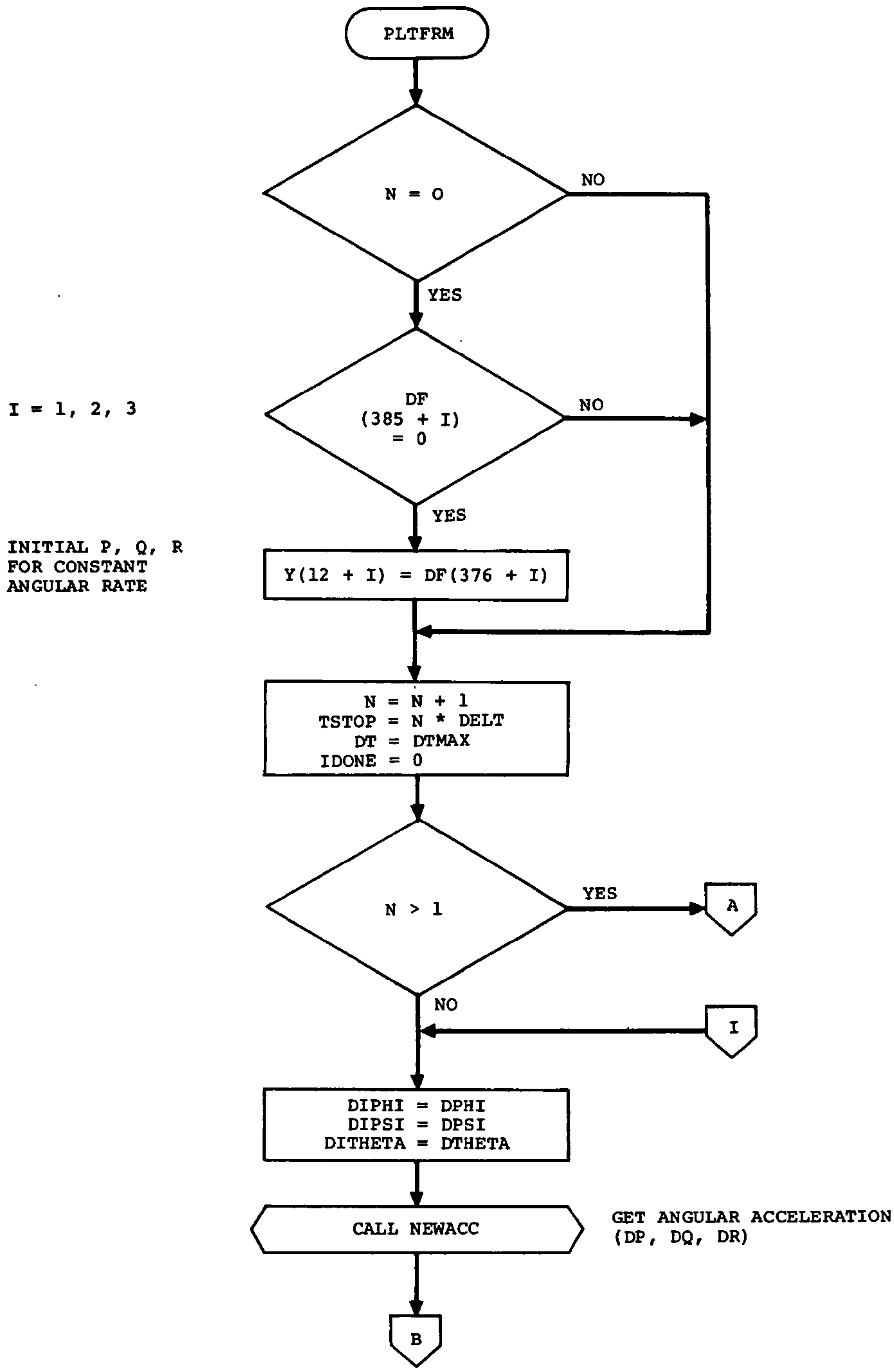

FIGURE 18

DETAILED FLOW DIAGRAM

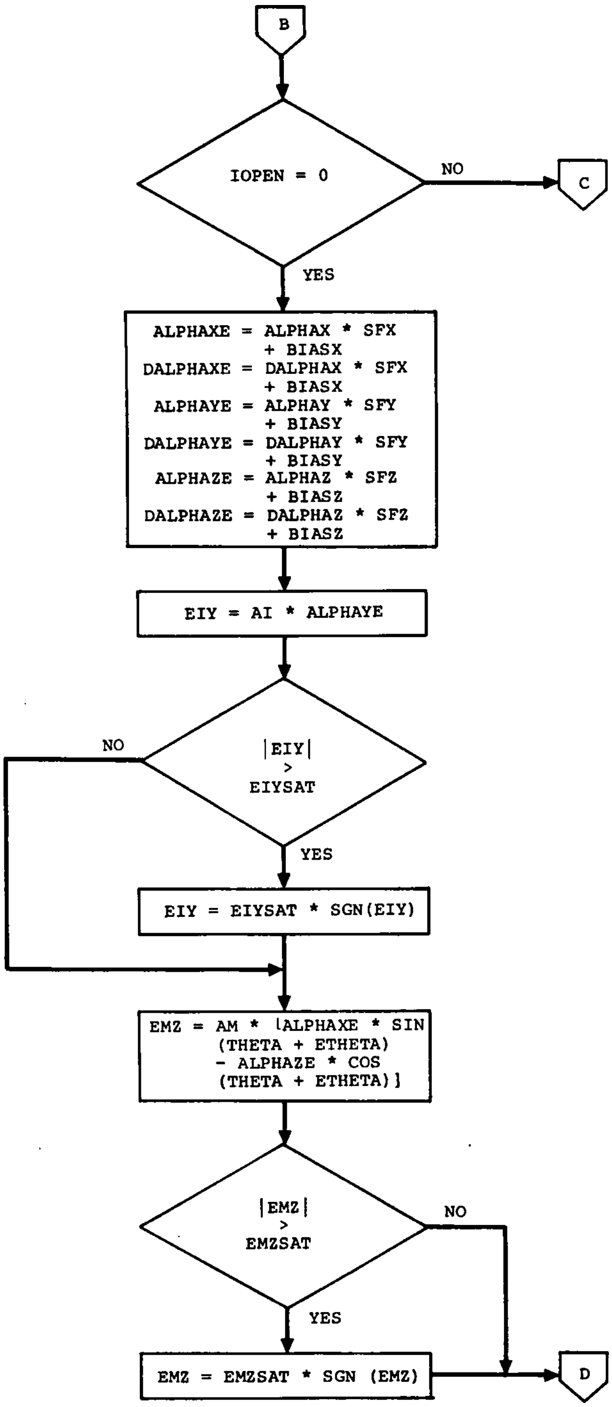

FIGURE 18 (Continued)

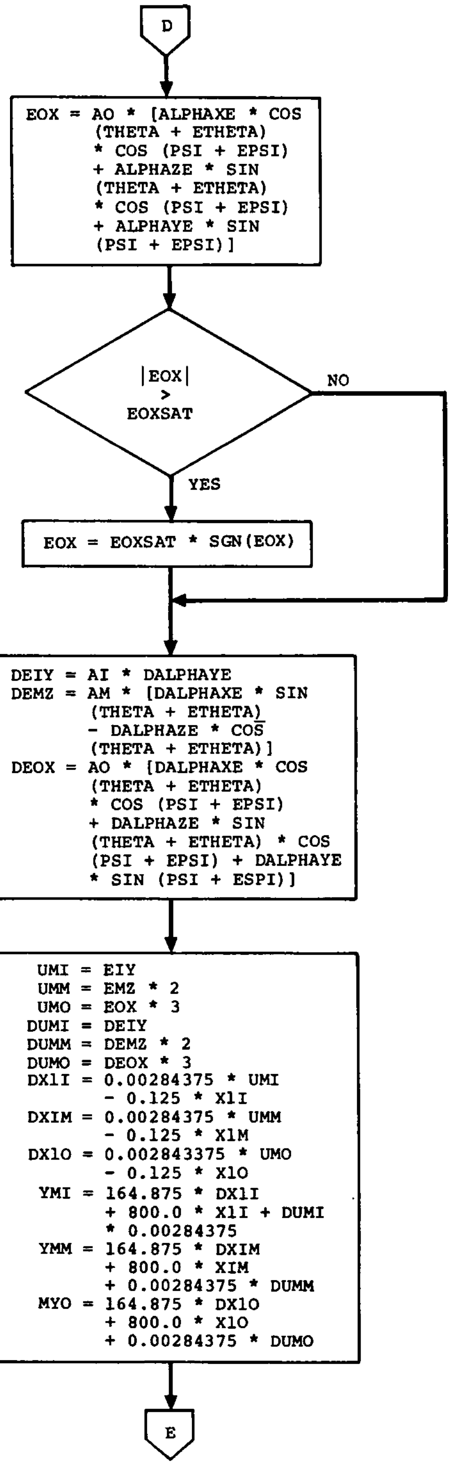

FIGURE 18 (Continued

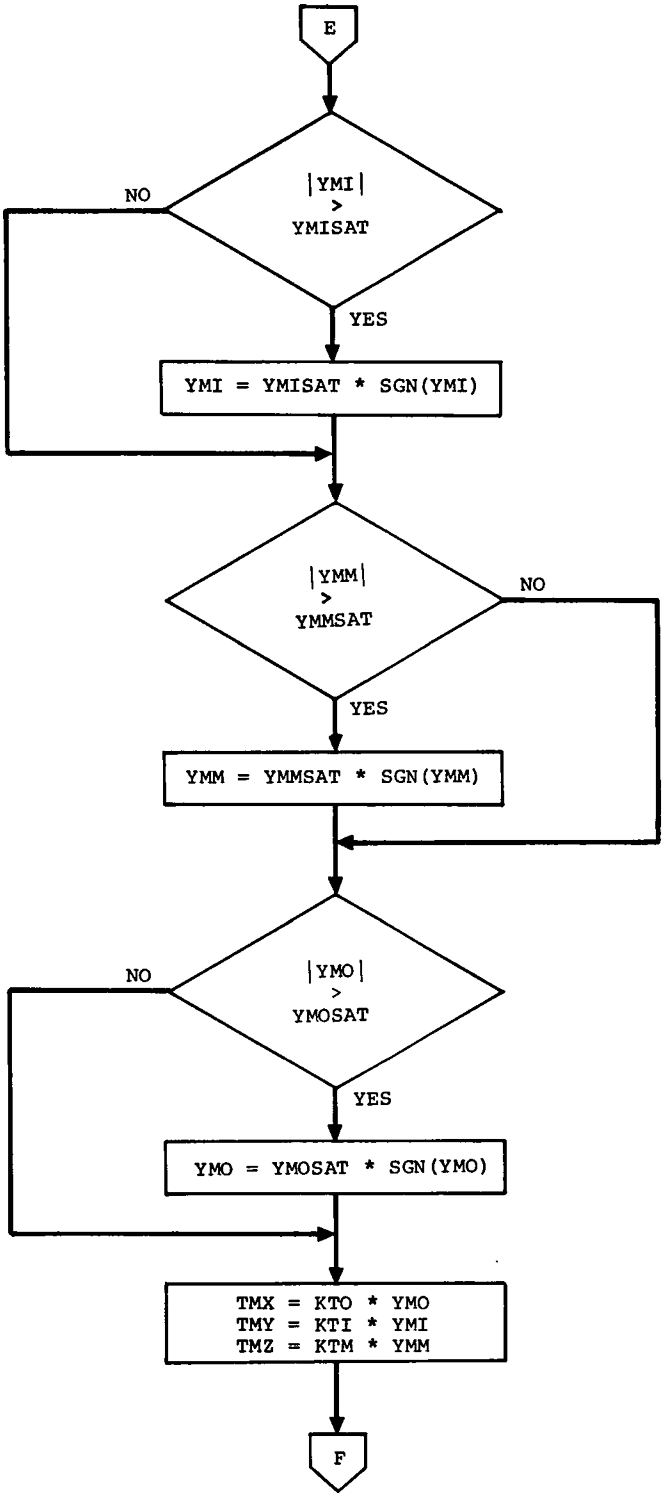

FIGURE 18 (Continued)

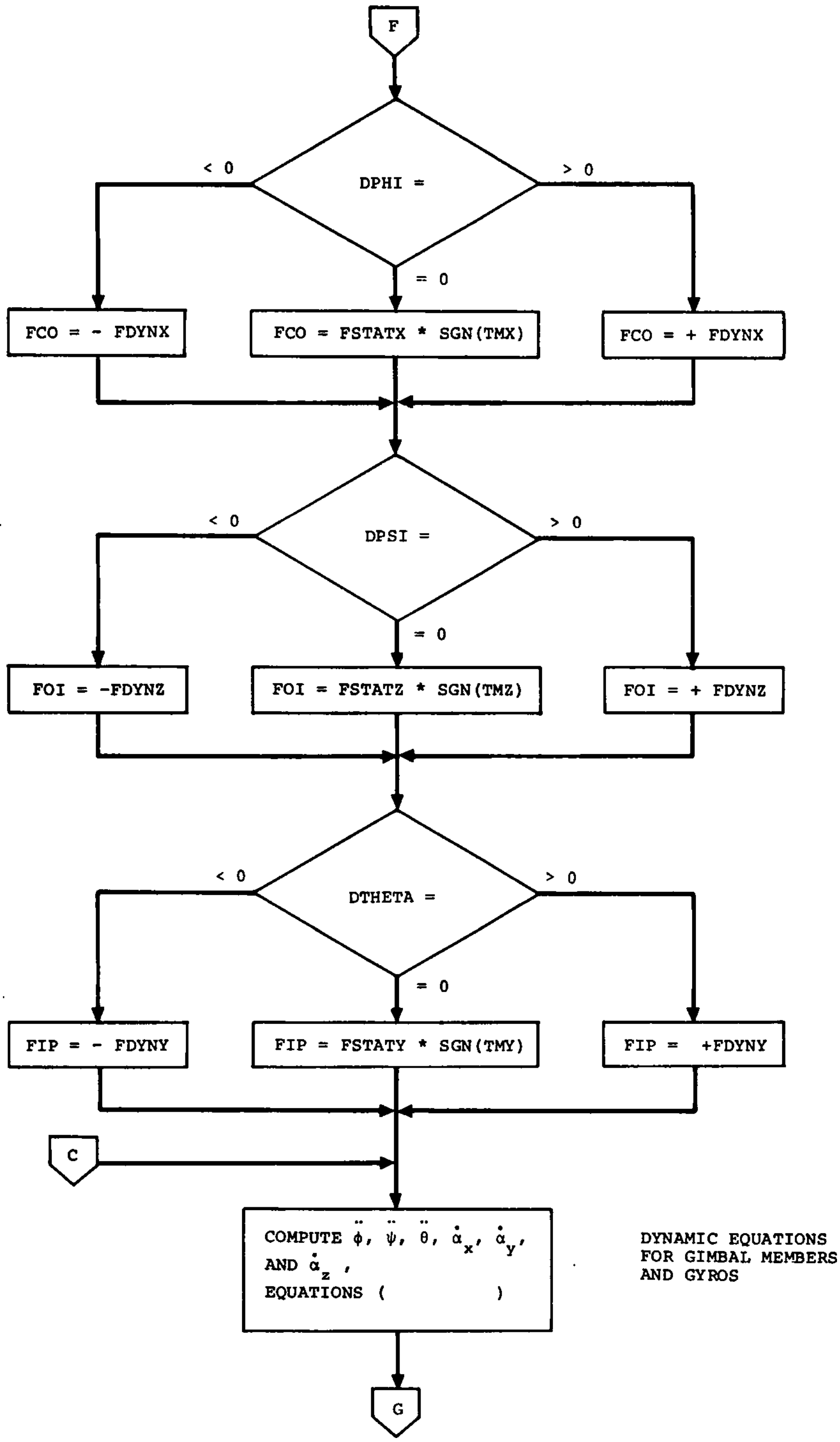

FIGURE 18 (Continued)

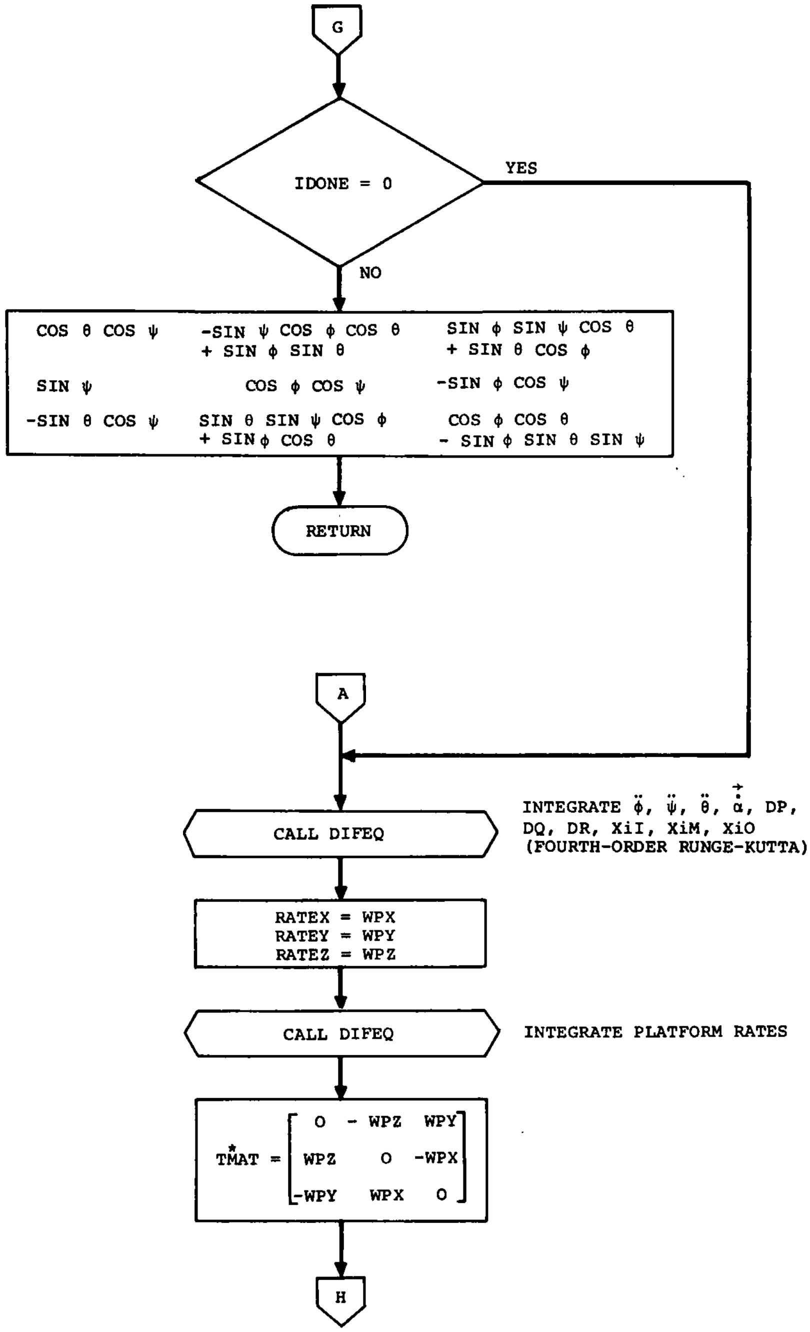

FIGURE 18 (Continued)

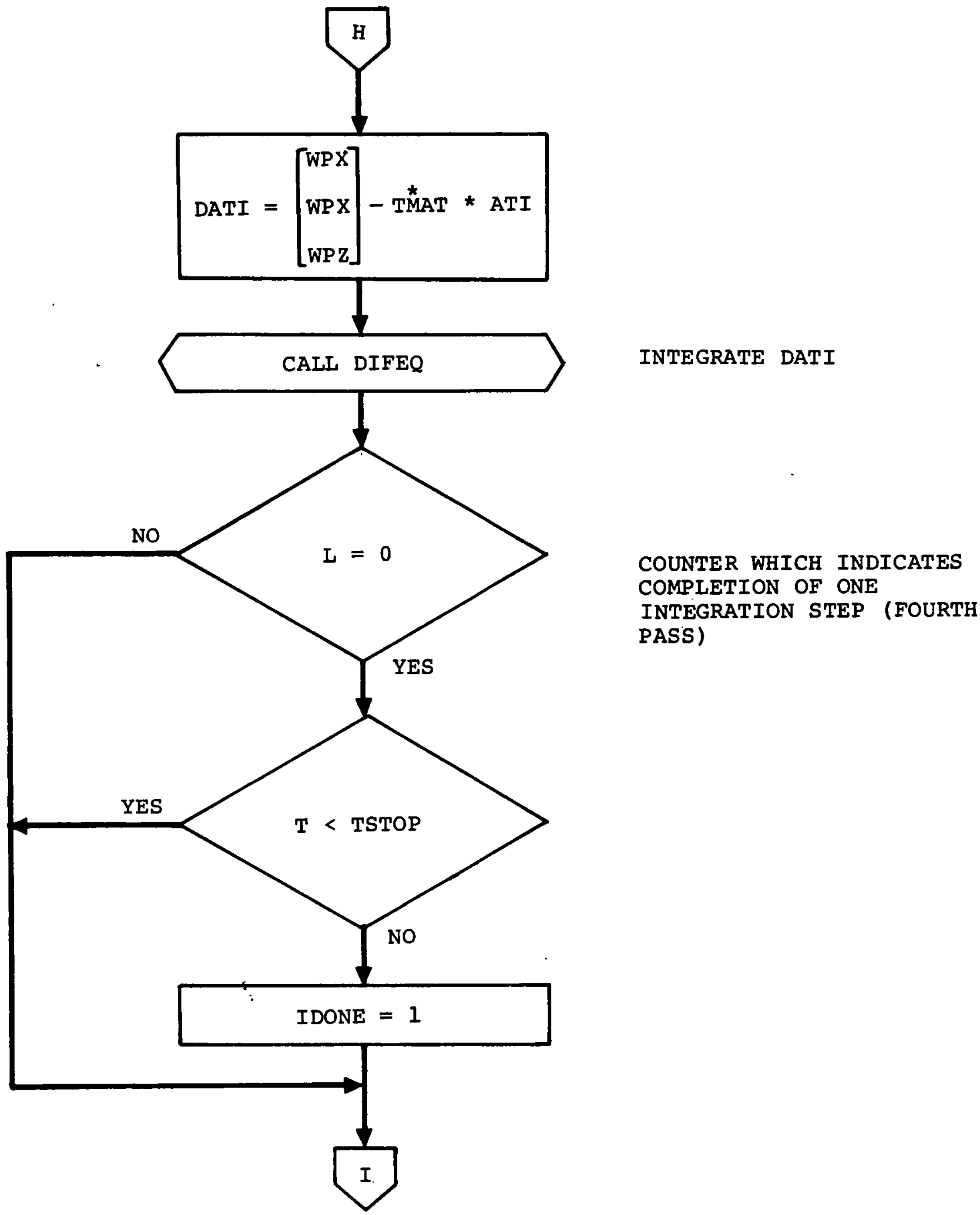

FIGURE 18 (Concluded)

INPUT COMMON DESCRIPTION

Subroutine PLTFRM Common BLK1

Location	Symbol	Description
1	PHI	Outer gimbal angle
2	PSI	Middle gimbal angle
3	THETA	Inner gimbal angle
4	DPHI	Outer gimbal angle rate
5	DPSI	Middle gimbal angle rate
6	DTHETA	Inner gimbal angle rate
62-64	HWX HWY HWZ	Gyro angular momentum
65-67	IGXI IGYI IGZI	Float moment of inertia about respective gyro input axes
68-70	IGXS IGYS IGZS	Float moment of inertia about respective gyro spin axes
71-73	IGXO IGYO IGZO	Float moment of inertia about respective gyro output axes
74-76	IPX IPY IPZ	Platform moments of inertia
77-79	IIX IIY IIZ	Inner gimbal moments of inertia
80-82	IOX IOY IOZ	Outer gimbal moments of inertia
83-85	DIP DDI DCO	Viscous damping

Location	Symbol	Description
92-94	SFX SFY SFZ	Scale factor-multiplicative perturbation to gyro error signal α
95-97	BIASX BIASY BIASZ	Additive perturbation to gyro error signal α
101	DTMAX	Integration time step
104-105	FSTATX FDYNX	Static and dynamic (Coulomb) friction torque between case and outer gimbal
106-107	FSTATY FDYNY	Static and dynamic (Coulomb) friction torque between inner gimbal and platform
108-109	FSTATZ FDYNZ	Static and dynamic (Coulomb) friction torque between inner and outer gimbals
110-112	AI AM AO	Preamp gains
113-115	EIYSAT EMZSAT EOXSAT	Preamp saturation limits
122-124	YMISAT YMMSAT YMOSAT	Compensation filter saturation limits
125-127	KTI KTM KTO	Torque motor gains
128-130	DGXO DGYO DGZO	Viscous damping on respective gyro output axes
131	DELT	Update time increment for each call to PLTFRM routine
223-225	EPHI EPSI ETHETA	Misalignment (offset) errors incorporated into respective gimbal angles in resolver

Location	Symbol	Description
201-209	TSV(1-9)	Estimated body-to-stable-member (platform transformation matrix
377-379	P,Q,R	Vehicle angular velocity
336-338	DP,DQ,DR	Vehicle angular acceleration

```
SUBROUTINE PLTFRM
COMMON/DFILE/DF(600)
COMMON/DRIFT/ATI(3),DATI(3),SCRTCH(7),TMAT(9)
COMMON/BLK1/Y(61),HWX,HWY,HWZ,IGXI,IGYI,IGZI,IGXS,IGYS,
 IGZS,IGXO,IGYO,IGZO,IPX,IPY,IPZ,IIX,IIY,IIZ,IOX,IOY,IOZ,
 DIP,DOI,DCO,FIP,FOI,FCO,TMX,TMY,TXZ,SFX,SFY,SFZ,BIASX,
 BIASY,BIASZ,EIY,EMZ,EOX,DTMAX,DT,T,FSTATX,FDYNX,FSTATY,
 FDYNY,FSTATZ,FDYNZ,AI,AM,AO,EIYSAT,EMZSAT,EOXSAT,UMI,
 UMM,UMO,YMI,YMM,YMO,YMISAT,YMMSAT,YMOSAT,KTI,KTM,KTO,
 DGXO,DGYO,DGZO,DELT,IOPEN,AIPHI,AIPSI,AOPHI,AOPSI,
 APPHI,APTHETA,DCHEK,DWIX,DWIY,DWIZ,DWOX,DWOY,DWOZ,DWPX,
 DWPY,DWPZ,GXPHI,GXPSI,GYPHI,GYPSI,GZPHI,GZPSI,L,L2,T2,
 MCOX,MIPY,MOIZ,WGXI,WGXO,WGXS,WGYI,WGYO,WGYS,WGZI,WGZO,
 WGZS,WIX,WIY,WIZ,WOX,WOY,WOZ,WPX,WPY,WPZ,DUMI,DUMM,
 DUMO,ANGPX,ANGPY,ANGPZ,RATEX,RATEY,RATEZ,WORK(7),LGXW,
 LGYW,LGZW,MGXW,MGYW,MGZW,MPYW,MIZW,MOXW,MA,MB,MC,AXPHI,
 AXPSI,AYPHI,AYPSI,AZPHI,AZPSI,APHI,APSI,ATHETA,BPHI,
 BPSI,CPHI,CPSI,TEMP1,TEMP2,TEMP3,EPHI,EPSI,ETHETA
EQUIVALENCE(Y(1),PHI),(Y(2),PSI),(Y(3),THETA),(Y(4)DPHI),
            (Y(5),DPSI),(Y(6),DTHETA),(Y(7),ALPHAX),
            (Y(8),ALPHAY,(Y(9),ALPHAZ),(Y(10),X1I),
            (Y(11),X1M),(Y(12),X1O),(Y(13),P),(Y(14),Q),
            (Y(15),R),(Y(16),D1PHI),(Y(17),D1PSI,
            (Y(18),D1THETA),(Y(19),D2PHI,(Y(20),D2PSI),
            (Y(21),D2THETA),(Y(22),DALPHAX),(Y(23),DALPHAY),
            (Y(24),DALPHAZ),(Y(25),DX1I),(Y(26),DX1M),
            (Y(27),DX1O),(Y(28),DP),(Y(29),DQ),(Y(30),DR)
DIMENSION SET(222)
EQUIVALENCE (SET(1),Y(1))

DATA (SET(62) = 4.34E5,4.34E5,4.34E5),
     (SET(65) = 650.8,650.8,650.8),
     (SET(68) = 724.9,724.9,724.9),
     (SET(71) = 367.3,367.3,367.3),
     (SET(74) = 4.2085E5,2.6303E5,4.2085E5),
     (SET(77) = 3.5015E5,5.2270E5,5.3658E5),
     (SET(80) = 1.0631E6,1.0067E6,8.8841E5),
     (SET(83) = 4.0E4,4.0E4,4.0E4),
     (SET(101) = 0.0009765625),
     (SET(104) = 1.76539E6,1.4123E6),
     (SET(106) = 1.76539E6,1.4123E6),
     (SET(108) = 1.76539E6,1.4123E6),
     (SET(110) = 1650.0,1650.0,1650.0),
     (SET(113) = 1.0E3,1.0E3,1.0E3),
     (SET(122) = 1.0E3,1.0E3,1.0E3),
     (SET(125) = 1.5185163E7,1.5185163E7,1.5185163E7),
     (SET(128) = 4.75E5,4.75E5,4.75E5)
```

```
      REAL IGXI,IGYI,IGZI,IGXS,IGYS,IGZS,IGXO,IGYO,IGZO,IPX,
       IPY,IPZ,IIX,IIY,IIZ,IOX,IOY,IOZ,MIPY,MOIZ,MCOX,KTI,
       KTM,KTO,LGXW,LGYW,LGZW,MGXW,MGYW,MGZW,MPYW,MIZW,MOXW,
       MA,MB,MC,MOZY,MIZY,MIXZ,MPZY,MPYX,MIYX,MPXZ
      DATA(SFX=1.0),SFY=1.0),(SFZ=1.0)
      DIMENSION TSV(9)
      EQUIVALENCE (TSV,DF(201))
      IF(N,NE.0) GO TO 4
      DO 3 I=1,3
      IF(DF(385+I).NE.0.)GO TO 3
      Y(12+I) = DF(376+I)
    3 CONTINUE
    4 N = N+1
      TSTOP = N * DELT
      DT = DTMAX
      IDONE = 0
      IF(N.GT.1) GO TO 200
   10 D1PHI = DPHI
      D1PSI = DPSI
      D1THETA = DTHETA
      CALL NEWACC(T,DP,DQ,DR)
      SPH = SIN(PHI)
      SPS = SIN(PSI)
      STH = SIN(THETA)
      CPH = COS(PHI)
      CPS = COS(PSI)
      CTH = COS(THETA)
      IF(IOPEN.NE.0) GO TO 131
      SPHE = SIN(PHI+EPHI)
      SPSE = SIN(PHI+EPSI)
      STHE = SIN(THETA+ETHETA)
      CPHE = COS(PHI+EPHI)
      CPSE = COS(PSI+EPSI)
      CTHE = COS(THETA+ETHETA)
```

```
ALPHAXE = ALPHAX*SFX + BIASX
DALPHAXE = DALPHAX*SFX + BIASX
ALPHAYE = ALPHAY*SFY + BIASY
DALPHAYE = DALPHAY*SFY + BIASY
ALPHAZE = ALPHAZ*SFZ + BIASZ
DALPHAZE = DALPHAZ*SFZ + BIASZ
EIY = AI * ALPHAYE
IF(ABS(EIY).GT.EIYSAT) EIY = EIYSAT * SGN(EIY)
EMZ = AM * (ALPHAXE*STHE - ALPHAZE*(CTHE))
IF(ABS(EMZ).GT.EMZSAT) EMZ = EMZSAT * SGN(EMZ)
EOX = AO * (ALPHAXE*CTHE*CPSE+ALPHAZE*STHE*CPSE
      +ALPHAYE*SPSE)
IF(ABS(EOX).GT.EOXSAT) EOX = EOXSAT * SGN(EOX)
DEIY = AI * DALPHAYE
DEMZ = AM * (DALPHAXE*STHE - DALPHAZE*CTHE)
DEOX = AO * (DALPHAXE*CTHE*CPSE+DALPHAZE*STHE*CPSE
       +DALPHAYE*SPSE)
UMI = EIY
DUMI = DEIY
UMM = EMZ * 2.0
DUMM = DEMZ * 2.0
UMO = EOX * 3.0
DUMO = DEOX * 3.0
DX1I = 0.00284375*UMI - 0.125*X1I
DX1M = 0.00284375*UMM - 0.125*X1M
DX1O = 0.00284375*UMO - 0.125*X1O
YMI = 164.875*DX1I + 800.0*X1I + 0.00284375*DUMI
YMM = 164.875*DX1M + 800.0*X1M + 0.00284375*DUMM
YMO = 164.875*DX1O + 800.0*X1O + 0.00284375*DUMO
IF(ABS(YMI).GT.YMISAT) YMI = YMISAT * SGN(YMI)
IF(ABS(YMM).GT.YMMSAT) YMM = YMMSAT * SGN(YMM)
IF(ABS(YMO).GT.YMOSAT) YMO = YMOSAT * SGN(YMO)
TMX = KTO * YMO
```

```
    TMY = KTI * YMI
    TMZ = KTM * YMM
    IF(DPHI)120,121,122
120 FCO = -FDYNX
    GO TO 123
121 FCO = FSTATX * SGN(TMX)
    TO TO 123
122 FCO = FDYNX
123 IF(DPSI)124,125,126
124 FOI = -FDYNZ
    TO TO 127
125 FOI = FSTATZ * SGN(TMZ)
    GO TO 127
126 FOI = FDYNZ
127 IF(DTHETA)128,129,130
128 FIP = -FDYNY
    GO TO 131
129 FIP = FSTATY * SGN(TMY)
    GO TO 131
130 FIP = FDYNY
131 CONTINUE
    WOX = P - DPHI
    WOY = Q*CPH - R*SPH
    WOZ = Q*SPH + R*CPH
    DWOX = DP
    DWOY = DQ*CPH - DR*SPH - DPHI*WOZ
    DWOZ = DQ*SPH + DR*CPH + DPHI*WOY
    WIX = WOX*CPS - WOY*SPS
    WIY = WOX*SPS + WOY*CPS
    WIZ = WOZ - DPSI
    DWIX = DP*CPS - DWOY*SPS - WIY*DPSI
    DWIY = DP*SPS + DWOY*CPS + WIX*DPSI
```

```
DWIZ = DWOZ
WPX = WIX*CTH + WIZ*STH
WPY = WIY - DTHETA
WPZ = -WIX*STH + WIZ*CTH
DWPX = DTHETA*WPZ + DWIX*CTH + DWOZ*STH
DWPY = DWIY
DWPZ = -DTHETA*WPX - DWIX*STH + DWOZ*CTH
WGXS = -WPY
WGXI = WPX
WGXO = WPZ + DALPHAX
WGYS = -WPZ
WGYI = WPY
WGYO = WPX + DALPHAY
WGZS = -WPY
WGZI = -WPZ
WGZO = WPX + DALPHAZ
MIPY = DIP*DTHETA + FIP - TMY
MOIZ = DOI*DPSI + FOI - TMZ
MCOX = DCO*DPHI + FCO - TMX
APTHETA = -((IGXS+IGYI+IGZS)/IPY + 1.)
APPHI = APTHETA * SPS
AIPSI = -(1. + STH**2*((IPX+IGXI)/IIZ)
        + CTH**2*((IPZ+IGYS+IGZI)/IIZ))
AIPHI = -STH * CTH * CPS * (IPX-IPZ+IGXI-IGYS-IGZI)/IIZ
AOPHI = -(1. + CPS**2*(IIX+CTH**2*(IPX+IGXI)
        + STH**2*(IPZ+IGYS+IGZI))/IOX + SPS**2*IIY/IOX)
AOPSI = -CTH * STH * CPS * (IPX+IGXI-IPZ-IGYS-IGZI)/IOX
AXPHI = IGXO/DGXO*STH*CPS
AXPSI = -IGXO/DGXO*CTH
AYPHI = -IGYO/DGYO*CTH*CPS
AYPSI = -IGYO/DGYO*STH
AZPHI = -IGZO/DGZO*CTH*CPS
```

```
AZPSI = -IGZO/DGZO*STH
HX = (IGXI+IGXO-IGXS)*WPY + HWX
HY = (IGYS+IGYO-IGYI)*WPY - HWY*ALPHAY
HZ = (IGZI+IGZO-IGZS)*WPY + HWZ
HPX = (IGXI-IGXS-IGXO)*WPX + HWX*ALPHAX
HPY = (IGYI+IGYO-IGYS)*WPZ + HWY
HPZ = (IGZS+IGZO-IGZI)*WPZ + HWZ*ALPHAZ
AOX = (HX*CTH*CPS + DGXO*STH*CPS)/IOX
AOY = (HY*STH*CPS - DGYO*CTH*CPS)/IOX
AOZ = (HZ*STH*CPS - DGZO*CTH*CPS)/IOX
AIX = (HX*STH - DGXO*OTH)/IIZ
AIY = (-HY*CTH - DGYO*STH)/IIZ
AIZ = (-HZ*CTH - DGZO*STH)/IIZ
APX = HPX/IPY
APY = HPY/IPY
APZ = HPZ/IPY
LGXW = (HWX*WGXI - (IGXI-IGXS)*WGXI*WGXS - IGXO*DWPZ)/DGXO
LGYW = (HWY*WGYI - (IGYI-IGYS)*WGYI*WGYS - IGYO*DWPX)/DGYO
LGZW = (HWZ*WGZI - (IGZI-IGZS)*WGZI*WGZS - IGZO*DWPX)/DGZO
MGXW = IGXI*DWPX+HWX*WPZ+(IGXO-IGXS)*WPZ*WPY
MGYW = (IGXO+IGYS+IGZI-IGXI-IGYO-IGZO)*WPX*WPZ-HWY*WPX
       -HWX*WPZ*ALPHAX-HWZ*WPX*ALPHAZ-(IGXS+IGYI
       +IGZS)*DWPY
MGZW = (IGYO+IGZO-IGYI-IGZS)*WPX*WPY+(HWZ-HWY*ALPHAY)*WPX
       -(IGYS+IGZI)*DWPZ
MOZY = (IOZ-IOY)*WOZ*WOY
MIZY = (IIZ-IIY)*WIZ*WIY + IIX*DWIX
MIXZ = (IIX-IIZ)*WIZ*WIX + IIY*DWIY
MPZY = (IPZ-IPY)*WPZ*WPY + IPX*DWPX
MPYX = (IPY-IPX)*WPX*WPY + IPZ*DWPZ
MIYX = (IIY-IIX)*WIX*WIY
MPXZ = (IPX-IPZ)*WPX*WPZ
MOXW = (MCOX-MOZY-MIZY*CPS-MIXZ*SPS-MIPY*SPS
       -MGXW*CTH*CPS-MGZW*STH*CPS-MPZY*CTH*CPS
       +MPYX*STH*CPS)/IOX - DWOX
```

```
    MIZW = (MOIZ-MIYX-(MPZY+MGXW)*STH-(MPYX-MGZW)*OTH)/IIZ
          -DWIZ
    MPYW = (MIPY-MPXZ+MGYW)/IPY - DWPY
    MA = MPYW - APX*LGXW - APY*LGYW - APZ*LGZW
    MB = MIZW - AIX*LGXW - AIY*LGYW - AIZ*LGZW
    MC = MOXW - AOX*LGXW - ACY*LGYW - AOZ*LGZW
    APHI = APPHI - APX*AXPHI - APY*AYPHI - APZ*AZPHI
    APSI = APX*AXPSI + APY*AYPSI + APZ*AZPSI
    ATHETA = APTHETA
    BPHI = AIPHI - AIX*AXPHI - AIY*AYPHI - AIZ*AZPHI
    BPSI = AIPSI - AIX*AXPSI - AIY*AYPSI - AIZ*AZPSI
    CPHI = AOPHI - AOX*AXPHI - AOY*AYPHI - AOZ*AZPHI
    CPSI = AOPSI - AOX*AXPSI - AOY*AYPSI - AOZ*AZPSI
    TEMP1 = MB*CPSI - MC*BPSI
    TEMP2 = BPHI*CPSI - BPSI*CPHI
    TEMP3 = MC*BPHI - MB*CPHI
    D2PHI = TEMP1/TEMP2
    D2PSI = TEMP3/TEMP2
    D2THETA = ((APSI*TEMP3 - APHI*TEMP1)/TEMP2 + MA)/ATHETA
    DALPHAX = LGXW - AXPHI*D2PHI - AXPSI*D2PSI
    DALPHAY = LGYW - AYPHI*D2PHI - AYPSI*D2PSI
    DALPHAZ = LGZW - AZPHI*D2PHI - AZPSI*D2PSI
    IF(IDONE.EQ.0) GO TO 200
    TSV(1) = CTH * CPS
    TSV(2) = SPS
    TSV(3) = -STH * CPS
    TSV(4) = -SPS*CPH*CTH + SPH*STH
    TSV(5) = CPH*CPS
    TSV(6) = STH*SPS*CPH + SPH*CTH
    TSV(7) = SPH*SPS*CTH + STH*CPH
    TSV(8) = -SPH*CPS
    TSV(9) = CPH*CTH - SPH*STH*SPS
    RETURN
200 CONTINUE
```

```
CALL DIFEQ(15,T,DT,Y,L)
RATEX = WPX
RATEY = WPY
RATEZ = WPZ
CALL DIFEQ(3,T2,DT,ANGPX,L2)
TMAT(2) = WPZ
TMAT(3) = -WPY
TMAT(4) = -TMAT(2)
TMAT(6) = WPX
TMAT(7) = -TMAT(3)
TMAT(8) = -TMAT(6)
CALL MXV(TMAT,ATI,DATI)
DATI(1) = WPX - DATI(1)
DATI(2) = WPY - DATI(2)
DATI(3) = WPZ - DATI(3)
CALL DIFEQ(3,T3,DT,ATI,L3)
IF(L.NE.0) GO TO 10
IF(T.LT.TSTOP) GO TO 10
IDONE = 1
GO TO 10
END
```

```
      SUBROUTINE NEWACC(T,DP,DQ,DR)
      COMMON/INAXIS/DELT,ALPHA,BETA,C1,C2,C3,C4,C5
      DOUBLE PRECISION TEMP1, TEMP2, U1, U2, U3
      DATA(INIT=0)
      IF(INIT.EQ.1) GO TO 10
      INIT = 1
      TEMP1 = DBLE(ALPHA)
      TEMP2 = DBLE(BETA)
      U1 = DCOS(TEMP1)*DCOS(TEMP2)
      U2 = DSIN(TEMP1)*DCOS(TEMP2)
      U3 = -(DSIN(TEMP2))
   10 DOMEG = C2*C3*COS(C3*T - C4) + C5
      DP = U1 * DOMEG
      DQ = U2 * DOMEG
      DR = U3 * DOMEG
      RETURN
      END
```

```
      SUBROUTINE DIFEQ (N,X,DX,Y,I)
      DIMENSION Y(1)
      N2=2*N
      N3=3*N
      DX2=DX/2.0
      IF (I) 20,10,20
   10 Y(4*N+1)=X
      X=X+DX2
   20 I=I+1
      DO 80 K=1,N
      KPN=K+N
      KPN2=K+N2
      KPN3=K+N3
      GO TO (30,40,40,70),I
   30 Y(KPN2)=Y(K)
      Y(KPN2)=Y(KPN)
      GO TO 50
   40 Y(KPN2)=Y(KPN2)+2.0*Y(KPN)
      IF (I-2) 60,50,60
   50 Y(K)=Y(KPN3)+DX2*Y(KPN)
      GO TO 80
   60 Y(K)=Y(KPN3)+DX*Y(KPN)
      GO TO 80
   70 Y(KPN2)=Y(KPN2)+Y(KPN)
      Y(K)=Y(KPN3)+DX*Y(KPN2)/6.0
   80 CONTINUE
      IF (I-3) 100,90,110
   90 X=X+DX2
  100 RETURN
  110 I=0
      RETURN
      END
```

```
      SUBROUTINE MXV(X,Y,Z)
      DIMENSION X(3,3),Y(3),Z(3)
      DO 10 I=1,3
      Z(I)=0.0
      DO 10 J=1,3
   10 Z(I)=Z(I)+X(I,J)*Y(J)
      RETURN
      END
```

```
      REAL FUNCTION SGN(X)
      IF(X) 10,20,30
   10 SGN = -1.0
      RETURN
   20 SGN = 0.0
      RETURN
   30 SGN = 1.0
      RETURN
      END
```

APPENDIX B

PLATFORM SIMULATION DATA

CGS Units	Description
$BIAS_x = 0.0$	Bias error, platform X-axis gyro
$BIAS_y = 0.0$	Bias error, platform Y-axis gyro
$BIAS_z = 0.0$	Bias error, platform Z-axis
$D_{co} = 4 \times 10^4 \dfrac{\text{dyne-CM}}{\text{rad/sec}}$	Viscous damping, case to outer gimbal
$D_{Ip} = 4 \times 10^4 \dfrac{\text{dyne-CM}}{\text{rad/sec}}$	Viscous damping, inner gimbal to platform
$D_{oI} = 4 \times 10^4 \dfrac{\text{dyne-CM}}{\text{rad/sec}}$	Viscous damping, outer gimbal to inner gimbal
$D_{gxO} = .475 \times 10^6 \dfrac{\text{dyne-CM}}{\text{rad/sec}}$	Output axis viscous damping, X-axis gyro
$D_{gyO} = .475 \times 10^6 \dfrac{\text{dyne-CM}}{\text{rad/sec}}$	Output axis viscous damping, Y-axis gyro
$D_{gzO} = .475 \times 10^6 \dfrac{\text{dyne-CM}}{\text{rad/sec}}$	Output axis viscous damping, Z-axis gyro
ESA $T_{II} = \pm 1000.0$ Volts	Preamp saturation limit - inner gimbal loop
ESA $T_{mm} = \pm 1000.0$ Volts	Preamp saturation limit - middle gimbal loop

CGS Units	Description
ESA T_{oo} = ±1000.0 Volts	Preamp saturation limit - outer gimbal loop
F_{co} – F_{Ip} – F_{oI} –	See components of FDYN and FSTAT; X, Y, and Z, respectively
$FDYN_x = 1.4123 \times 10^6$ dyne-CM	Coulomb friction torque, from case to outer gimbal
$FDYN_y = 1.4123 \times 10^6$ dyne-CM	Coulomb friction torque, from inner gimbal to platform
$FDYN_z = 1.4123 \times 10^6$ dyne-CM	Coulomb friction torque, from outer gimbal to inner gimbal
$FSTAT_x = 1.76539 \times 10^6$ dyne-CM	Static friction torque, from case to outer gimbal
$FSTAT_y = 1.76539 \times 10^6$ dyne-CM	Static friction torque, from inner gimbal to platform
$FSTAT_z = 1.76539 \times 10^6$ dyne-CM	Static friction torque, from outer gimbal to inner gimbal
$H_{\omega x} = .434 \times 10^6 \frac{\text{dyne-CM}}{\text{rad/sec}}$	Angular momentum of the platform X-axis gyro
$H_{\omega y} = .434 \times 10^6 \frac{\text{dyne-CM}}{\text{rad/sec}}$	Angular momentum of the platform Y-axis gyro

CGS Units	Description
$H_{\omega z} = .434 \times 10^6 \frac{\text{dyne-CM}}{\text{rad/sec}}$	Angular momentum of the platform Z-axis gyro
$I_{gxI} = 650.8$ gm-cm^2	Float moment of inertia X-gyro input axis
$I_{gxO} = 367.3$ g-cm^2	Float moment of inertia X-gyro output axis
$I_{gxS} = 724.9$ g-cm^2	Float moment of inertia X-gyro spin axis
$I_{gyI} = 650.8$ gm-cm^2	Float moment of inertia Y-gyro input axis
$I_{gyO} = 367.3$ gm-cm^2	Float moment of inertia Y-gyro output axis
$I_{gyS} = 724.9$ gm-cm^2	Float moment of inertia Y-gyro spin axis
$I_{gzI} = 650.8$ gm-cm^2	Float moment of inertia Z-gyro input axis
$I_{gzO} = 367.3$ gm-cm^2	Float moment of inertia Z-gyro output axis
$I_{gzS} = 724.9$ gm-cm^2	Float moment of inertia Z-gyro spin axis
$I_{Ix} = 3.5015 \times 10^5$ gm-cm^2	Inner gimbal X-axis moment of inertia
$I_{Iy} = 5.2270 \times 10^5$ gm-cm^2	Inner gimbal Y-axis moment of inertia
$I_{Iz} = 5.3658 \times 10^5$ gm-cm^2	Inner gimbal Z-axis moment of inertia

CGS Units	Description
$I_{ox} = 1.0631 \times 10^6$ gm-cm^2	Outer gimbal X-axis moment of inertia
$I_{oy} = 1.0067 \times 10^6$ gm-cm^2	Outer gimbal Y-axis moment of inertia
$I_{oz} = 8.8841 \times 10^5$ gm-cm^2	Outer gimbal Z-axis moment of inertia
$I_{px} = 4.2085 \times 10^5$ gm-cm^2	Platform X-axis moment of inertia
$I_{py} = 2.6303 \times 10^5$ gm-cm^2	Platform Y-axis moment of inertia
$I_{pz} = 4.2085 \times 10^5$ gm-cm^2	Platform Z-axis moment of inertia
$K_{aII} = 1650.0$	Preamp gain inner gimbal loop
$K_{amm} = 1650.0$	Preamp gain middle gimbal loop
$K_{aoo} = 1650.0$	Preamp gain outer gimbal loop
$K_{tII} = 1.5185163 \times 10^7 \frac{\text{dyne-CM}}{\text{amp}}$	Torque motor gain inner gimbal to platform
$K_{tmm} = 1.5185163 \times 10^7 \frac{\text{dyne-CM}}{\text{amp}}$	Torque motor gain outer to inner gimbal
$K_{too} = 1.2283712 \times 10^7 \frac{\text{dyne-CM}}{\text{amp}}$	Torque motor gain case to outer gimbal
$SF_x = 1.0$	Scale factor error term X-gyro

CGS Units	Description
$SF_y = 1.0$	Scale factor error term Y-gyro
$SF_z = 1.0$	Scale factor error term Z-gyro
$YMSAT_{II} = \pm 1000.0$ volts	Compensation filter saturation inner gimbal loop
$YMSAT_{mm} = \pm 1000.0$ volts	Compensation filter saturation middle gimbal loop
$YMSAT_{oo} = \pm 1000.0$ volts	Compensation filter saturation outer gimbal loop

APPENDIX C

NOTATION CONVENTION

I. MATRICES

Matrices are represented by a capital letter in brackets. In particular

$$\left[B_{cp}\right] = \text{direction cosine matrix, from case to platform}$$

Coordinate transformation matrices are represented by a pair of lower case subscripts; the first indicates the coordinate frame of the vector to be transformed and the second indicates the coordinate frame of the transformed vector.

II. VECTORS

Vectors are designated by a superwritten arrow

$$\vec{\omega} = \begin{bmatrix} \omega_x \\ \omega_y \\ \omega_z \end{bmatrix}$$

Unit vectors use ^ in place of an arrow over the describing symbol.

The coordinate frame in which the components of a vector are expressed is indicated by an identifying superscript. That is

$$\vec{\omega}_p^I = \text{The angular rate of } P \text{ expressed in } I \text{ coordinates}$$

A vector component is expressed by dropping the arrow and adding appropriate subscripts identifying the coordinate system and component. For example

$$\vec{\omega}^I = \begin{bmatrix} \omega_{Ix} \\ \omega_{Iy} \\ \omega_{Iz} \end{bmatrix}$$

III. VECTOR TIME DERIVATIVES

The time derivatives of a vector vary depending on the absolute rotational rate of the reference system in which it is computed. For this reason, it is necessary to indicate the coordinate system in which the time derivative is taken, as well as in which the components of the time derivative are expressed.

The notation $\dot{\vec{\omega}}$ or ${}^{i}\dot{\vec{\omega}}$ indicates a time derivative with respect to the inertial reference frame. Similarly, ${}^{p}\dot{\vec{\omega}}^{c}$ represents a time derivative with respect to the p reference frame with coordinates in the C frame.

APPENDIX D

TEST CASES AND RESULTS

Subroutine PLTFRM may be used to study the effects of vehicle motion on the attitude of the stable member, navigation base.

A driving program was prepared to call PLTFRM; the Apollo platform described by the system parameters in Appendix B was studied under the influence of stationary axis and coning motion.

I. STATIONARY AXIS MOTION

Stationary axis motion may be described as rotational motion about a single axis S" . The stationary axis of rotation is located by rotating an axis S (initially located along the vehicle X axis) α degrees about the Z-body axis and β degrees about the Y-body axis (Figure 19).

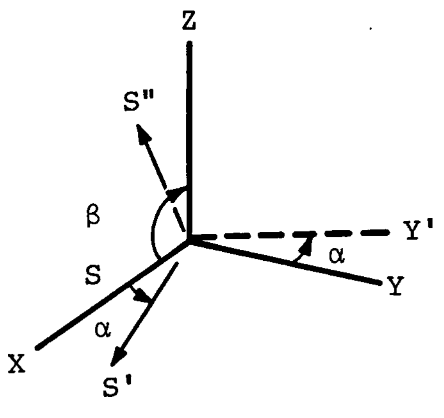

FIGURE 19

STATIONARY AXIS OF ROTATION

The rotational rate magnitude about the stationary axis described is

$$\Omega = C_1 + C_2 \sin (C_3 t - C_4) + C_5 t$$

where

C_1 — Constant rate (Bias)

C_2 — Amplitude of sinusoidal component of rate

C_3 — Frequency of sinusoid

C_4 — Phase shift

C_5 — Ramp component of rate

The closed form integral of Ω is

$$\gamma = C_1 t - \frac{C_2}{C_3} \left[\cos (C_3 t - C_4) \right] + \frac{C_5 t^2}{2} + \gamma_0$$

for the definite integral $t = 0$ to $t = t_f$

$$\gamma = C_1 t_f - \frac{C_2}{C_3} \left[\cos (C_3 t_f - C_4) - \cos C_4 \right] + \frac{C_5 t_f^2}{2}$$

The rate Ω may be expressed as a vector $\vec{\omega}^v$ in vehicle coordinates by multiplying a unit vector of direction cosines $\hat{\beta}$.

$$\hat{B} = \begin{bmatrix} \cos\alpha\cos\beta \\ \sin\alpha\cos\beta \\ -\sin\beta \end{bmatrix} = \begin{bmatrix} b_1 \\ b_2 \\ b_3 \end{bmatrix}$$

$$\vec{\omega}^v = \Omega\hat{B}$$

The reference attitude matrix [T] body to inertial frame may be calculated

$$[T] = \left[T_0\right]\left\{I + [L]\sin\gamma + [L]^2(1 - \cos\gamma)\right\}$$

where

$$[L] = \begin{bmatrix} 0 & -b_3 & b_2 \\ b_3 & 0 & -b_1 \\ -b_2 & b_1 & 0 \end{bmatrix}$$

and $[T_0]$ = initial value of [T].

The matrix [T] represents the closed-form transformation from the body system of the vehicle to the reference inertial frame. The transformation may be compared with $[B_{cp}]$, Equation 2-20, when evaluated with the system Euler angles, and the variation between these transformations represents the platform error.

II. CONING MOTION

Coning motion is more complicated than stationary axis motion. The body coordinate system (Figure 20) is initially rotated through an angle θ about the Y_I axis, which establishes the body coordinate system at $t = 0$. The total body angular rate $\vec{\omega}$ is composed of a rate $\vec{\omega}_p$ aligned with Z_I and another $\vec{\omega}_s$ along Z_B. The body rates are

$$\omega_x = -\omega_p \sin\theta \sin\phi$$

$$\omega_y = \omega_p \sin\theta \cos\phi$$

$$\omega_z = \omega_s + \omega_p \cos\theta$$

where

$$\phi = \omega_s t$$

The reference attitude matrix [T] may be calculated an element at a time and compared with $[B_{cp}]$.

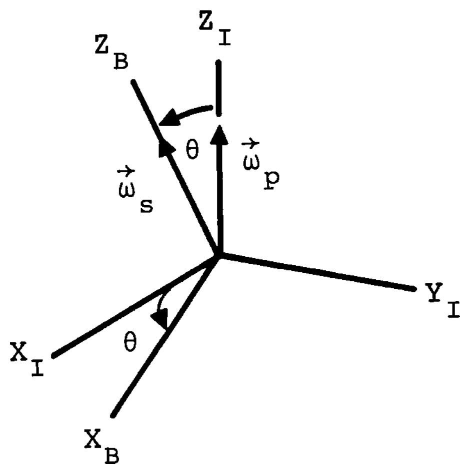

FIGURE 20

CONING MOTION AXES OF ROTATION

The elements of [T] are

$$t_{11} = \cos\psi \cos\theta \cos\phi - \sin\psi \sin\phi$$

$$t_{12} = -\cos\psi \cos\theta \sin\phi - \sin\psi \cos\phi$$

$$t_{13} = \cos\psi \sin\theta$$

$$t_{21} = \sin\psi \cos\theta \cos\phi + \cos\psi \sin\phi$$

$$t_{22} = -\sin\psi \cos\theta \sin\phi + \cos\psi \cos\phi$$

$$t_{23} = \sin\psi \sin\theta$$

$$t_{31} = -\sin\theta\cos\phi$$

$$t_{32} = \sin\theta\sin\phi$$

$$t_{33} = \cos\theta$$

where

$$\psi = \omega_{pt}$$

$$\phi = \omega_{st}$$

and θ = the initial rotation about the Y_I axis establishing the body to inertial attitude at $t = 0$.

III. ATTITUDE ERRORS

The attitude error of the stable member may be expressed as a function of the row vectors making up the reference transformation [T] and $[B_{cp}]$ as evaluated from the simulated platform Euler angles.

Let

$$T = \begin{bmatrix} T_1 \\ T_2 \\ T_3 \end{bmatrix} \quad \text{and} \quad \begin{bmatrix} B_{cp} \end{bmatrix} = \begin{bmatrix} B_1 \\ B_2 \\ B_3 \end{bmatrix}$$

where

$$T_1 = \begin{bmatrix} t_{11} & t_{12} & t_{13} \end{bmatrix}$$

$$T_2 = \begin{bmatrix} t_{21} & t_{22} & t_{23} \end{bmatrix}$$

$$T_3 = \begin{bmatrix} t_{31} & t_{32} & t_{33} \end{bmatrix}$$

and B_1, B_2, and B_3 are the respective row vectors constituting equation 2-20.

Assuming EXP is small, the X-axis attitude error EXP is calculated by

$$EXP = \frac{1}{2} \left\{ T_3 \cdot B_2 - B_3 \cdot T_2 \right\}$$

Similarly

$$EYP = \frac{1}{2} \left\{ T_1 \cdot B_3 - B_1 \cdot T_3 \right\}$$

and

$$EZP = \frac{1}{2} \left\{ T_2 \cdot B_1 - B_2 \cdot T_1 \right\}$$

For the purpose of evaluating the IMU system performance, a time-history of EXP, EYP, and EZP was studied. The criteria used for evaluating the attitude error were the norm, mean, and variance-of-attitude errors (EXP, EYP, and EZP). The norm is defined as the root mean square (rms) of the attitude angles and represents a total attitude error.

IV. TEST CASES

Each test case run includes a time plot of the above-mentioned parameters. (A representative group of test cases is included.) Each case is identified based on the preceding discussion of the driving functions. Test cases include step response, slewing, and sinusoidal stationary axis (STAXIS) cases as well as coning motion.

Test Case 1, 30°/sec Y-axis step response. Stationary axis motion with $\alpha = 90°$, $\beta = 0°$, $Cl = 30°$, 512 plot points per second.

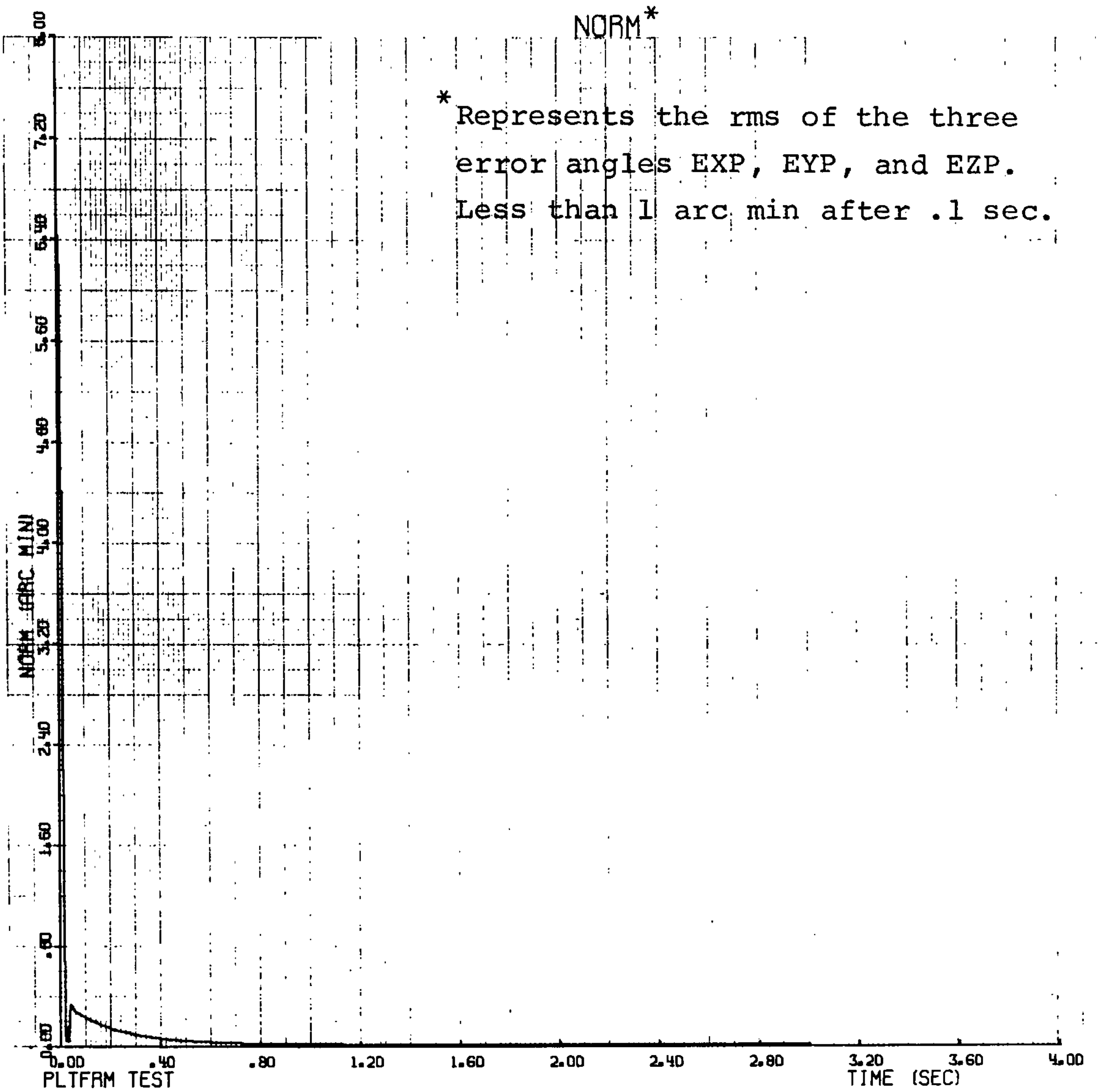
NORM*
*Represents the rms of the three error angles EXP, EYP, and EZP. Less than 1 arc min after .1 sec.
NORM (ARC MIN)
0.00
.80
1.60
2.40
3.20
4.00
4.80
5.60
6.40
7.20
8.00
0.00
.40
.80
1.20
1.60
2.00
2.40
2.80
3.20
3.60
4.00
PLTFRM TEST
TIME (SEC)

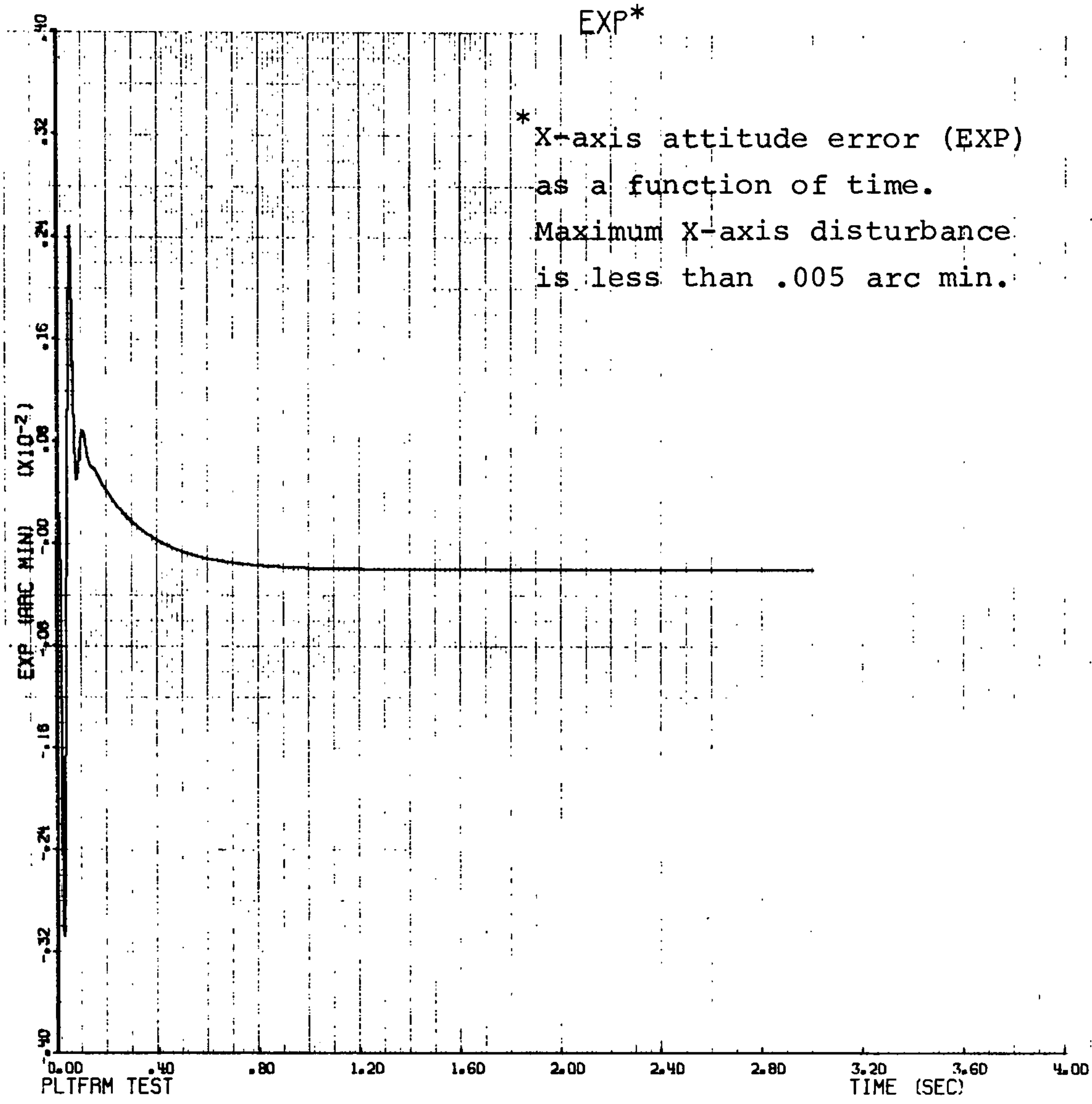

*X-axis attitude error (EXP) as a function of time. Maximum X-axis disturbance is less than .005 arc min.

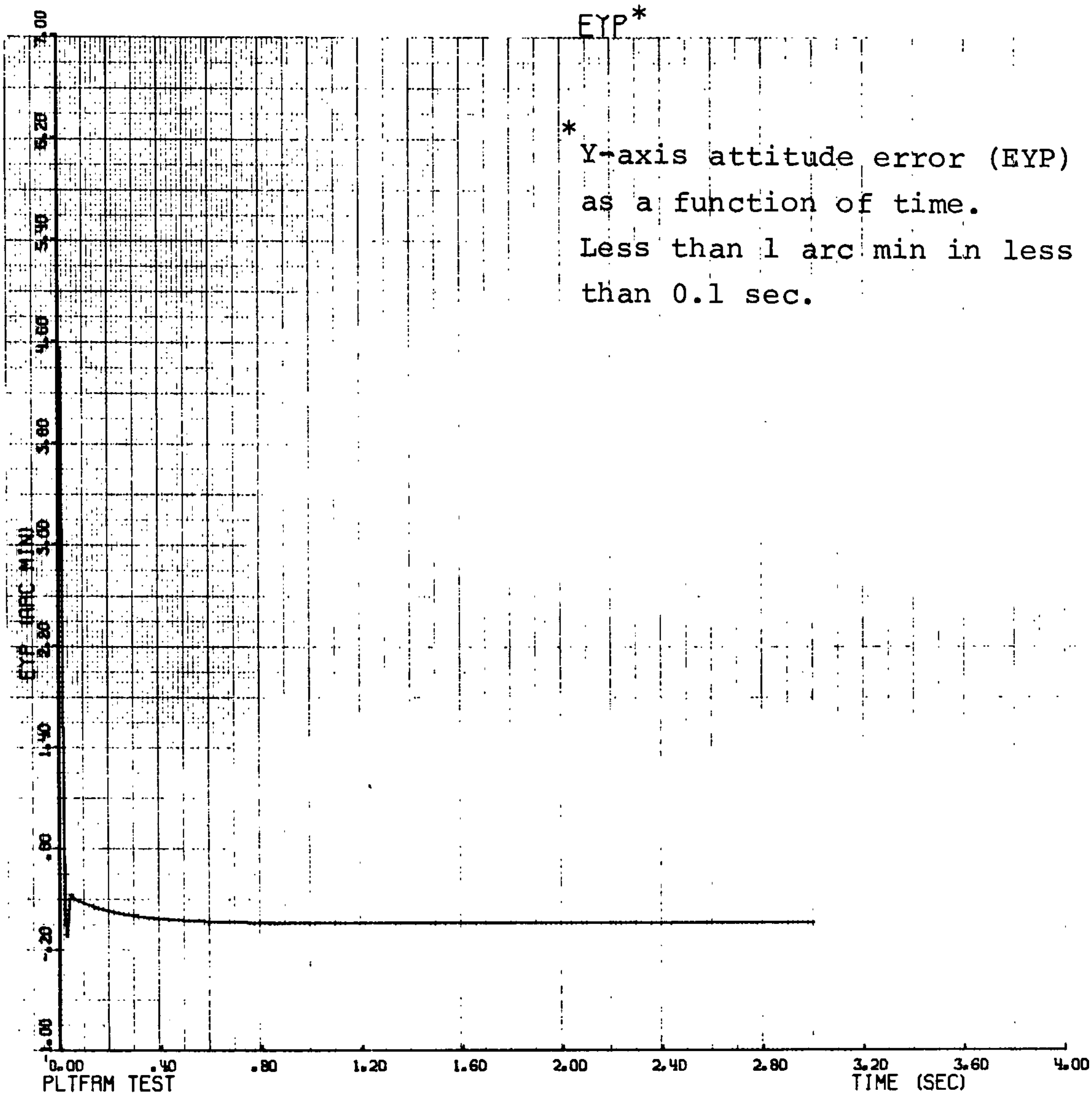
EYP*
7.00
6.20
5.40
4.60
3.80
3.00
2.20
1.40
.60
-.20
-1.00
EYP (ARC MIN)
0.00
.40
.80
1.20
1.60
2.00
2.40
2.80
3.20
3.60
4.00
PLTFRM TEST
TIME (SEC)
* Y-axis attitude error (EYP) as a function of time. Less than 1 arc min in less than 0.1 sec.

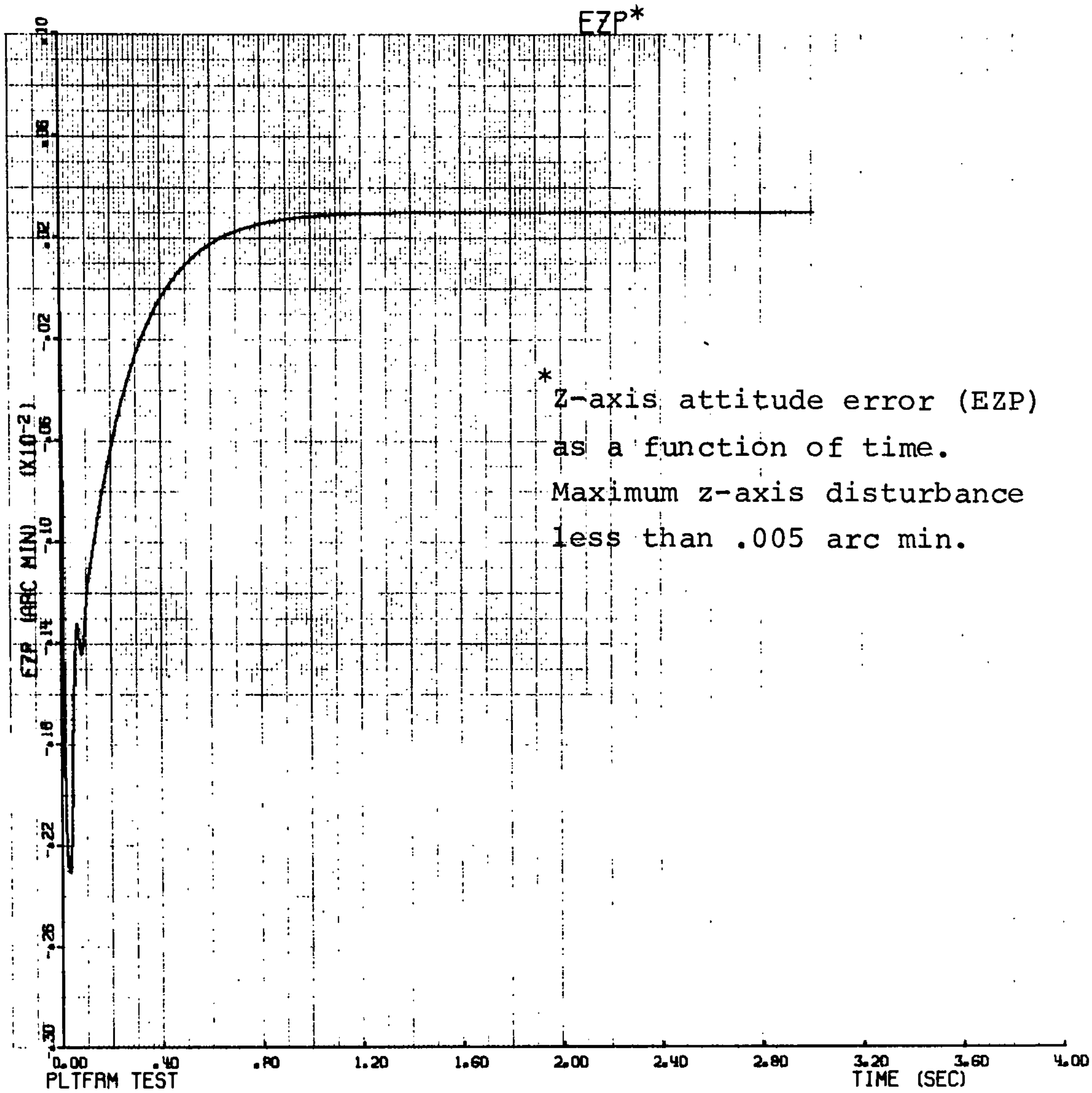

*Z-axis attitude error (EZP) as a function of time. Maximum z-axis disturbance less than .005 arc min.

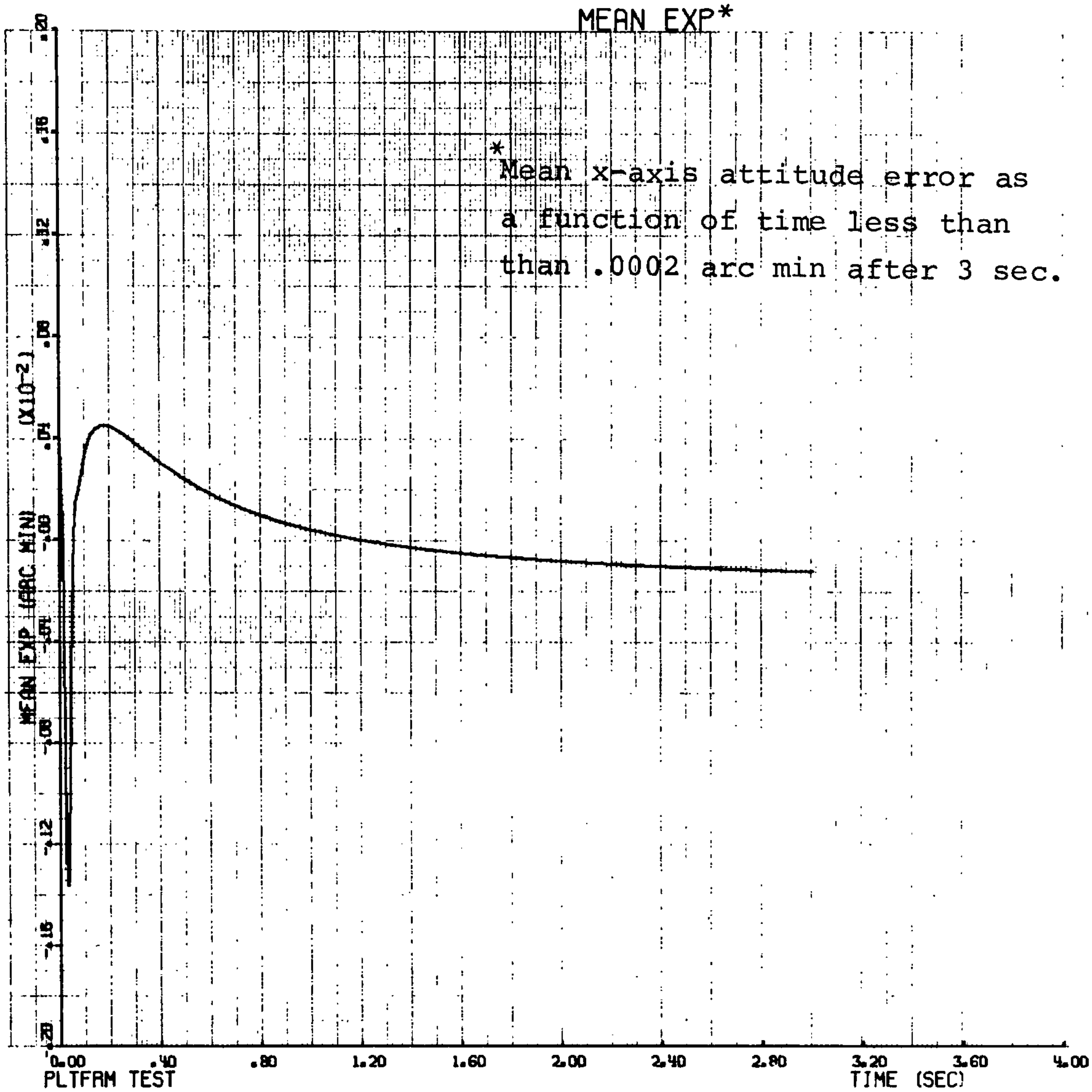

*Mean x-axis attitude error as a function of time less than than .0002 arc min after 3 sec.

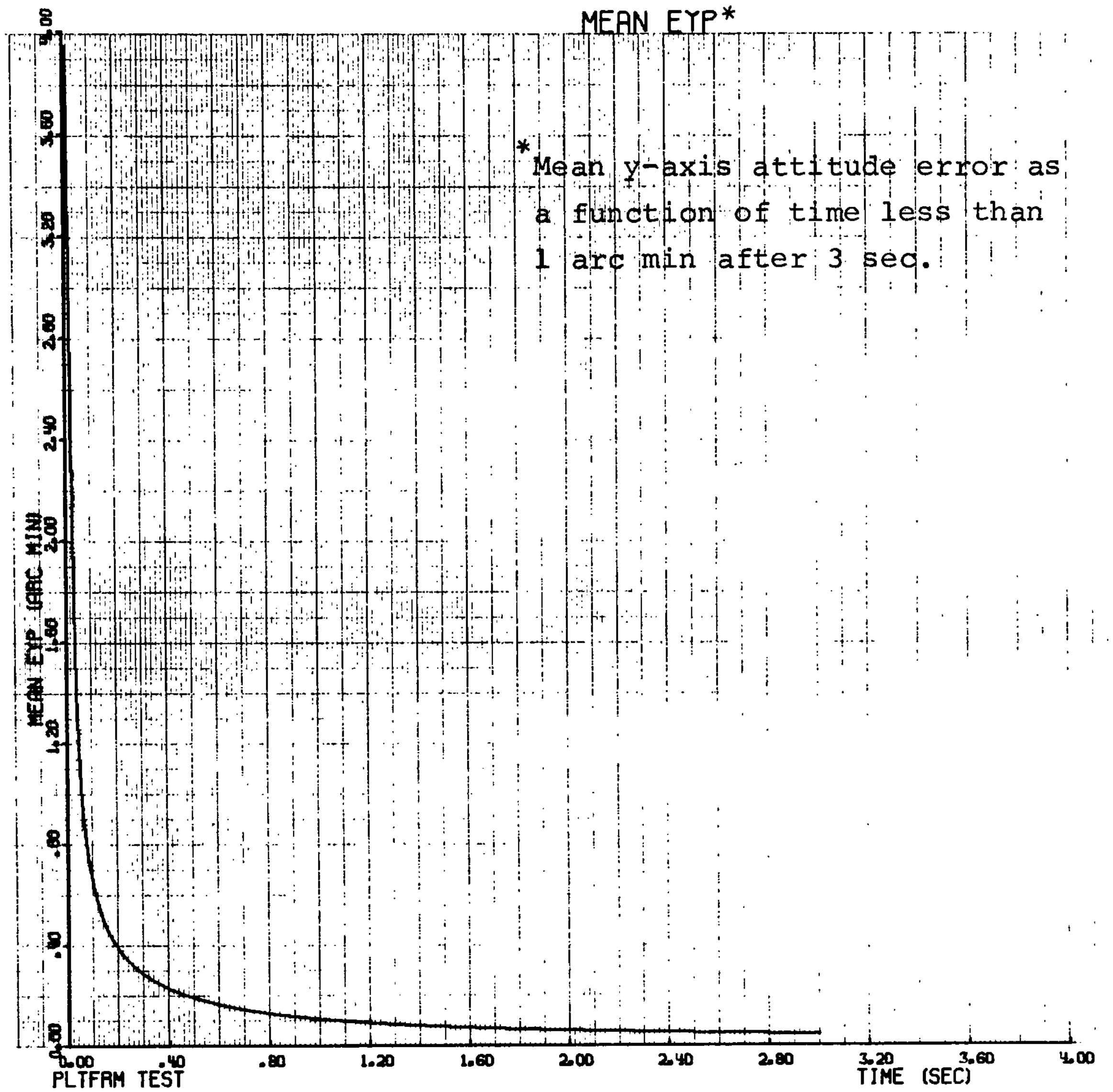

*Mean y-axis attitude error as a function of time less than 1 arc min after 3 sec.

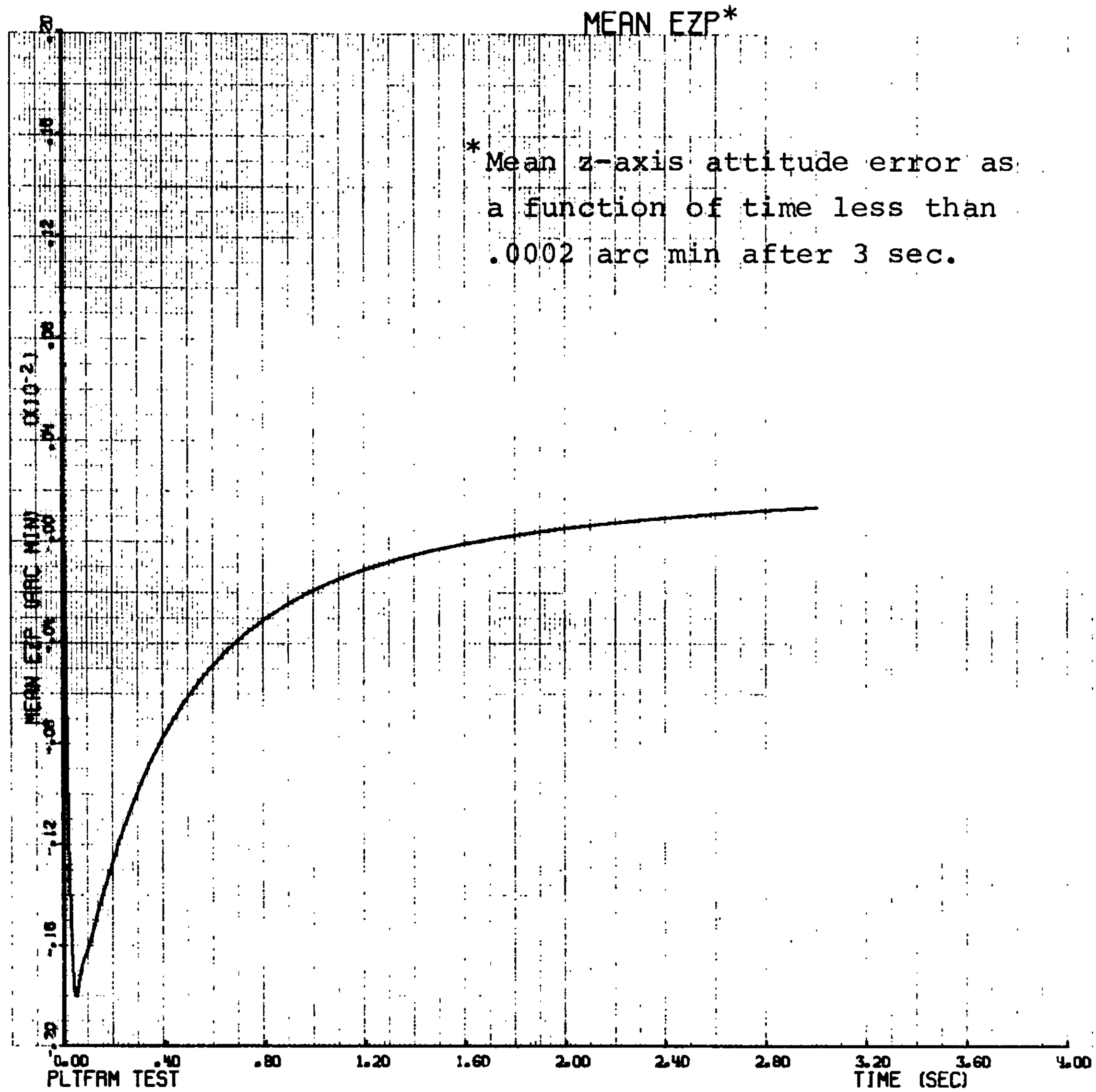
MEAN EZP*
*Mean z-axis attitude error as a function of time less than .0002 arc min after 3 sec.
MEAN EZP (ARC MIN) (X10-2)
.20
.16
.12
.08
.04
.00
-.04
-.08
-.12
-.16
-.20
0.00
.40
.80
1.20
1.60
2.00
2.40
2.80
3.20
3.60
4.00
PLTFRM TEST
TIME (SEC)

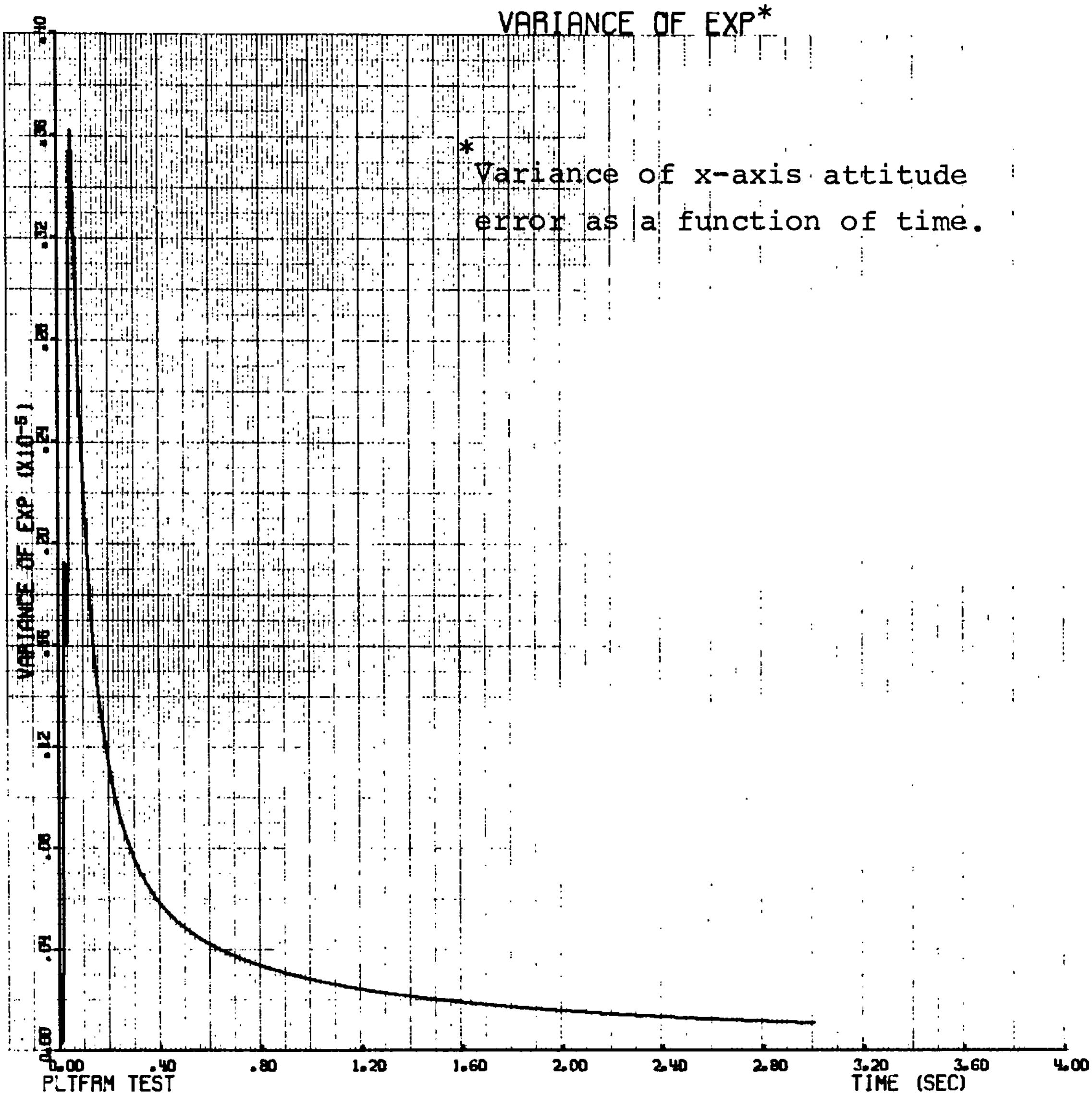

*Variance of x-axis attitude error as a function of time.

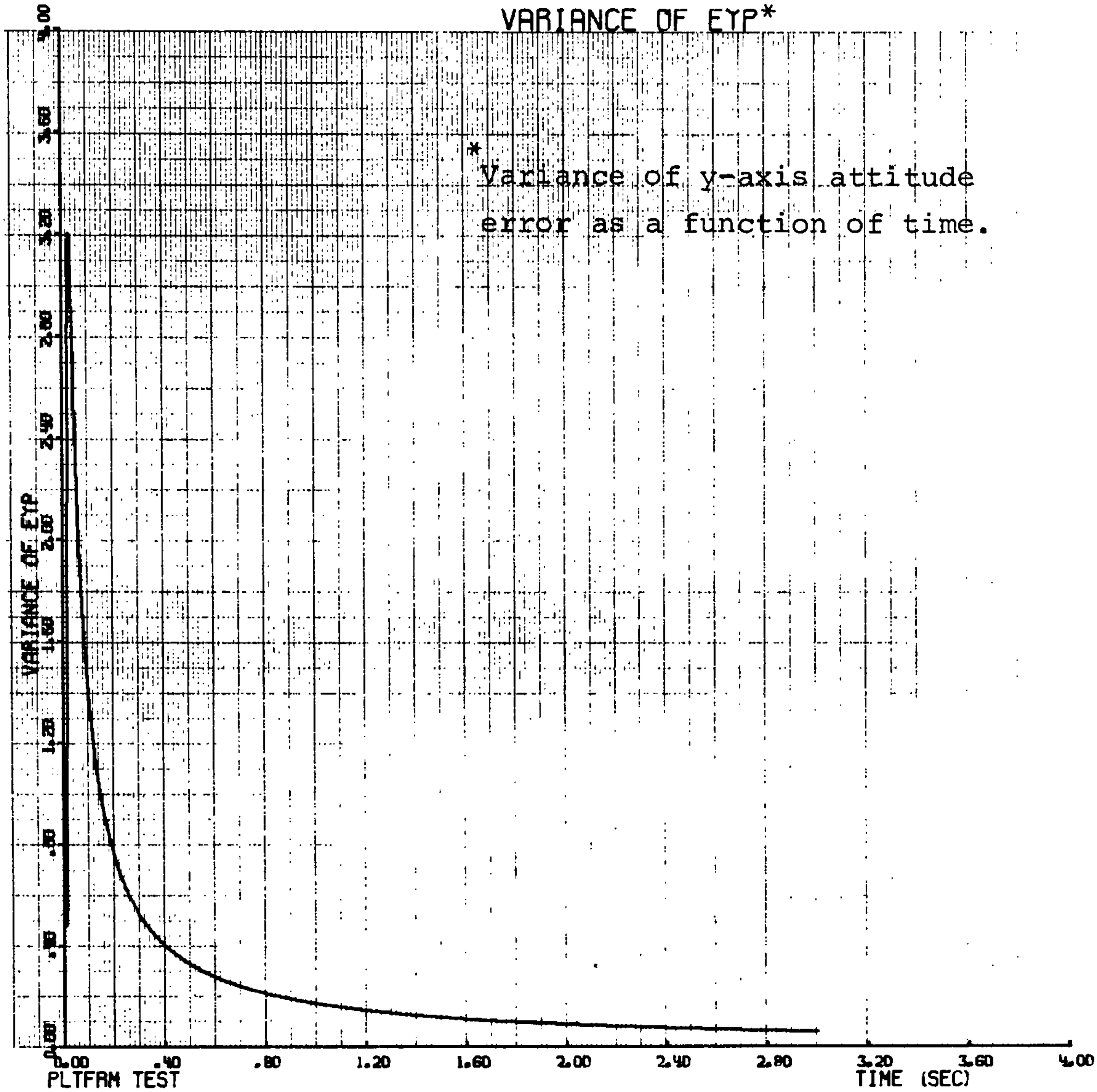
VARIANCE OF EYP*
*Variance of y-axis attitude error as a function of time.
VARIANCE OF EYP
0.00
.40
.80
1.20
1.60
2.00
2.40
2.80
3.20
3.60
4.00
PLTFRM TEST
TIME (SEC)

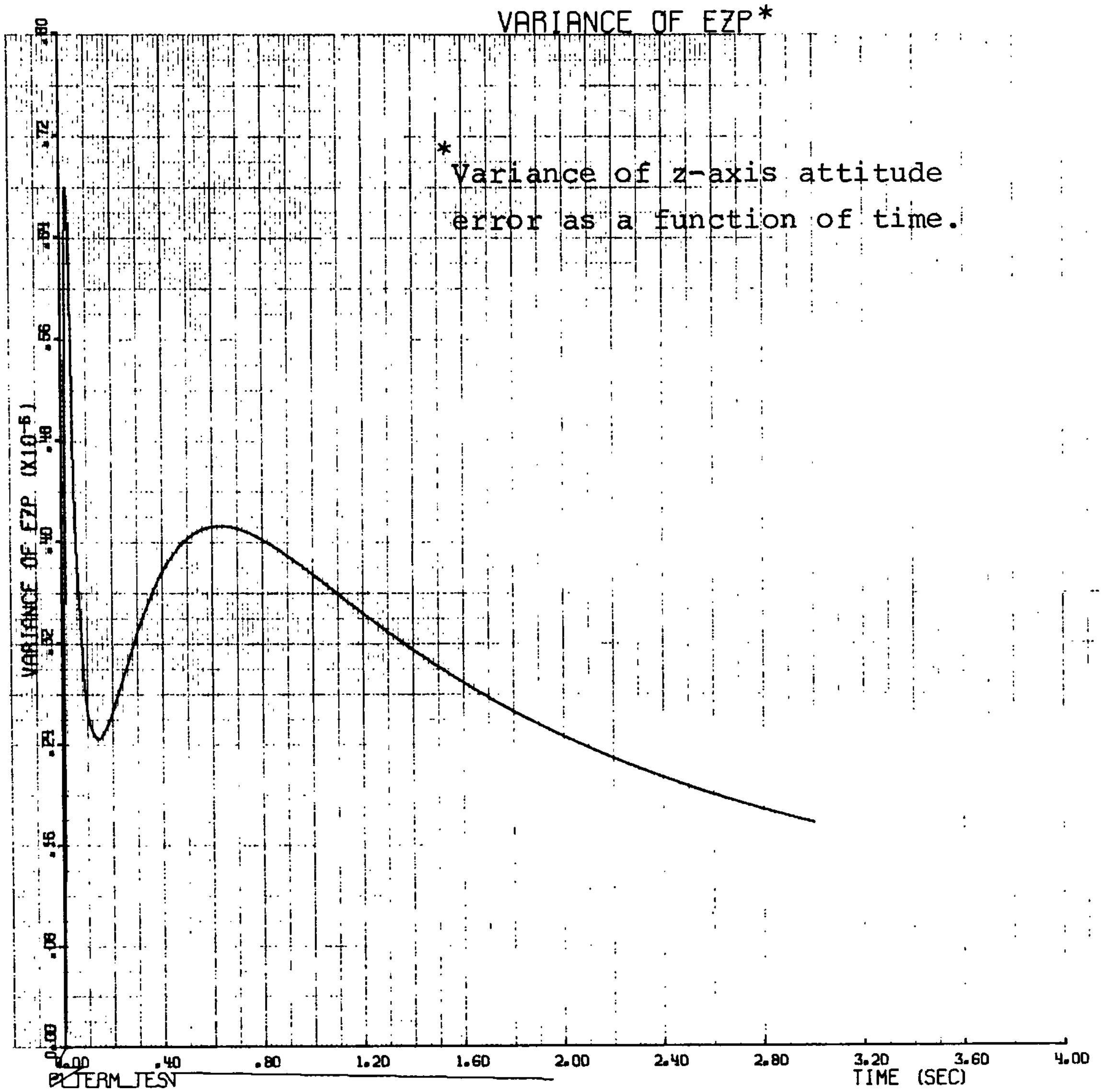
VARIANCE OF EZP*
*Variance of z-axis attitude error as a function of time.
VARIANCE OF EZP (X10^{-6})
0.00
.08
.16
.24
.32
.40
.48
.56
.64
.72
.80
0.00
.40
.80
1.20
1.60
2.00
2.40
2.80
3.20
3.60
4.00
TIME (SEC)
PLTERM TEST

Test Case 2, Slewing. Stationary axis motion with $C_1 = 30°/\text{sec}$, $\alpha = 45°$, $\beta = -30°$ (512 plot points/sec). The disturbance between 4 and 6 seconds results from the system experiencing gimbal lock.

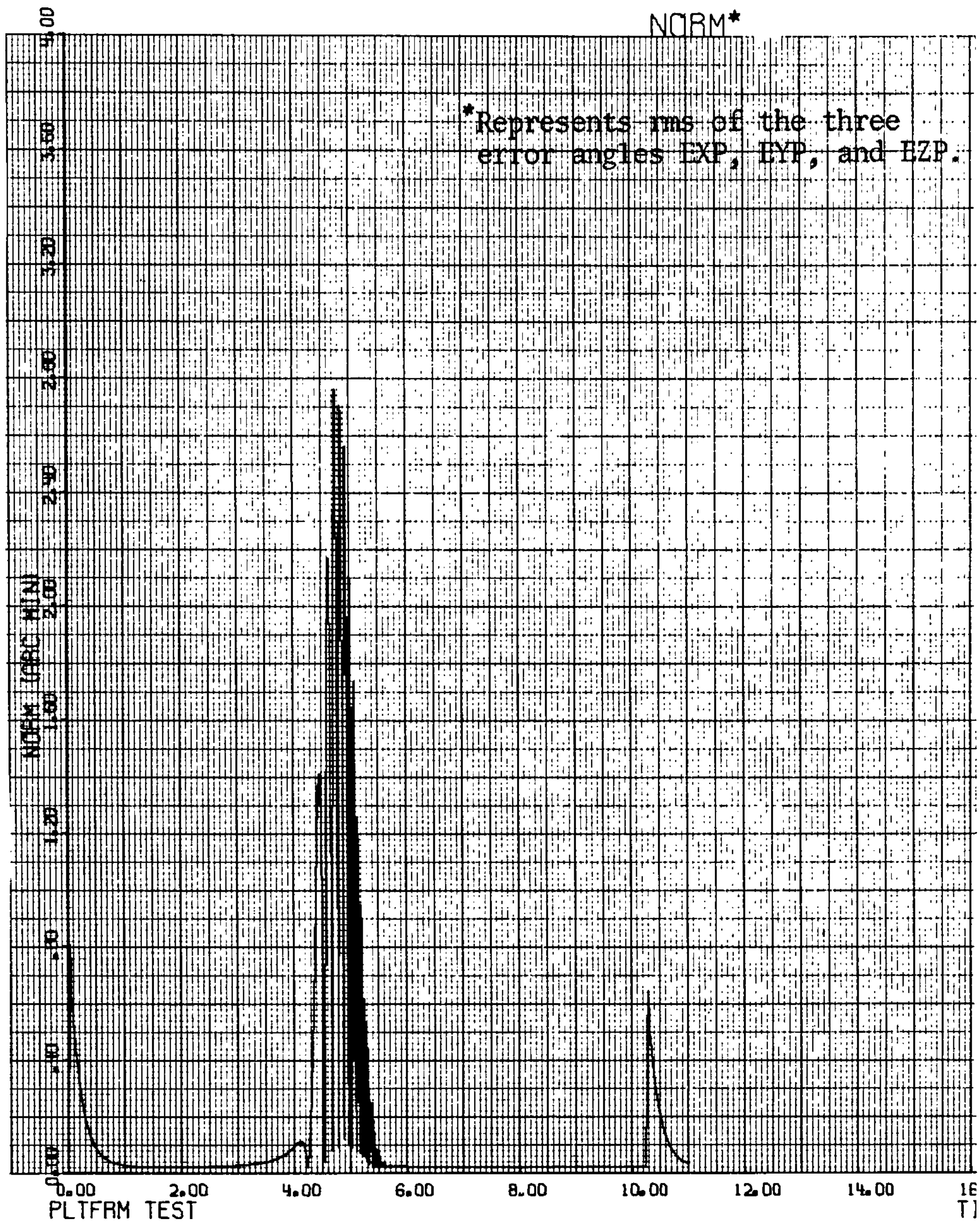
NORM*
*Represents rms of the three error angles EXP, EYP, and EZP.
NORM (ARC MIN)
0.00
.40
.80
1.20
1.60
2.00
2.40
2.80
3.20
3.60
4.00
0.00
2.00
4.00
6.00
8.00
10.00
12.00
14.00
PLTFRM TEST

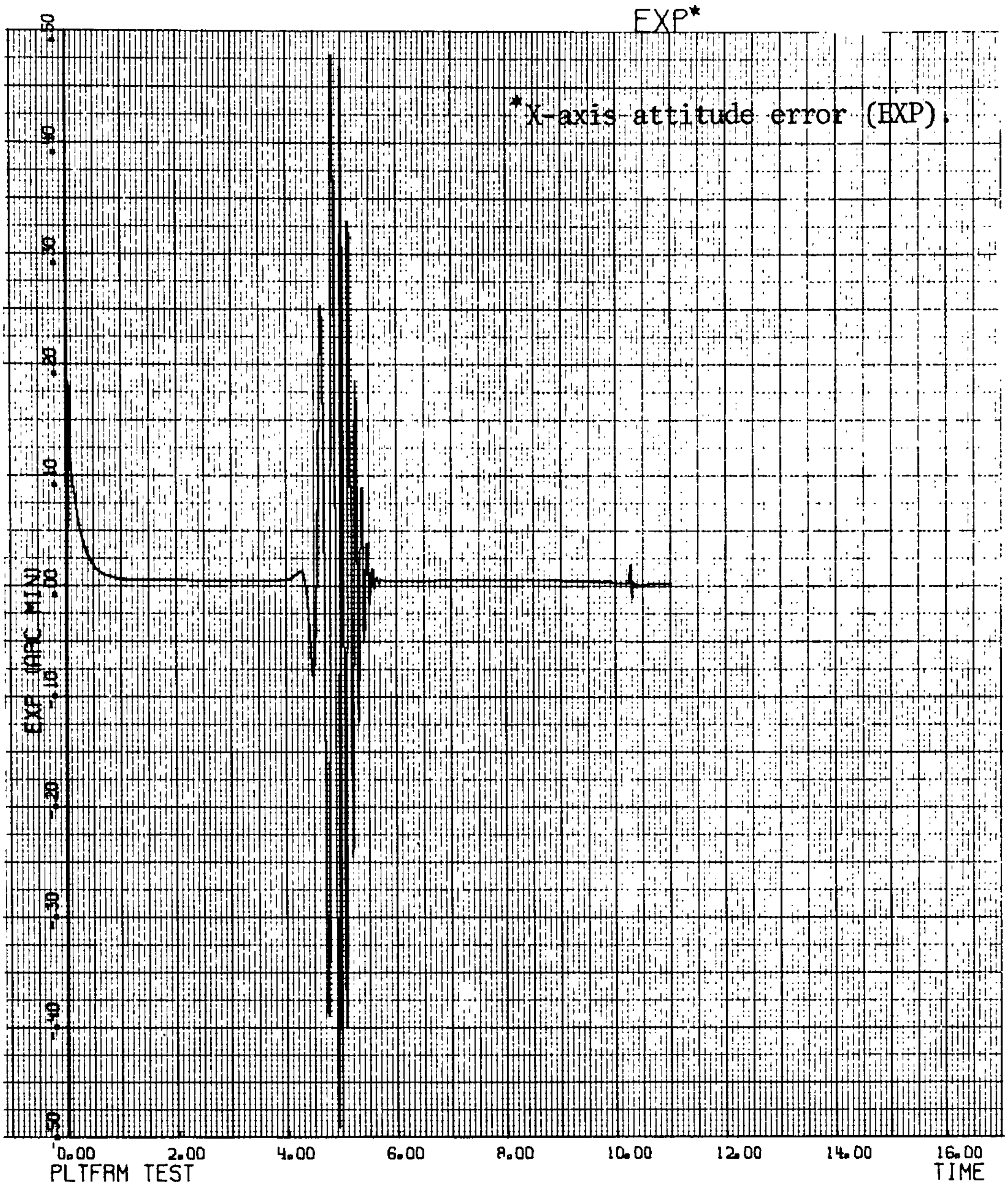
EXP*
*X-axis attitude error (EXP).
EXP (ARC MIN)
.50
.40
.30
.20
.10
.00
-.10
-.20
-.30
-.40
-.50
0.00
2.00
4.00
6.00
8.00
10.00
12.00
14.00
16.00
PLTFRM TEST
TIME

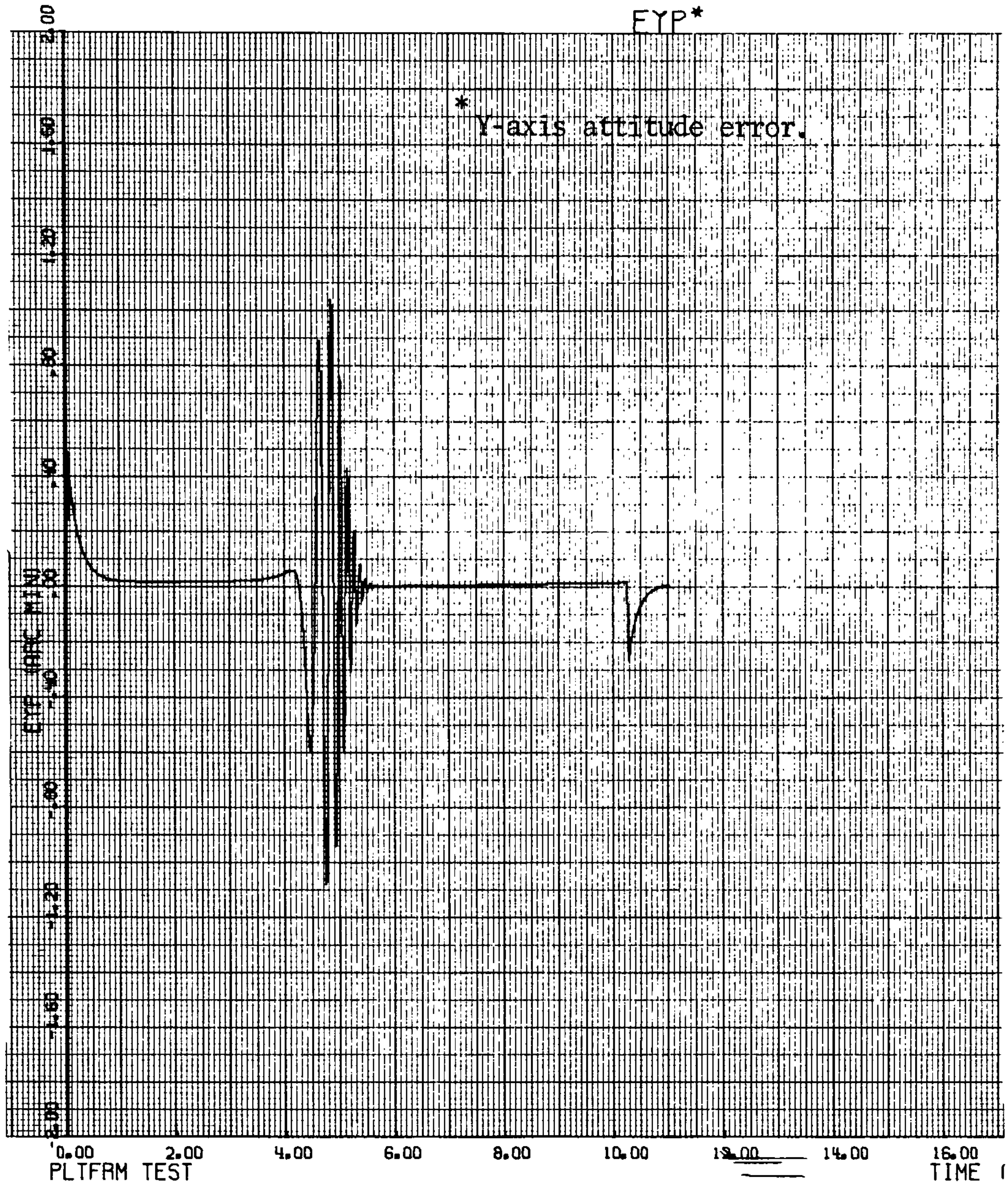
EYP*
*Y-axis attitude error.
EYP (ARC MIN)
PLTFRM TEST
TIME

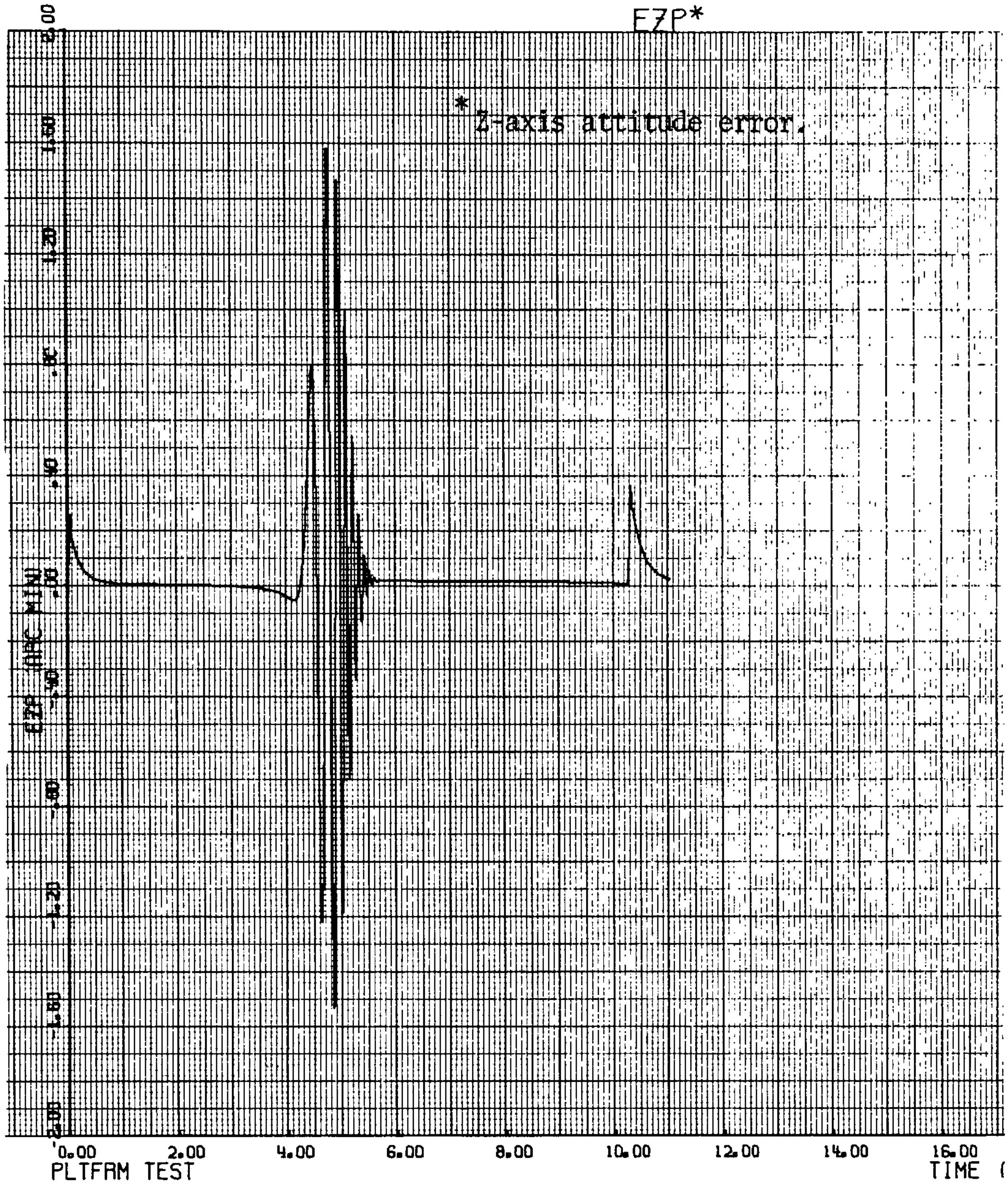

*Z-axis attitude error.

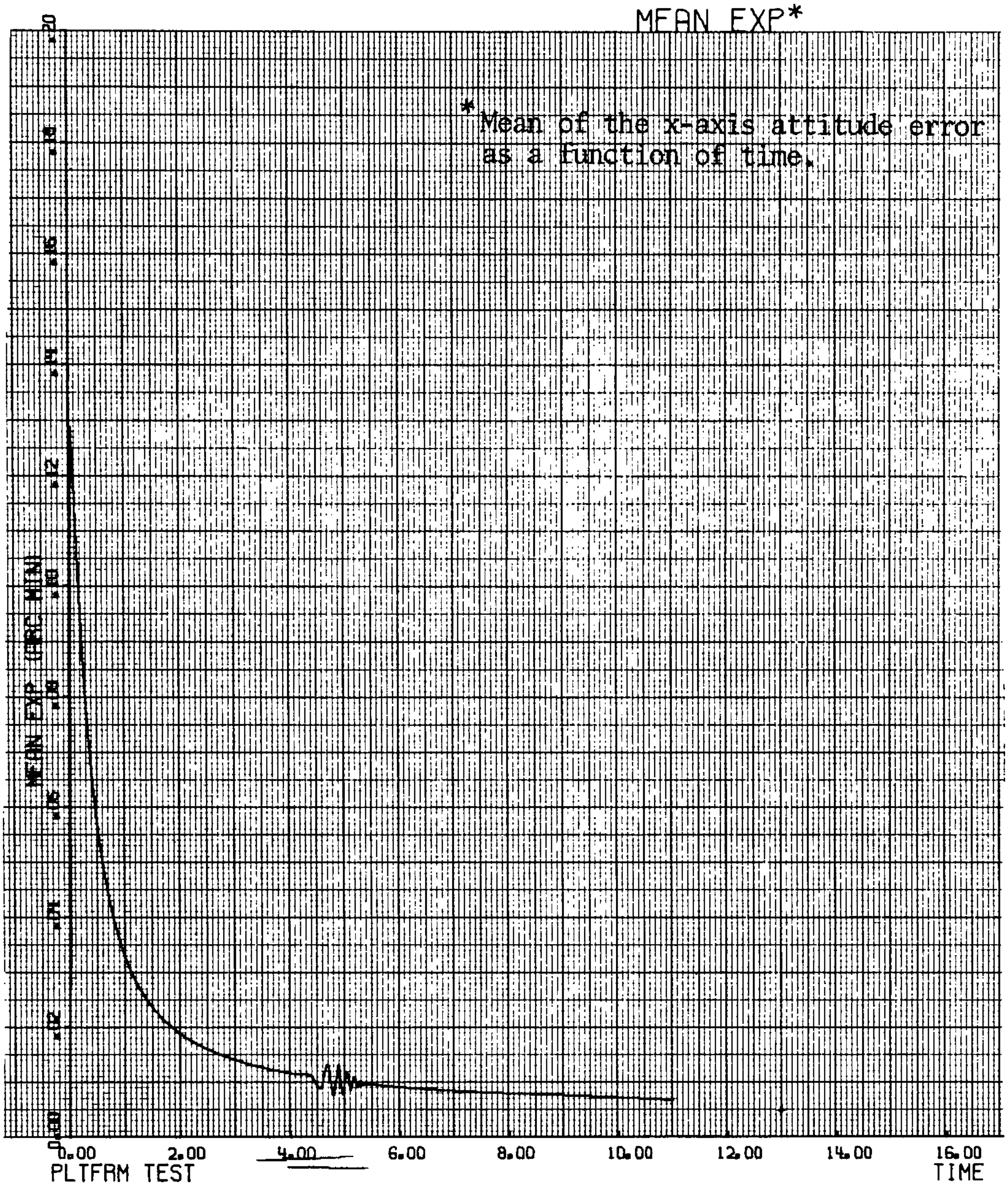
MEAN EXP*
*Mean of the x-axis attitude error as a function of time.
MEAN EXP (ARC MIN)
0.00
2.00
4.00
6.00
8.00
10.00
12.00
14.00
16.00
PLTFRM TEST
TIME

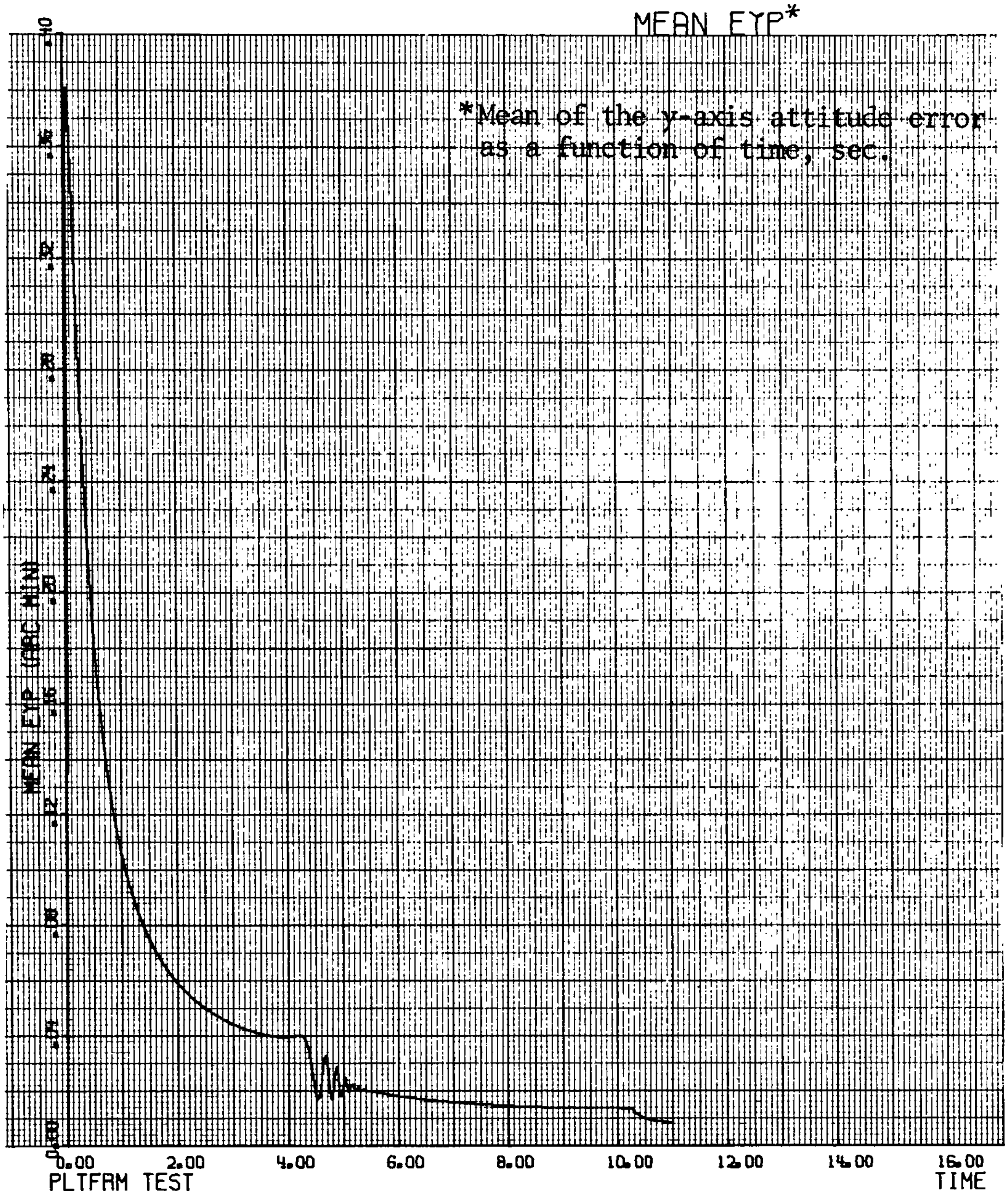
MEAN EYP*
*Mean of the y-axis attitude error
as a function of time, sec.
MEAN EYP (ARC MIN)
0.00
2.00
4.00
6.00
8.00
10.00
12.00
14.00
16.00
PLTFRM TEST
TIME

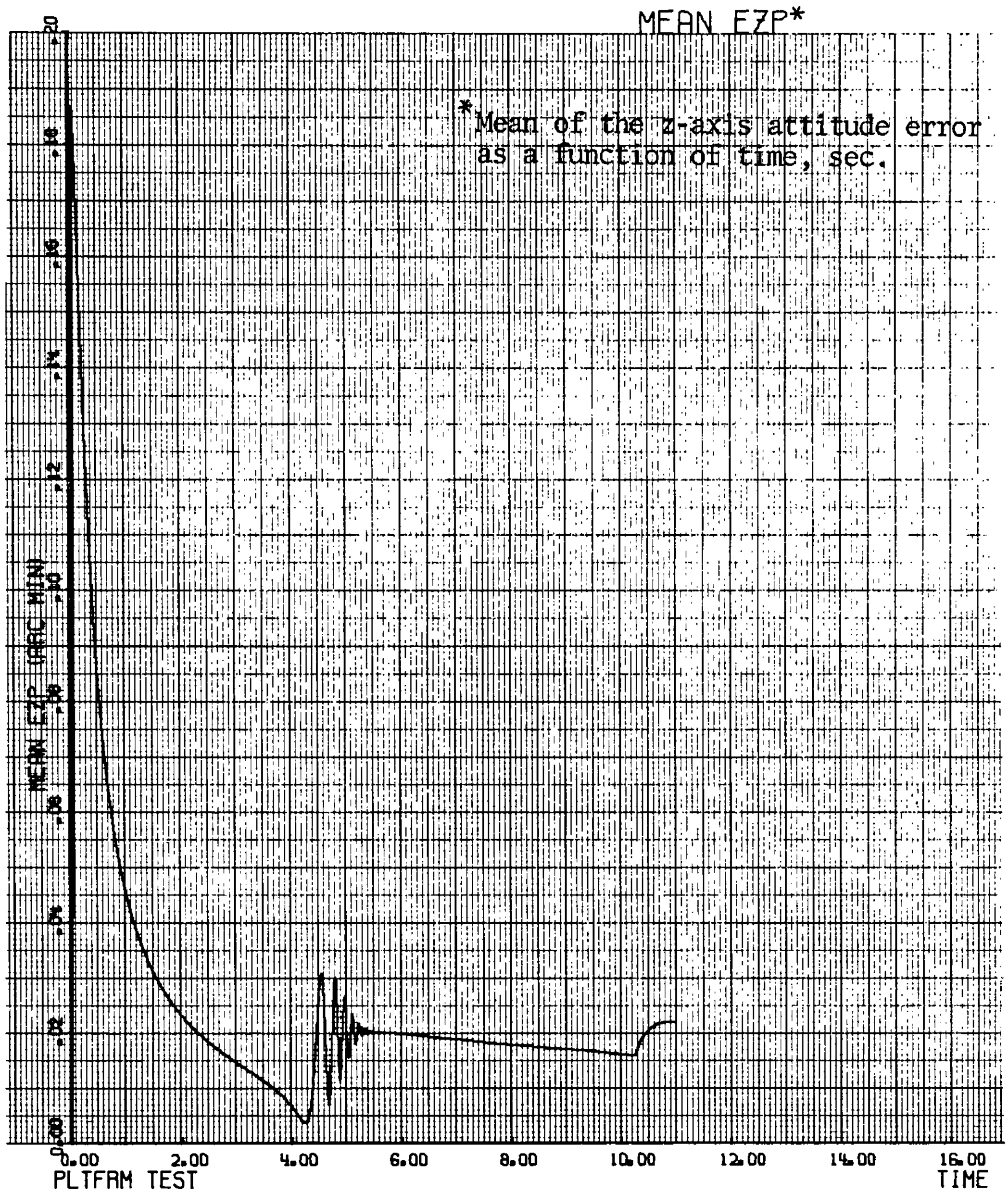
MEAN EZP*
*Mean of the z-axis attitude error
as a function of time, sec.
MEAN EZP (ARC MIN)
.20
.18
.16
.14
.12
.10
.08
.06
.04
.02
0.00
0.00
2.00
4.00
6.00
8.00
10.00
12.00
14.00
16.00
PLTFRM TEST
TIME

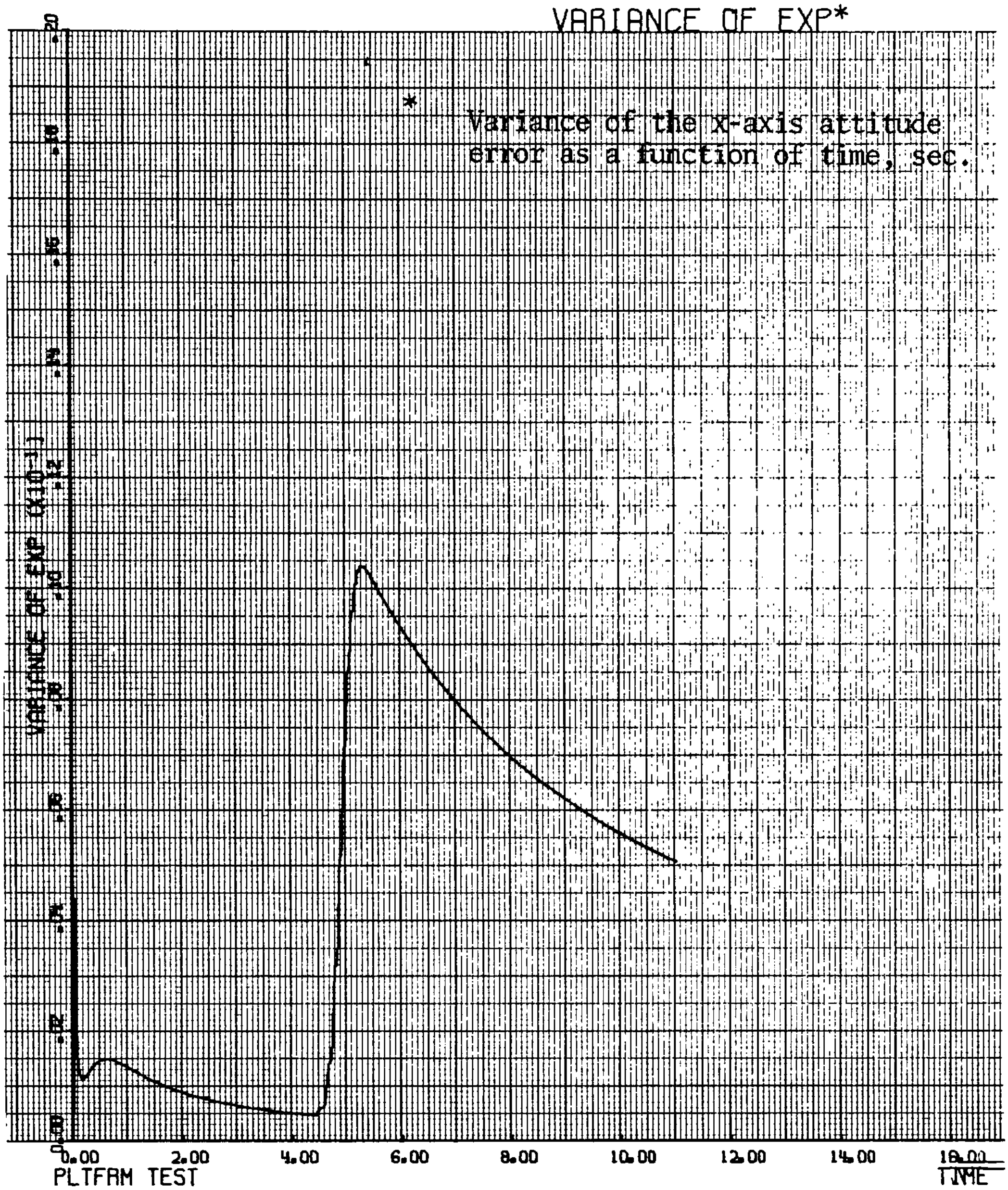

* Variance of the x-axis attitude error as a function of time, sec.

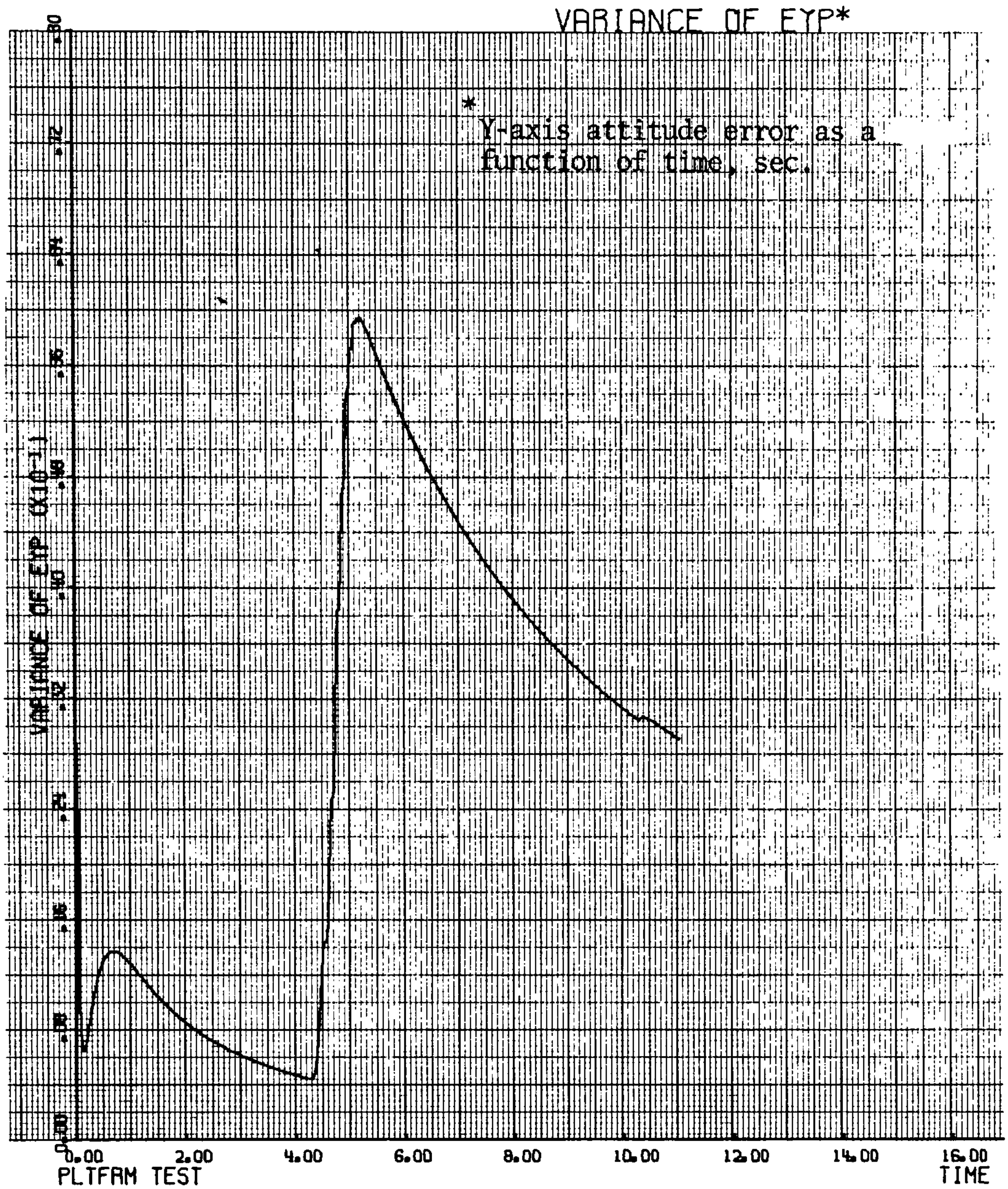
VARIANCE OF EYP*
* Y-axis attitude error as a function of time, sec.
VARIANCE OF EYP (X10-1)
0.00
2.00
4.00
6.00
8.00
10.00
12.00
14.00
16.00
PLTFRM TEST
TIME

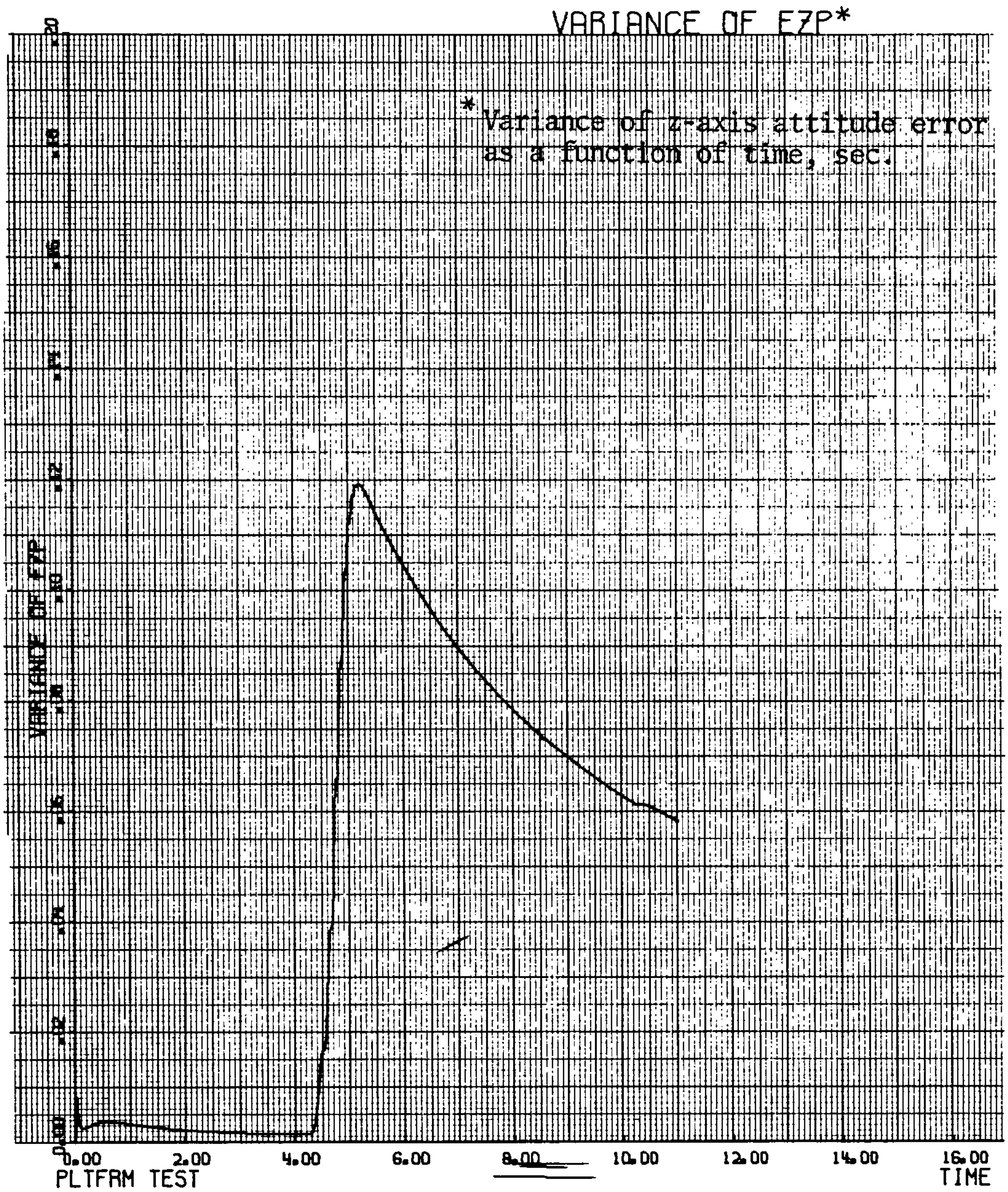
VARIANCE OF EZP*
*Variance of z-axis attitude error
as a function of time, sec.
VARIANCE OF EZP
0.00
2.00
4.00
6.00
8.00
10.00
12.00
14.00
16.00
PLTFRM TEST
TIME

Test Case 3, Sinusoidal Stationary Axis Motion (Y-axis). STAXIS with $C_1 = 30°/sec$, $C_3 = 0.1$ Hz, $\alpha = 90°$, $\beta = 0°$ (512 plot points/sec). Discontinuity at 0, 5, and 10 seconds is due to friction effect when the gimbal rate changes direction.

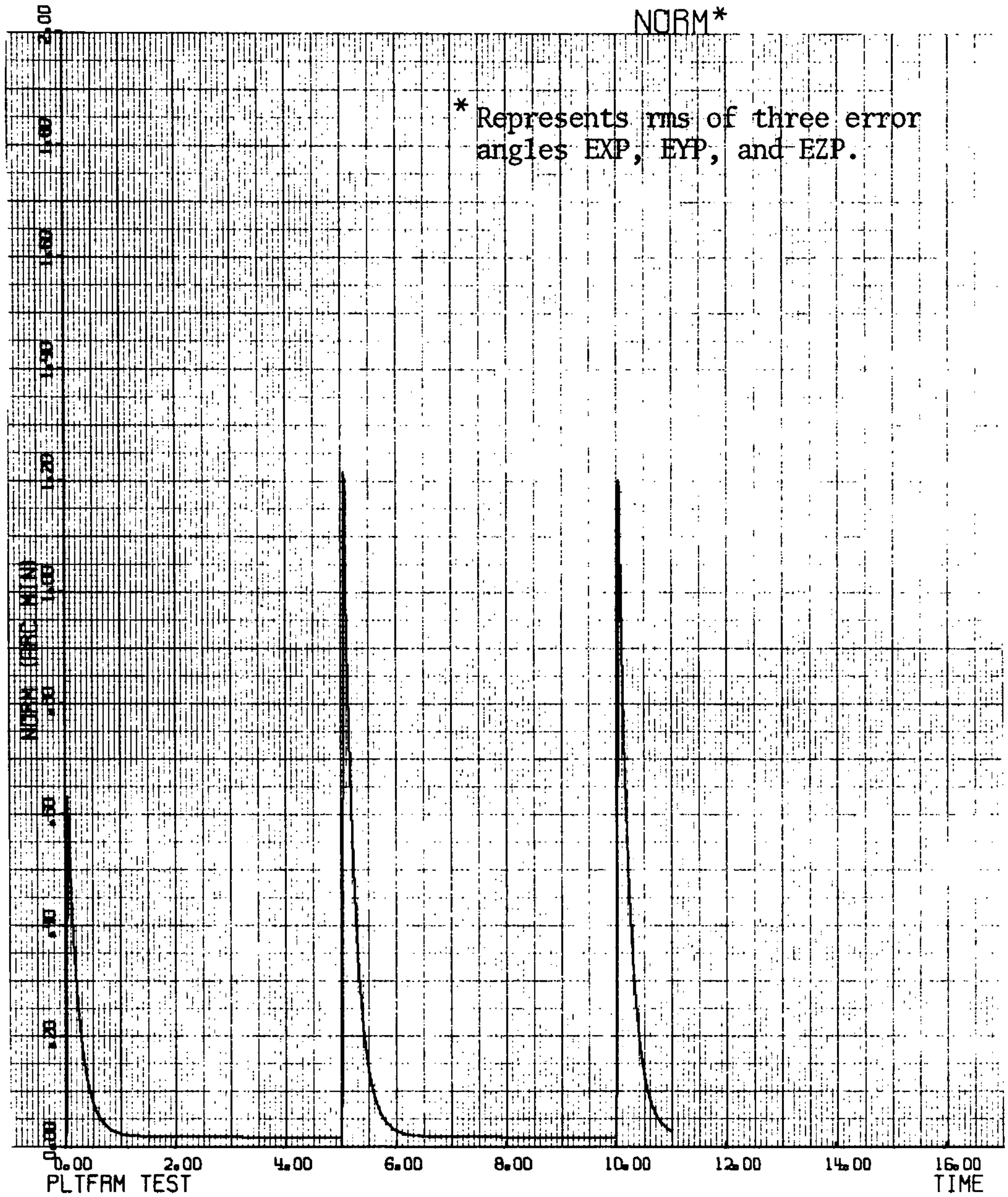
NORM*
* Represents rms of three error angles EXP, EYP, and EZP.
NORM (ARC MIN)
0.00
2.00
4.00
6.00
8.00
10.00
12.00
14.00
16.00
PLTFRM TEST
TIME

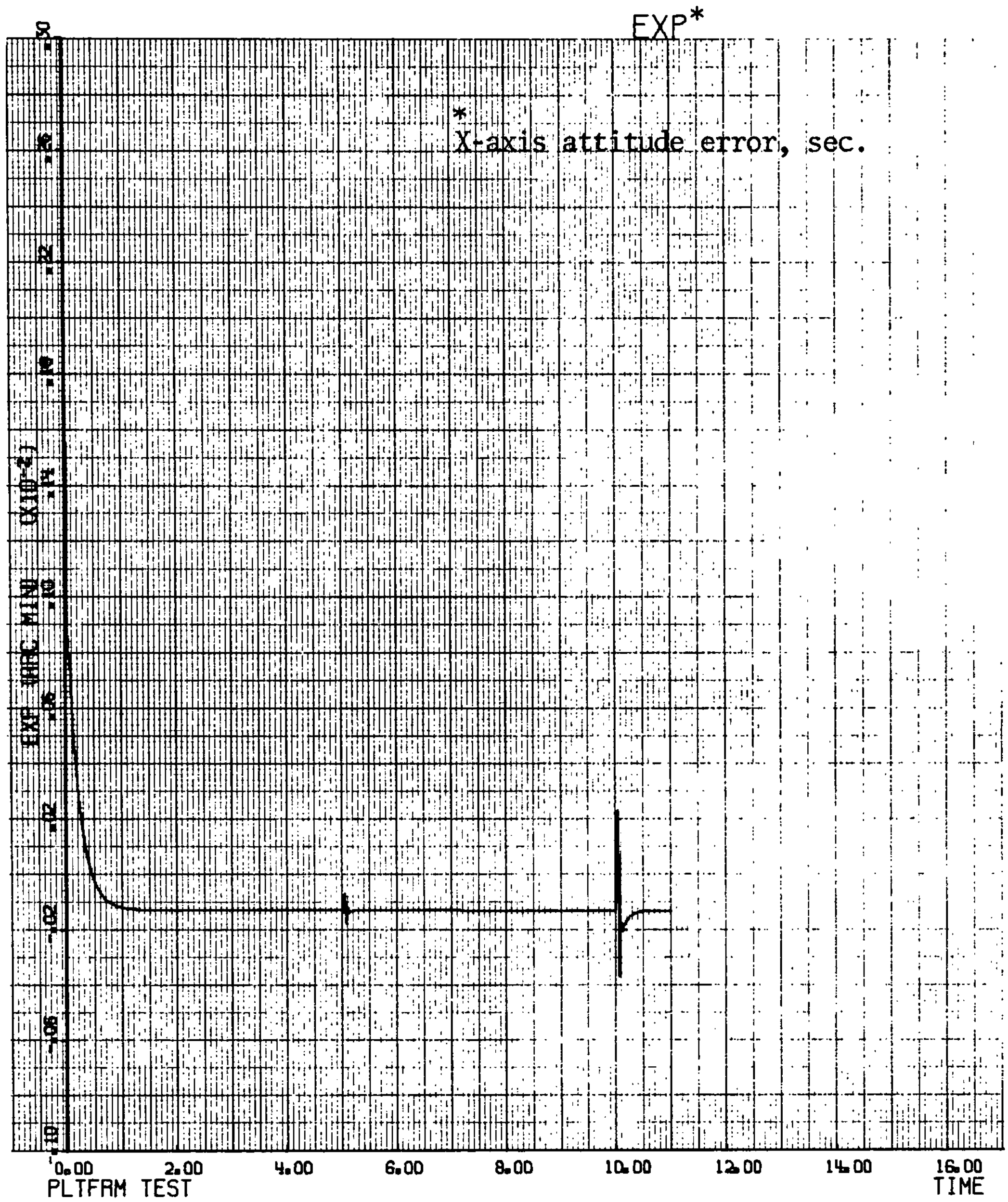
EXP*
* X-axis attitude error, sec.
EXP (ARC MIN) (X10^-2)
.30
.26
.22
.18
.14
.10
.06
.02
-.02
-.06
-.10
0.00
2.00
4.00
6.00
8.00
10.00
12.00
14.00
16.00
PLTFRM TEST
TIME

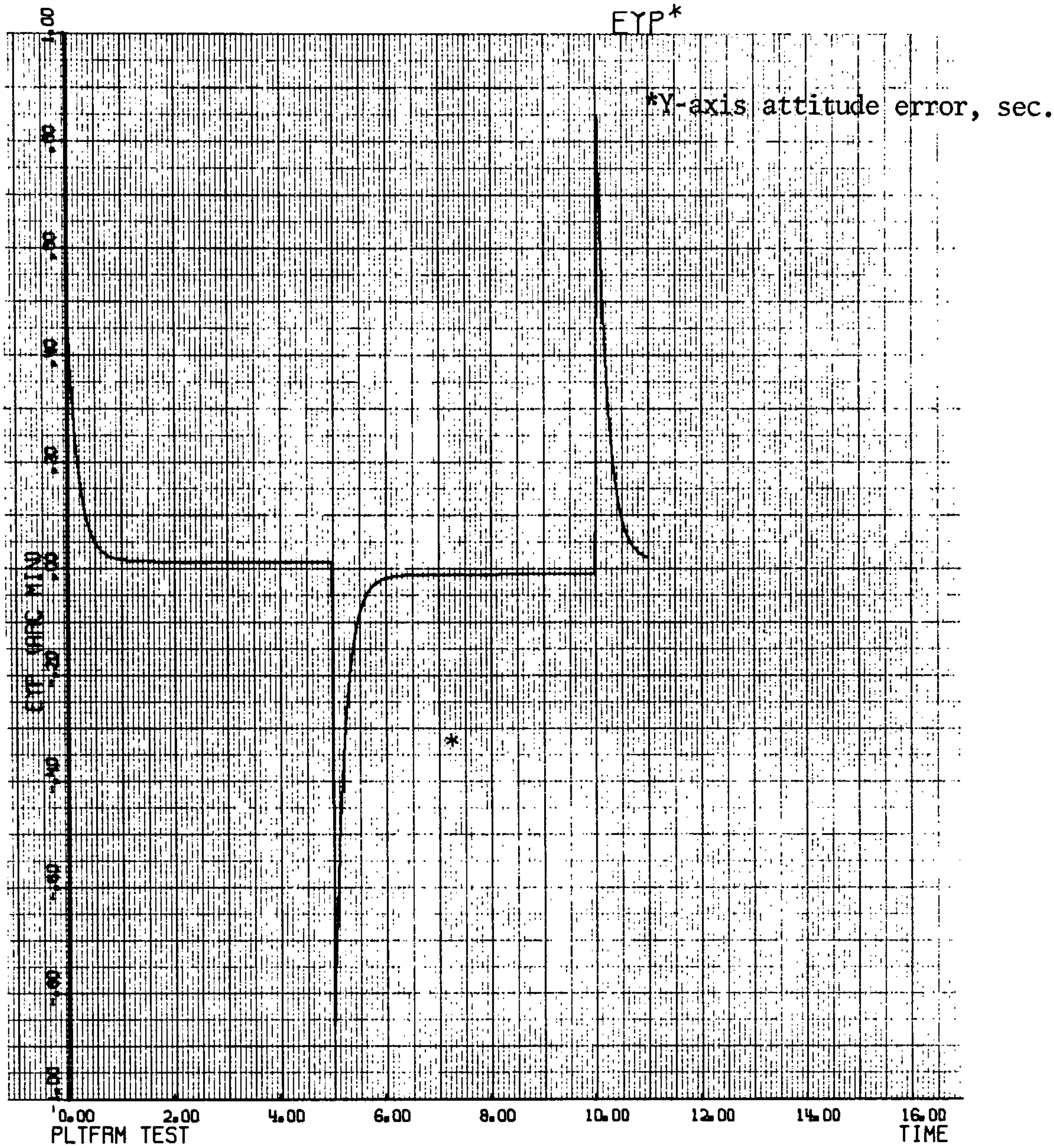
EYP*
*Y-axis attitude error, sec.
EYP (ARC MIN)
1.00
.80
.60
.40
.20
.00
-.20
-.40
-.60
-.80
-1.00
0.00
2.00
4.00
6.00
8.00
10.00
12.00
14.00
16.00
PLTFRM TEST
TIME
*

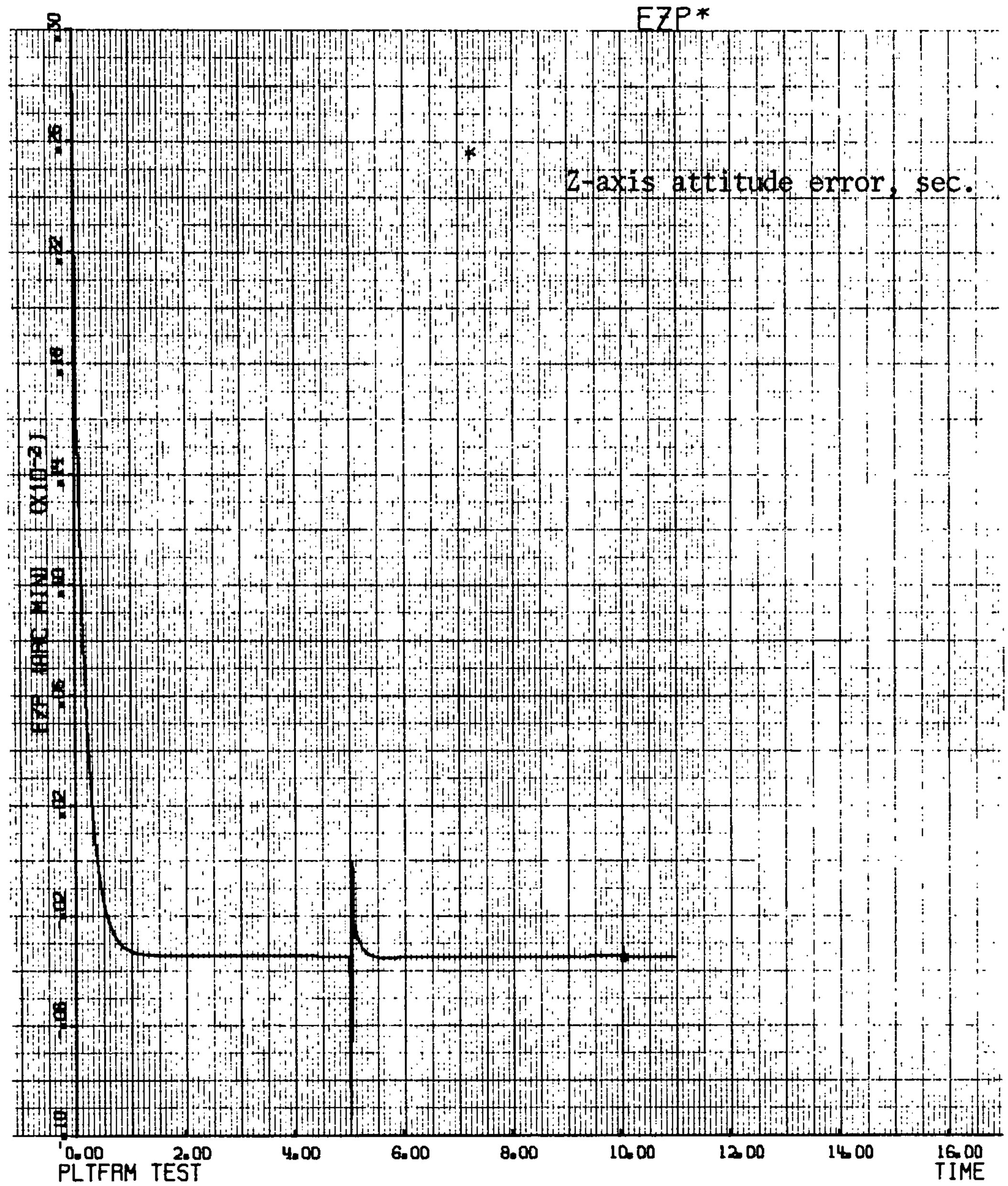
EZP*
*
Z-axis attitude error, sec.
0.00
2.00
4.00
6.00
8.00
10.00
12.00
14.00
16.00
PLTFRM TEST
TIME

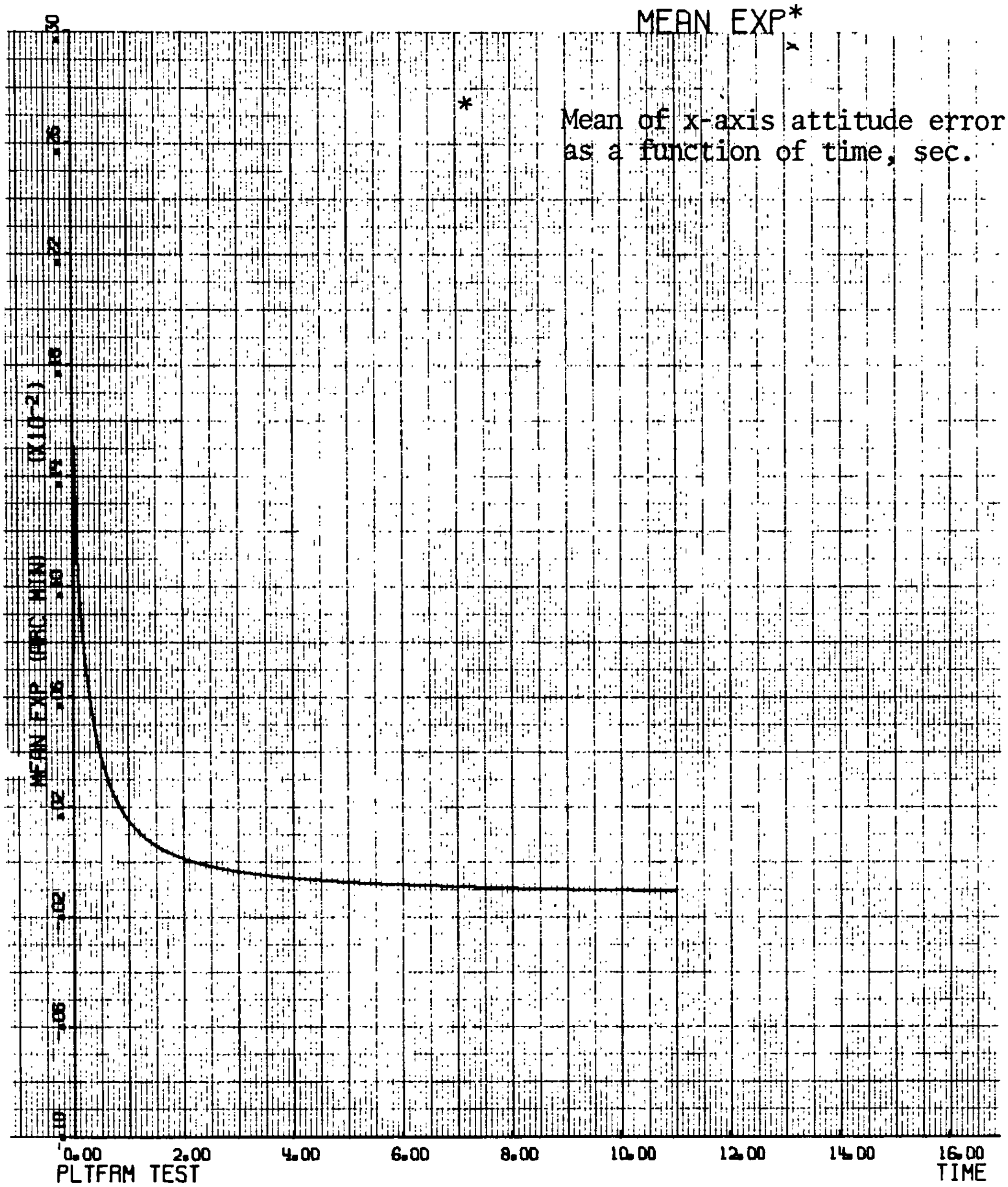
MEAN EXP*
Mean of x-axis attitude error
as a function of time, sec.
MEAN EXP (ARC MIN) (X10-2)
0.00
2.00
4.00
6.00
8.00
10.00
12.00
14.00
16.00
PLTFRM TEST
TIME

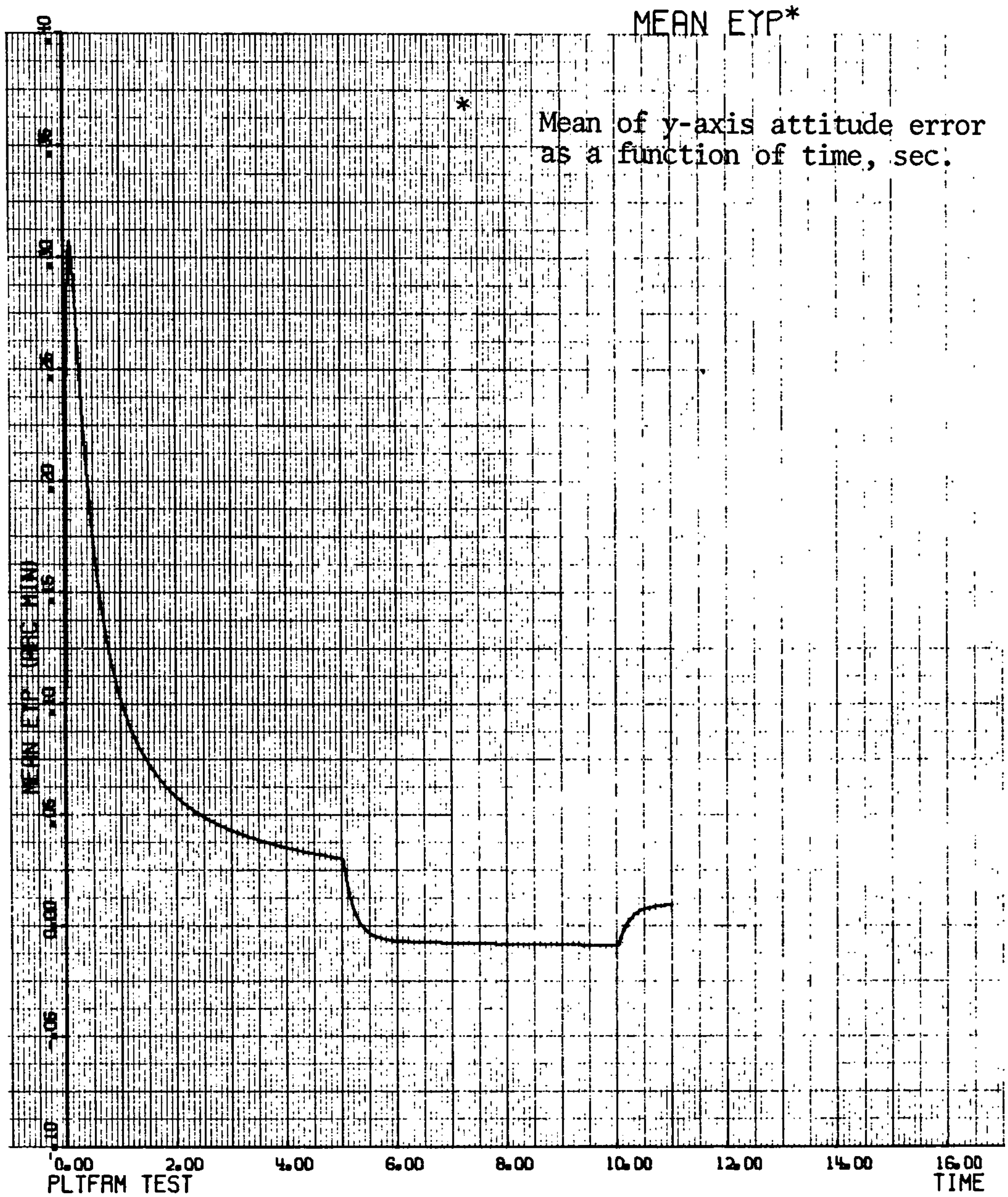
MEAN EYP*
* Mean of y-axis attitude error as a function of time, sec.
MEAN EYP (ARC MIN)
.40
.35
.30
.25
.20
.15
.10
.05
0.00
-.05
-.10
0.00
2.00
4.00
6.00
8.00
10.00
12.00
14.00
16.00
PLTFRM TEST
TIME

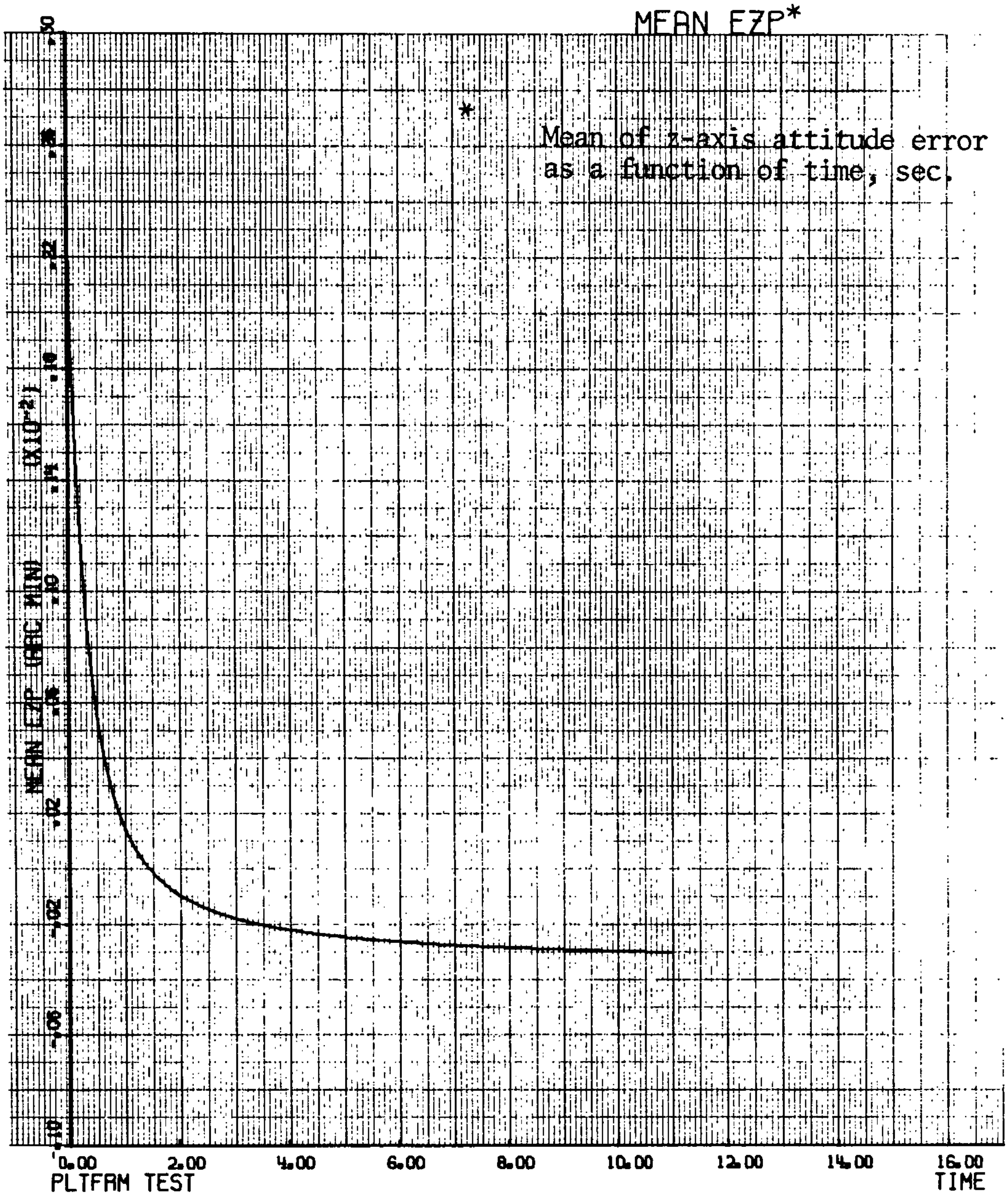
MEAN EZP*
* Mean of z-axis attitude error as a function of time, sec.
MEAN EZP (ARC MIN) (X10^-2)
.30
.26
.22
.18
.14
.10
.06
.02
-.02
-.06
-.10
0.00
2.00
4.00
6.00
8.00
10.00
12.00
14.00
16.00
PLTFRM TEST
TIME

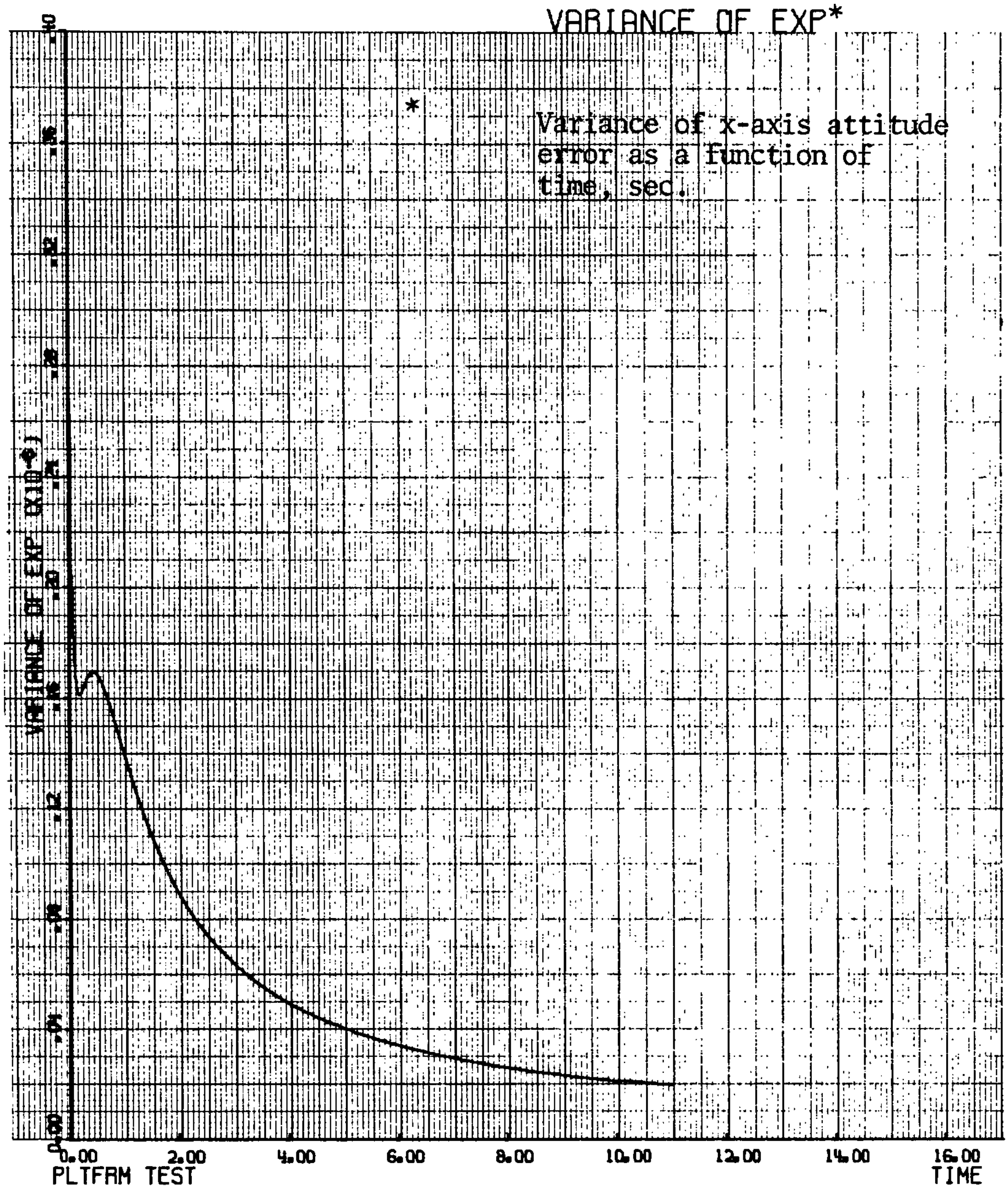
VARIANCE OF EXP*
*
Variance of x-axis attitude error as a function of time, sec.
VARIANCE OF EXP (X10^-6)
0.00
.04
.08
.12
.16
.20
.24
.28
.32
.36
.40
0.00
2.00
4.00
6.00
8.00
10.00
12.00
14.00
16.00
PLTFRM TEST
TIME

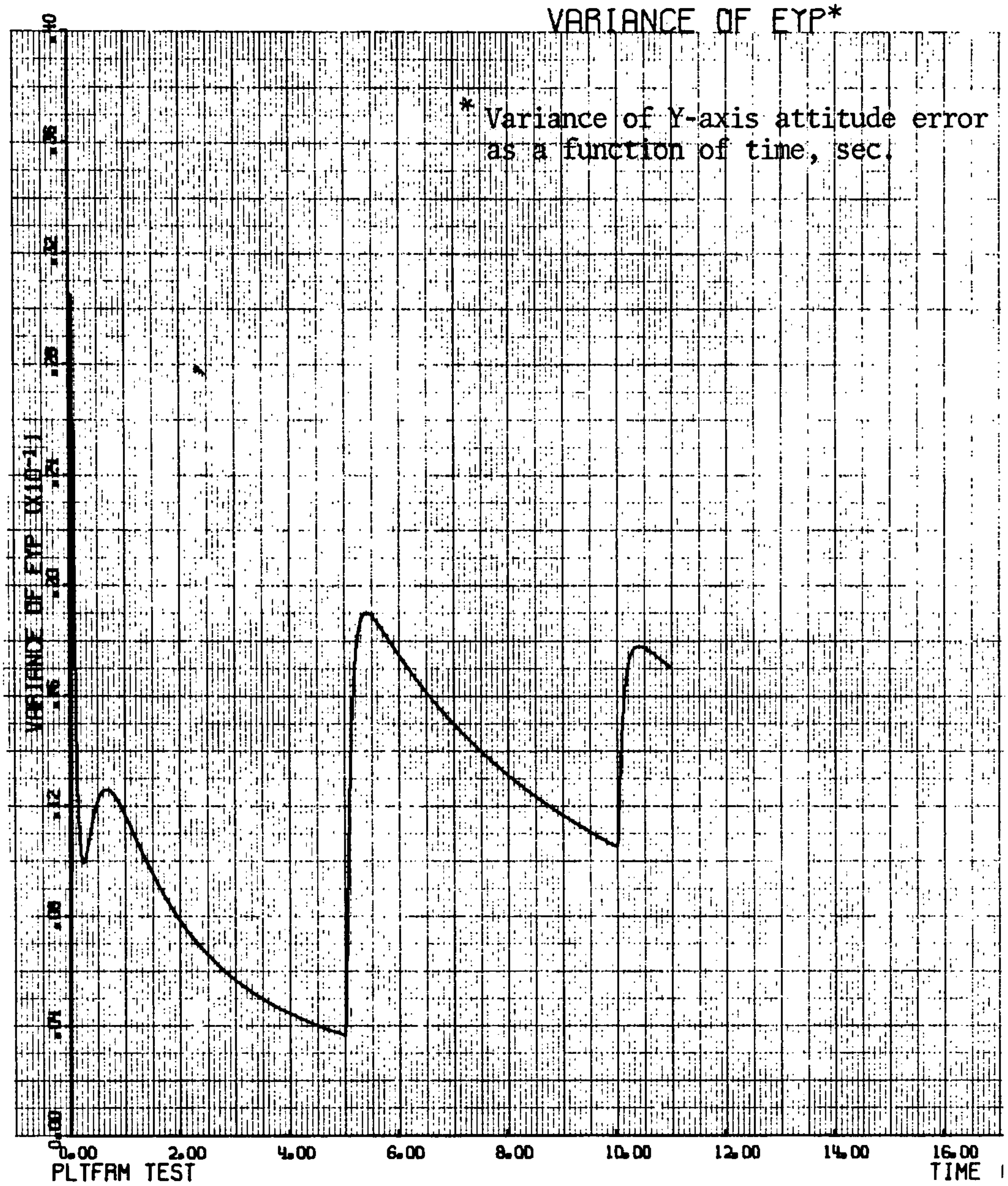
VARIANCE OF EYP*
* Variance of Y-axis attitude error as a function of time, sec.
VARIANCE OF EYP (X10-1)
0.00
.04
.08
.12
.16
.20
.24
.28
.32
.36
.40
0.00
2.00
4.00
6.00
8.00
10.00
12.00
14.00
16.00
PLTFRM TEST
TIME

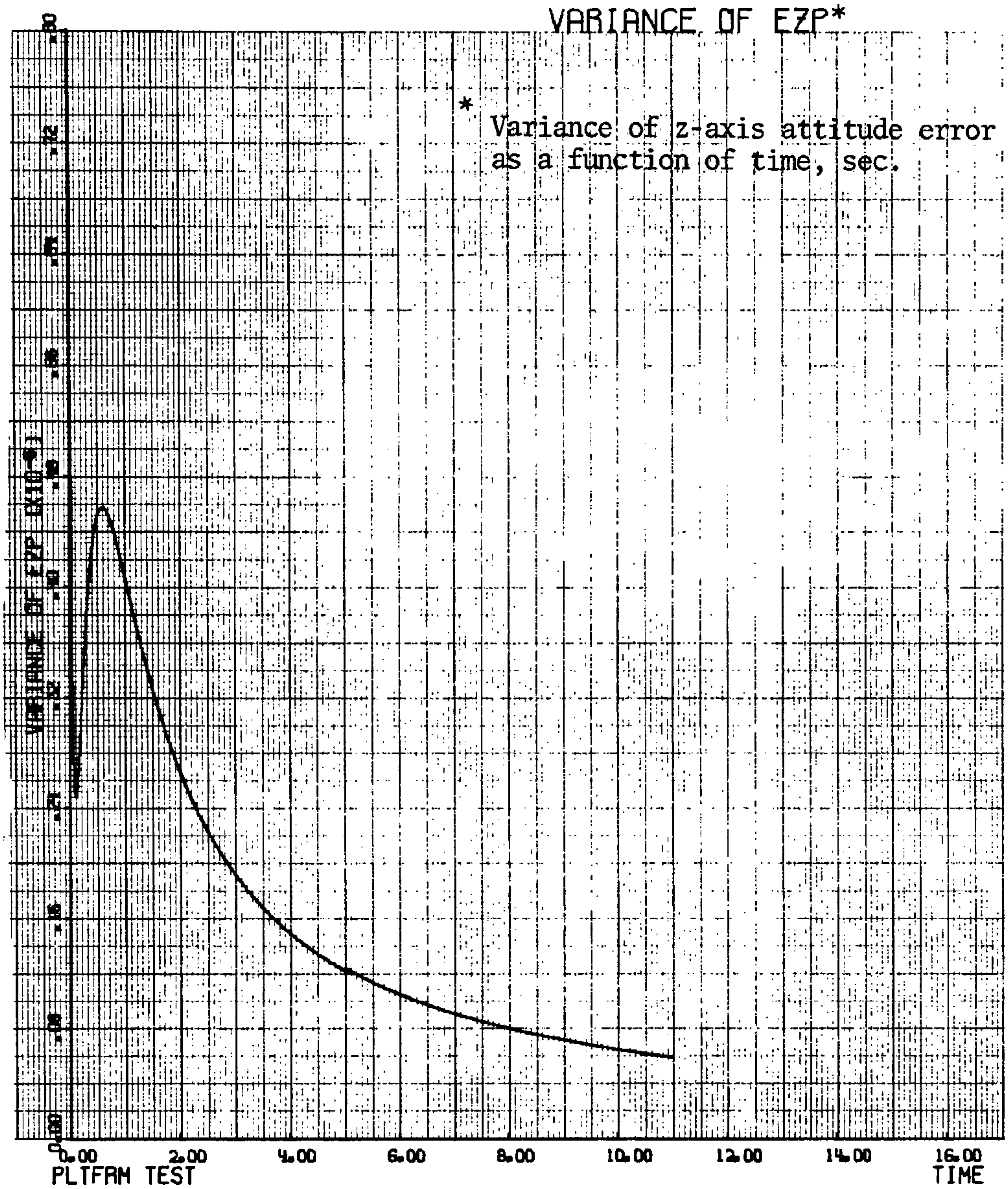

* Variance of z-axis attitude error as a function of time, sec.

<u>Test Case 4, Coning Motion</u>. Coning with $\theta = 30°$, $\omega_s = 16°/\mathrm{sec}$, $\omega_p = 8°/\mathrm{sec}$ (128 plot points/sec). Severe coning motion effects result.

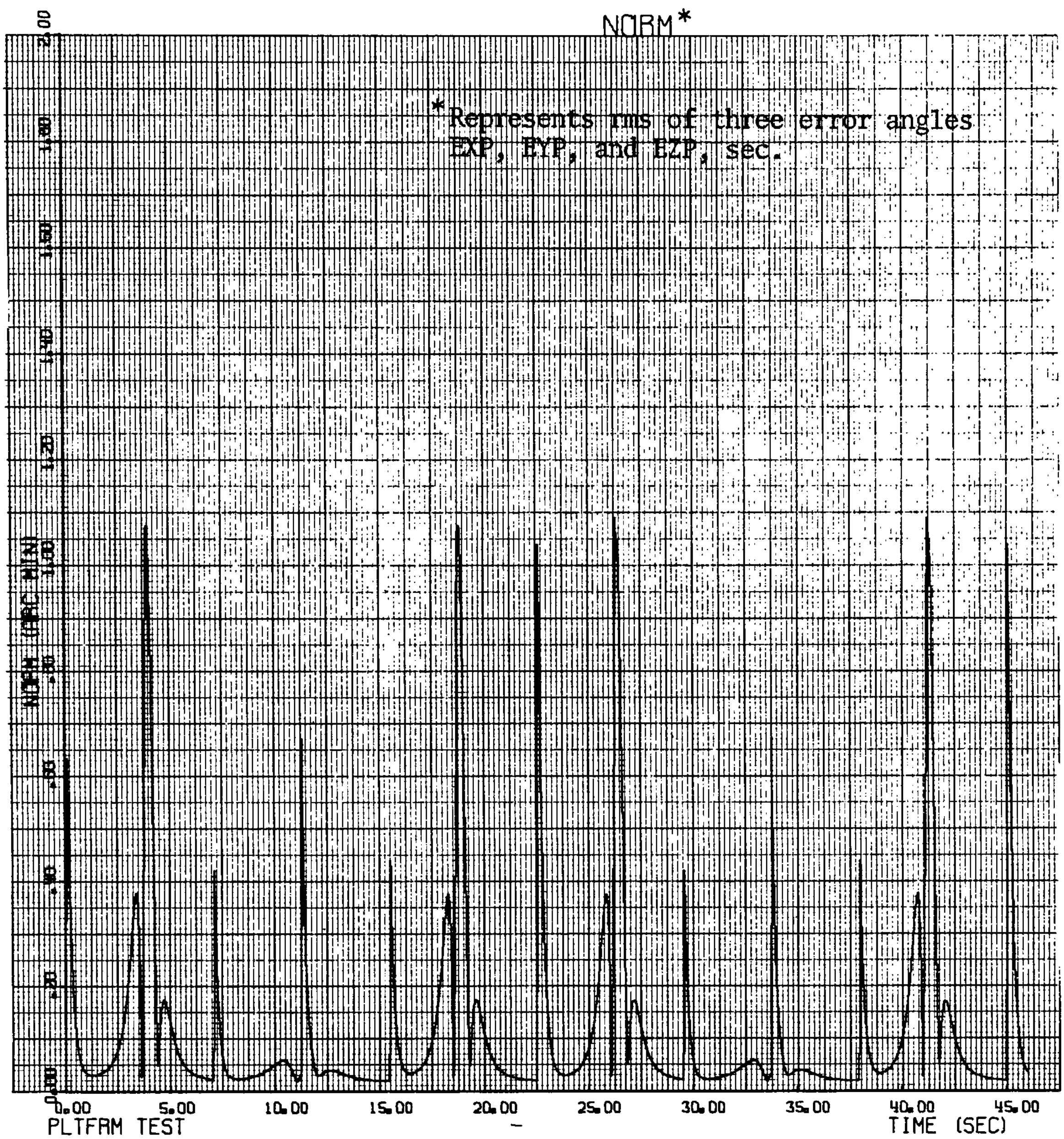
NORM*
*Represents rms of three error angles EXP, EYP, and EZP, sec.
NORM (ARC MIN)
0.00
.20
.40
.60
.80
1.00
1.20
1.40
1.60
1.80
2.00
0.00
5.00
10.00
15.00
20.00
25.00
30.00
35.00
40.00
45.00
PLTFRM TEST
TIME (SEC)

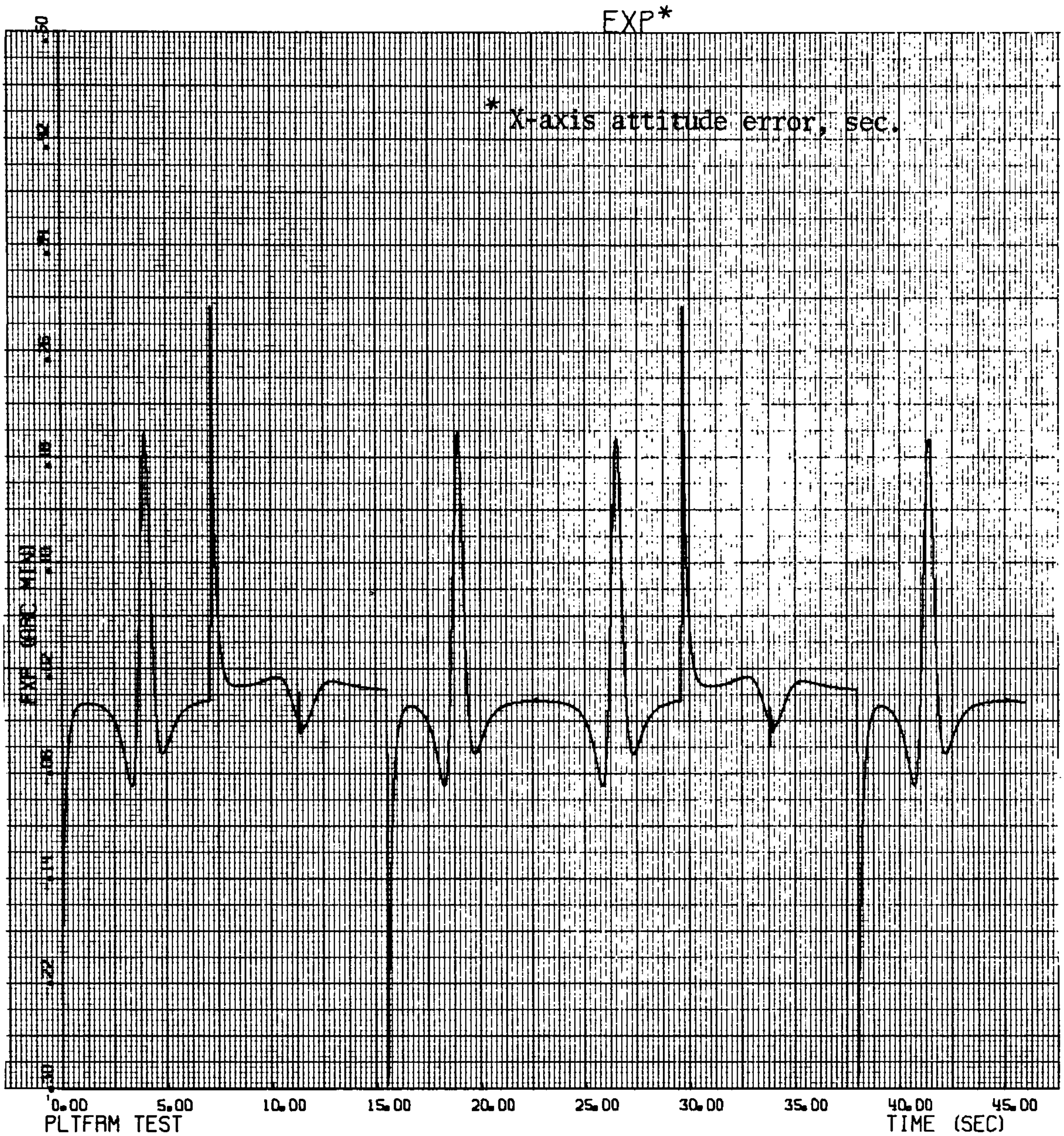
EXP*
* X-axis attitude error, sec.
EXP (ARC MIN)
0.00
5.00
10.00
15.00
20.00
25.00
30.00
35.00
40.00
45.00
PLTFRM TEST
TIME (SEC)

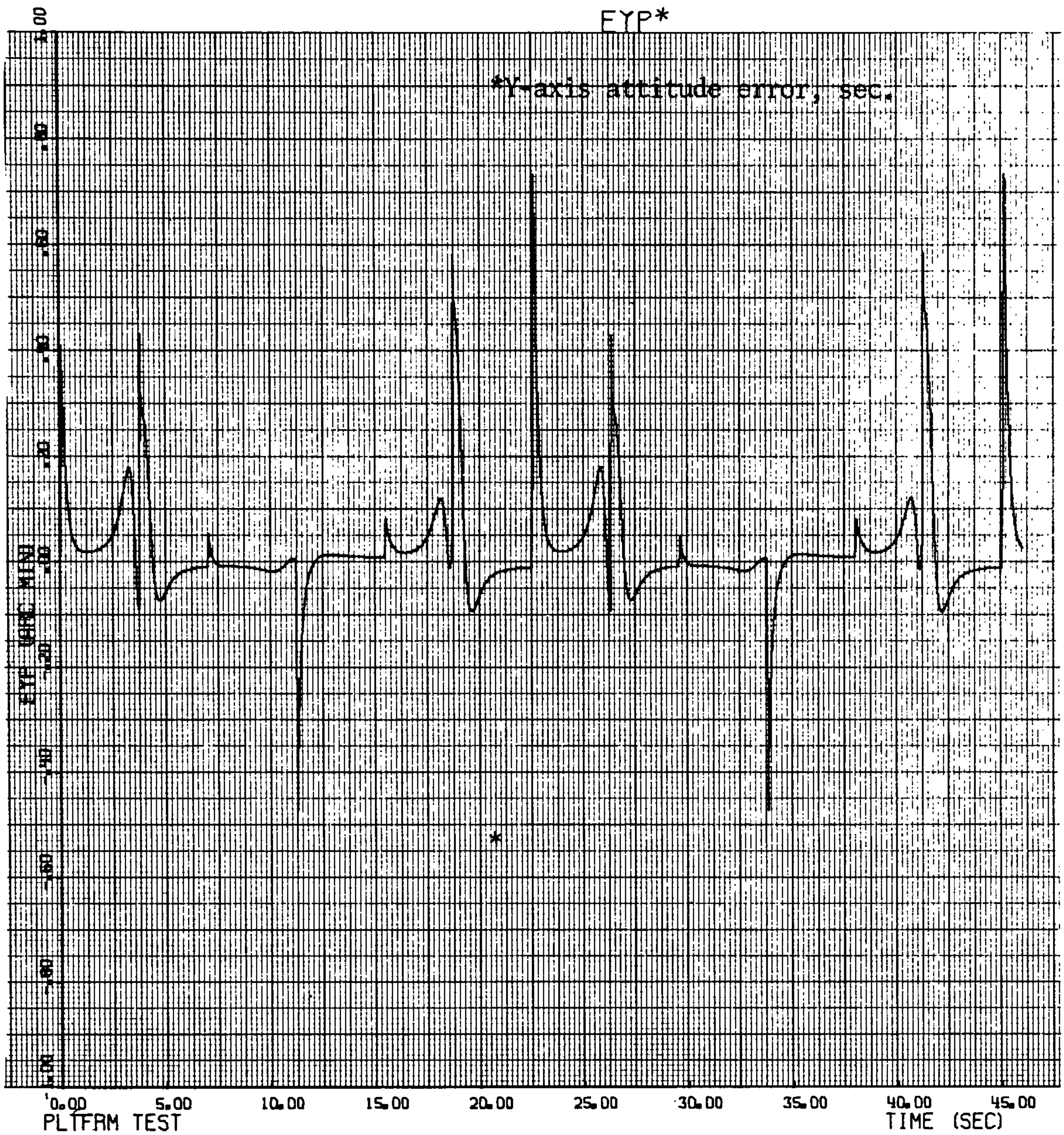
EYP*
*Y-axis attitude error, sec.
EYP (ARC MIN)
0.00
5.00
10.00
15.00
20.00
25.00
30.00
35.00
40.00
45.00
PLTFRM TEST
TIME (SEC)

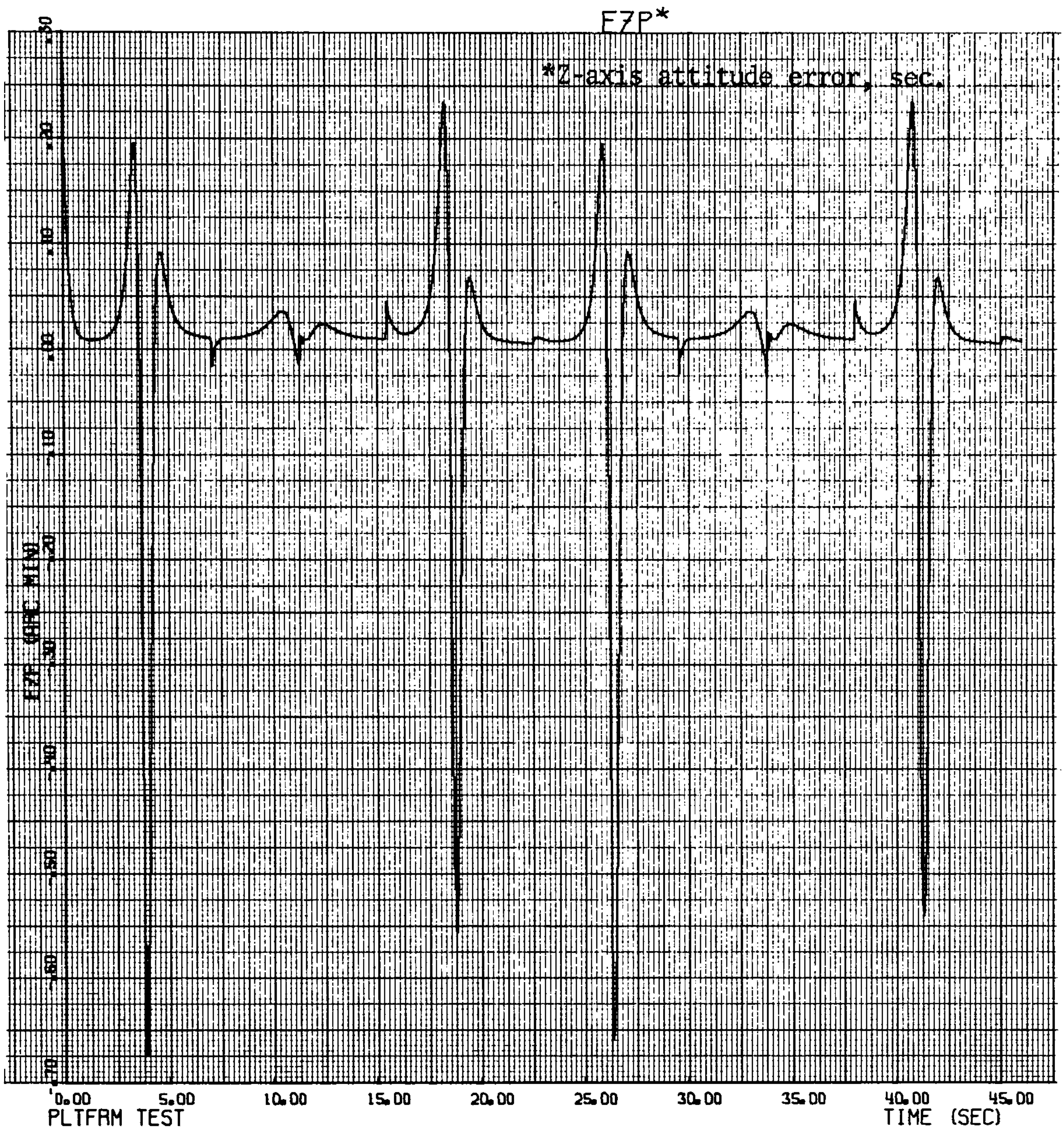
EZP*
*Z-axis attitude error, sec.
EZP (ARC MIN)
.30
.20
.10
.00
-.10
-.20
-.30
-.40
-.50
-.60
-.70
0.00
5.00
10.00
15.00
20.00
25.00
30.00
35.00
40.00
45.00
PLTFRM TEST
TIME (SEC)

*

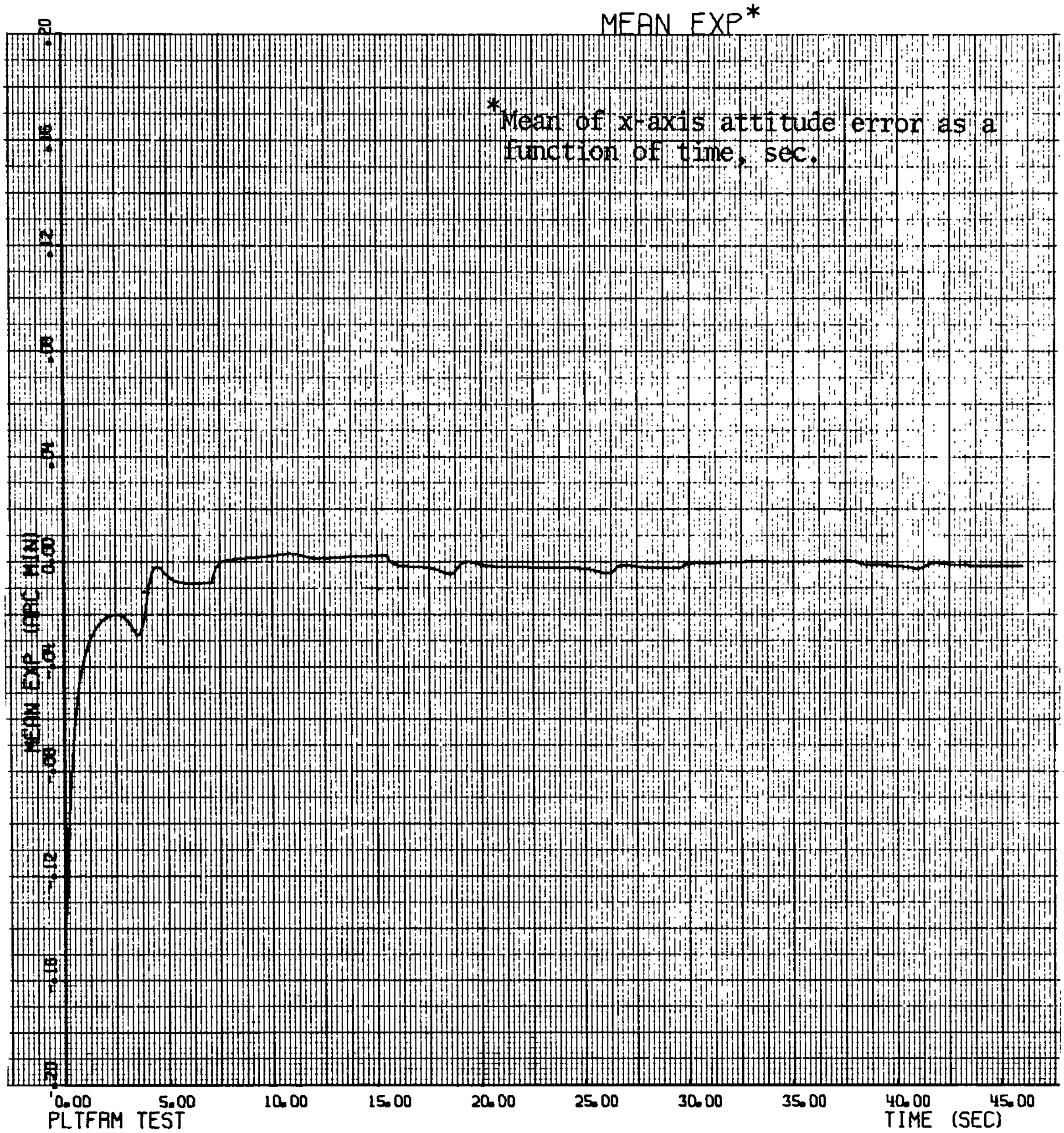
MEAN EXP*
*Mean of x-axis attitude error as a function of time, sec.
.20
.16
.12
.08
.04
0.00
-.04
-.08
-.12
-.16
-.20
MEAN EXP (ARC MIN)
0.00
5.00
10.00
15.00
20.00
25.00
30.00
35.00
40.00
45.00
PLTFRM TEST
TIME (SEC)

MEAN EYP*

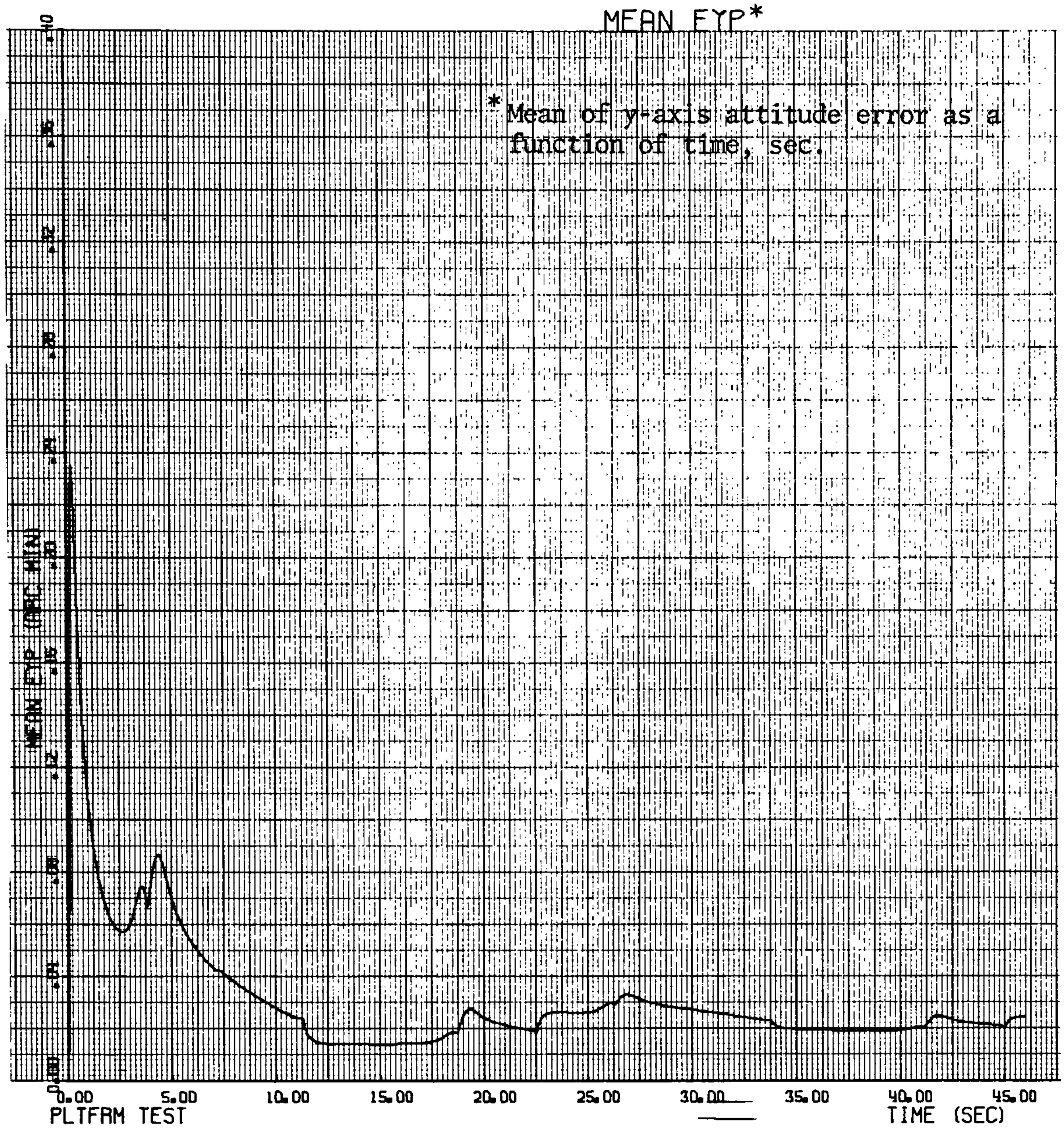
*Mean of y-axis attitude error as a function of time, sec.
MEAN EYP (ARC MIN)
0.00
5.00
10.00
15.00
20.00
25.00
30.00
35.00
40.00
45.00
PLTFRM TEST
TIME (SEC)

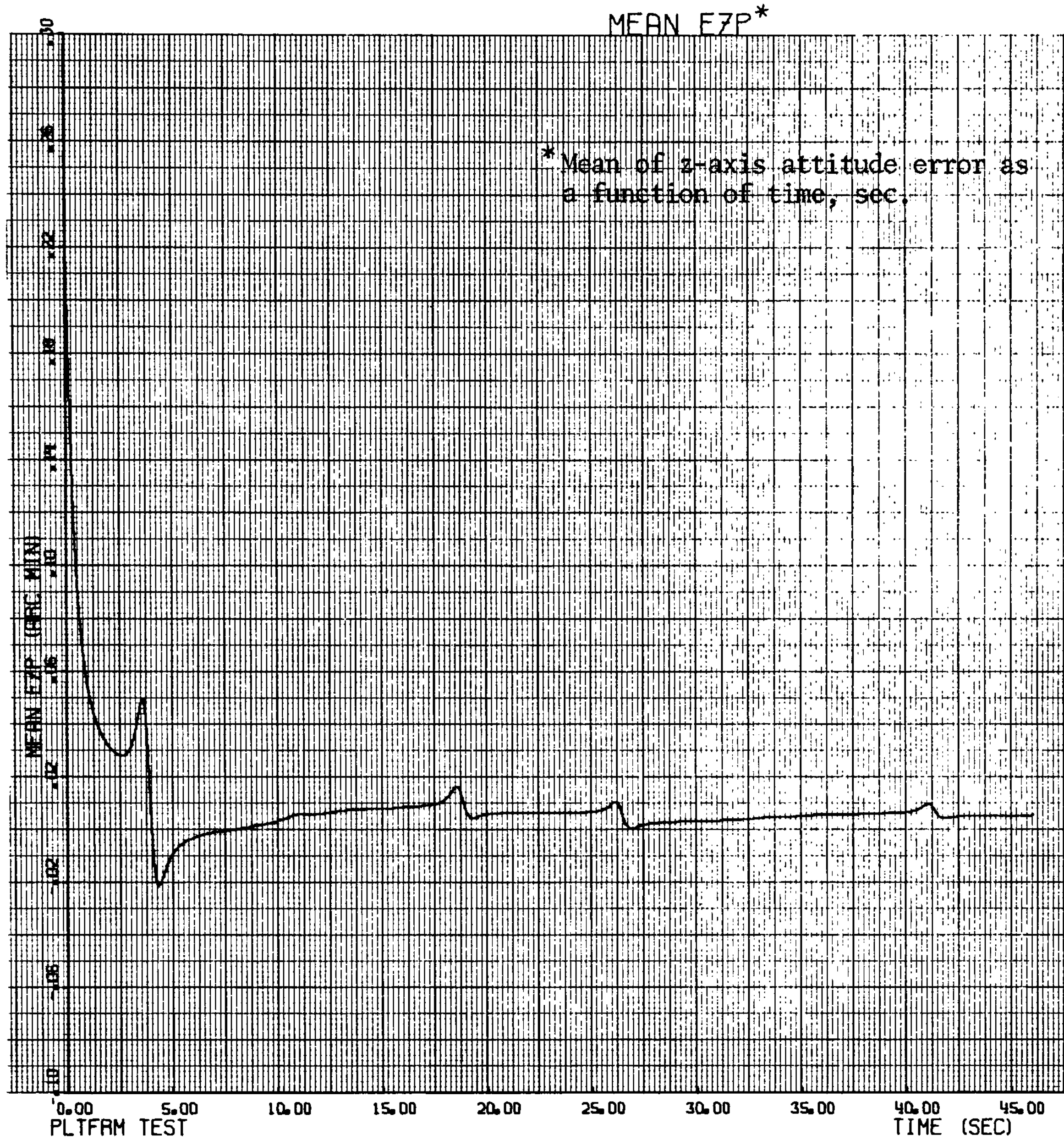

MEAN EZP*
*Mean of z-axis attitude error as a function of time, sec.
MEAN EZP (ARC MIN)
0.00
5.00
10.00
15.00
20.00
25.00
30.00
35.00
40.00
45.00
PLTFRM TEST
TIME (SEC)

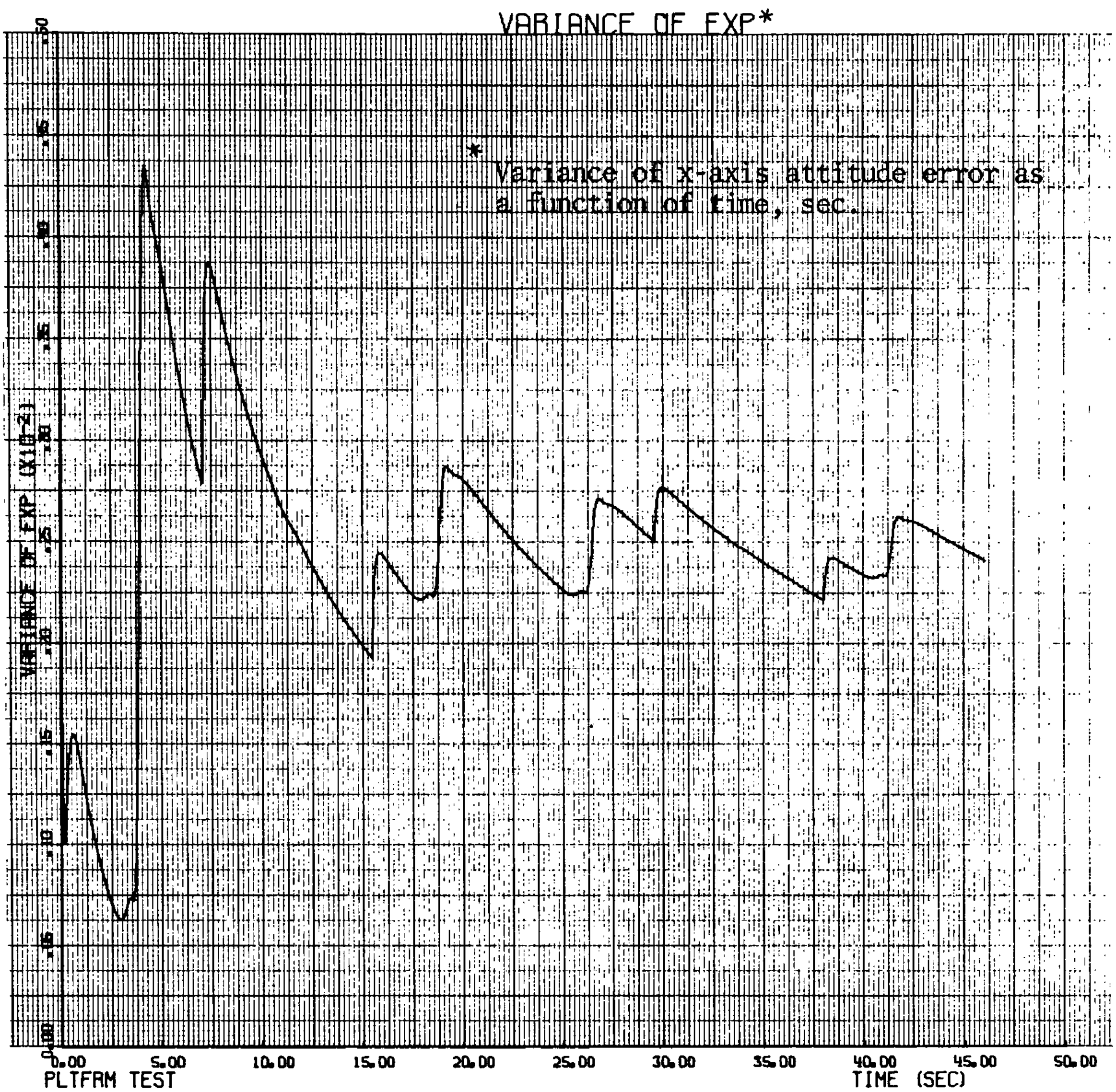
VARIANCE OF EXP*
* Variance of x-axis attitude error as a function of time, sec.
VARIANCE OF EXP (X10-2)
0.00
.05
.10
.15
.20
.25
.30
.35
.40
.45
.50
0.00
5.00
10.00
15.00
20.00
25.00
30.00
35.00
40.00
45.00
50.00
PLTFRM TEST
TIME (SEC)

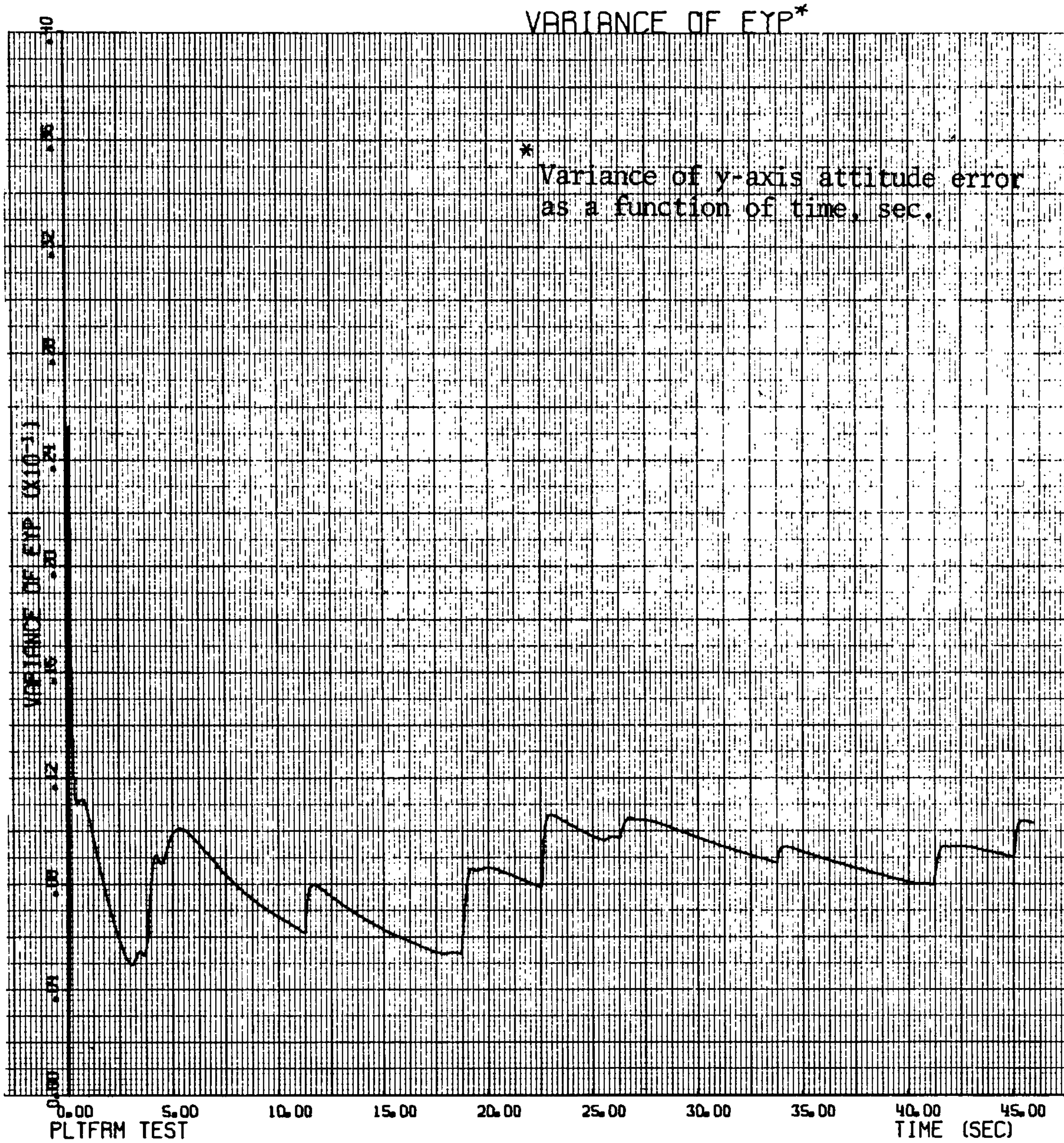
VARIANCE OF EYP*
* Variance of y-axis attitude error as a function of time, sec.
VARIANCE OF EYP (X10⁻¹)
0.00
.04
.08
.12
.16
.20
.24
.28
.32
.36
.40
0.00
5.00
10.00
15.00
20.00
25.00
30.00
35.00
40.00
45.00
PLTFRM TEST
TIME (SEC)

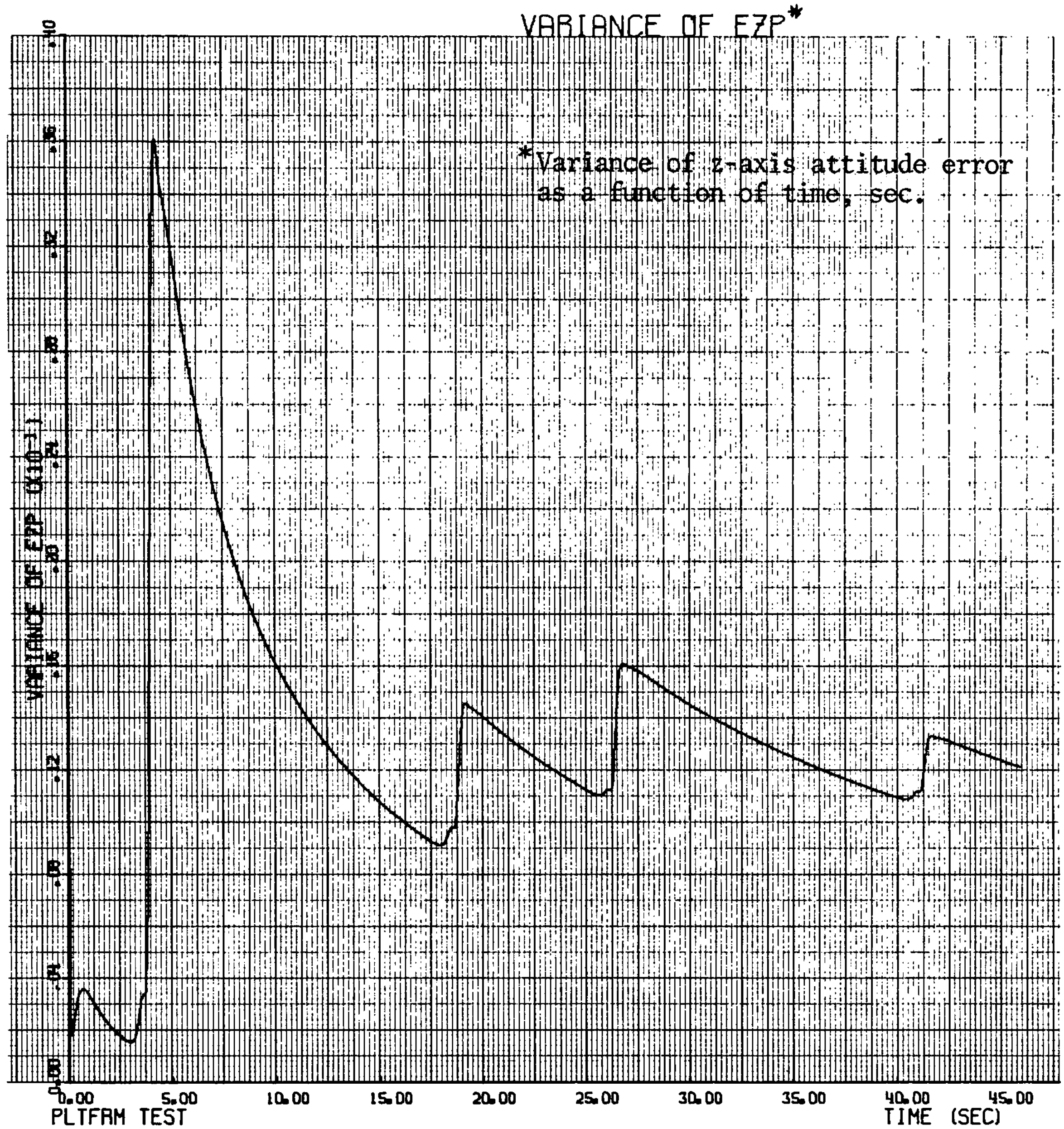
VARIANCE OF EZP*
*Variance of z-axis attitude error
as a function of time, sec.
VARIANCE OF EZP (X10⁻¹)
0.00
.04
.08
.12
.16
.20
.24
.28
.32
.36
.40
0.00
5.00
10.00
15.00
20.00
25.00
30.00
35.00
40.00
45.00
PLTFRM TEST
TIME (SEC)